REPORT NO. 714104/A/006-2

# COAST GUARD

## OFFICE OF
## RESEARCH & DEVELOPMENT

CONTRACT NO. DOT-CG-03,592-A

AD 727524

# OCEANOGRAPHIC OBSERVATIONS AND THEORETICAL ANALYSIS OF OIL SLICKS DURING THE CHEVRON SPILL, MARCH 1970


STEPHEN P. MURRAY
W. G. SMITH
CHOULE J. SONU





COASTAL STUDIES INSTITUTE
LOUISIANA STATE UNIVERSITY
BATON ROUGE, LOUISIANA 70803




JULY 1970

FINAL REPORT

Prepared for: COMMANDANT (DAT)
U.S. COAST GUARD HEADQUARTERS
WASHINGTON, D.C., 20591

DATE: 4 DECEMBER 1970

This report has been submitted in fulfillment of contract DOT-CG-03592-A and is promulgated subject to the following qualifications:

The contents of this report reflect the views of the Coastal Studies Institute of Louisiana State University,

which is responsible for the facts and the accuracy of the data presented herein. The contents do not necessarily reflect the official views or policy of the Coast Guard. This report does not constitute a standard, specification or regulation.

J. R. IVERSEN
Captain, U. S. Coast Guard
Chief, Applied Technology Division
Office of Research and Development
U. S. Coast Guard Headquarters
Washington, D. C. 20591

# Oceanographic Observations and Theoretical Analysis of Oil Slicks During the Chevron Spill, March 1970

Stephen P. Murray
W. G. Smith
Choule J. Sonu
Coastal Studies Institute
Louisiana State University
Baton Rouge, Louisiana 70803

July 1970

FINAL REPORT



Prepared for
Department of Transportation
United States Coast Guard
Washington, D.C. 20591

The contents of this report reflect the views of the Coastal Studies Institute of Louisiana State University, which is responsible for the facts and the accuracy of the data presented herein. The contents do not necessarily reflect the official views or policy of the Department of Transportation. This report does not constitute a standard, specification or regulation.

## ABSTRACT

Oceanographic observations near the Chevron spilling well off the Mississippi Delta in March, 1970, revealed relative roles of various physical factors of the regional estuarine system in the behavior of oil slicks. Surface stress from the wind was most important; at speeds above 15 mph the slick orientation was generally determined by the wind direction. The wind also indirectly affected oil which was sunk by dispersant in that wind waves promoted mixing, which in turn affected the vertical stability, hence eventually the velocity profile. Wind setups and setdowns were correlated with downward and upward isopycnal movements, respectively. Both calculations and observations showed that tidal currents produced an L-shaped slick geometry when winds were below about 15 mph. The diurnal rotation of the tidal currents served to limit the excursion length of oil from the source, keeping it short of the nearest shore. The presence of fresh water from the Mississippi River in the surface layer and the consequent development of convergence lines often formed a natural barrier, preventing oil from encroaching upon the shore. Theoretical analysis using turbulent diffusion theory disclosed that the area and length of a steady-state oil slick increased with oil discharge but decreased with the current speed and the lateral diffusion coefficient. Slick width increased with the rate of discharge and decreased with current speed but was independent of the diffusion coefficient. The width/length ratio of an oil slick, which was notably independent of current speed, was controlled only by the diffusion coefficient and the oil discharge. In order to be able to predict oil slick behavior, understanding of the interaction between these multiple factors is essential and, for that end, the use of a multiple-sensor array with automatic data transfer and processing capability is recommended.

CONTENTS

FIGURES

TABLES

## NOTATION

| | |
|---|---|
| $A$ | slick area |
| $C$ | concentration; $C(y = R)$ is the concentration at the visible boundary of the slick |
| $F$ | fetch |
| $g$ | acceleration because of gravity; or grams |
| $h$ | thickness or depth |
| $H_{1/3}$ | significant height of waves |
| $K$ | diffusion coefficient, diffusion coefficient of oil |
| $K_o$ | modified Bessel function of 2nd Kind and Zero Order |
| $\ell^*$ | scale length or average eddy size |
| $L$ | slick length |
| $Q$ | rate of emission (of oil) |
| $r$ | distance from the origin |
| $R(\xi)$ | the Lagrangian autocorrelation function |
| $t$ | various time parameters |
| $T$ | time |
| $U$ | mean horizontal current speed |
| $U_w$ | wind speed at 10-meter height |
| $v'$ | turbulent velocity in $y$ direction |
| $(\overline{v'^2})^{1/2}$ | intensity of turbulence, usually of oil |
| $W$ | slick width |
| $\theta$ | one-half the initial angle of dispersion of the slick, $\tan\theta = \frac{d\sigma}{dx} = (\overline{v'^2})^{1/2}/U$ |
| $M$ | millimicrons |
| $\xi$ | the lag time |
| $\rho$ | density |
| $\sigma^2$ | the variance of particle displacements from the source |
| $\phi$ | in polar coordinates, the argument |

# INTRODUCTION

When the Chevron production platform MP-41C caught fire and burned in February 1970, a situation was created which at the time appeared to be potentially a prelude to a disaster of major scale. Efforts to extinguish the costly fire were almost certain to lead to large losses of crude oil into the sea, and much of this seemed likely to wash ashore in various areas of the marshes on the mainland.

Figure 1 indicates the location of the accident (platform 41C); it is north and east of the Mississippi Delta and near the entrance of the Gulf outlet channel. Water depths in the general vicinity are from 20 to 50 feet. Before direct measurements were begun, a search for literature giving indications of circulation patterns in the area was made.

Scruton (1956) measured 24-hour diurnal current profiles at several stations in the Main Pass area. Two of these were in the passages into Breton Sound lying to the east and west of Breton Island. In these, ebb and flood current direction were necessarily constrained to inward and outward flow. Surface currents showed a net outward flow at the time of measurement, which was in agreement with the wind direction at the time. Another station, away from the passes and within 3 miles of the site of the 41C platform, showed more variability in flow direction but indicated even higher residual outward (in this case southeastward) flow at the surface. Scruton felt that the residual outward flow in this last case was also caused in part by the wind and by transfer of fresh water from the river out to sea at the surface. He indicated that maximum currents at times of

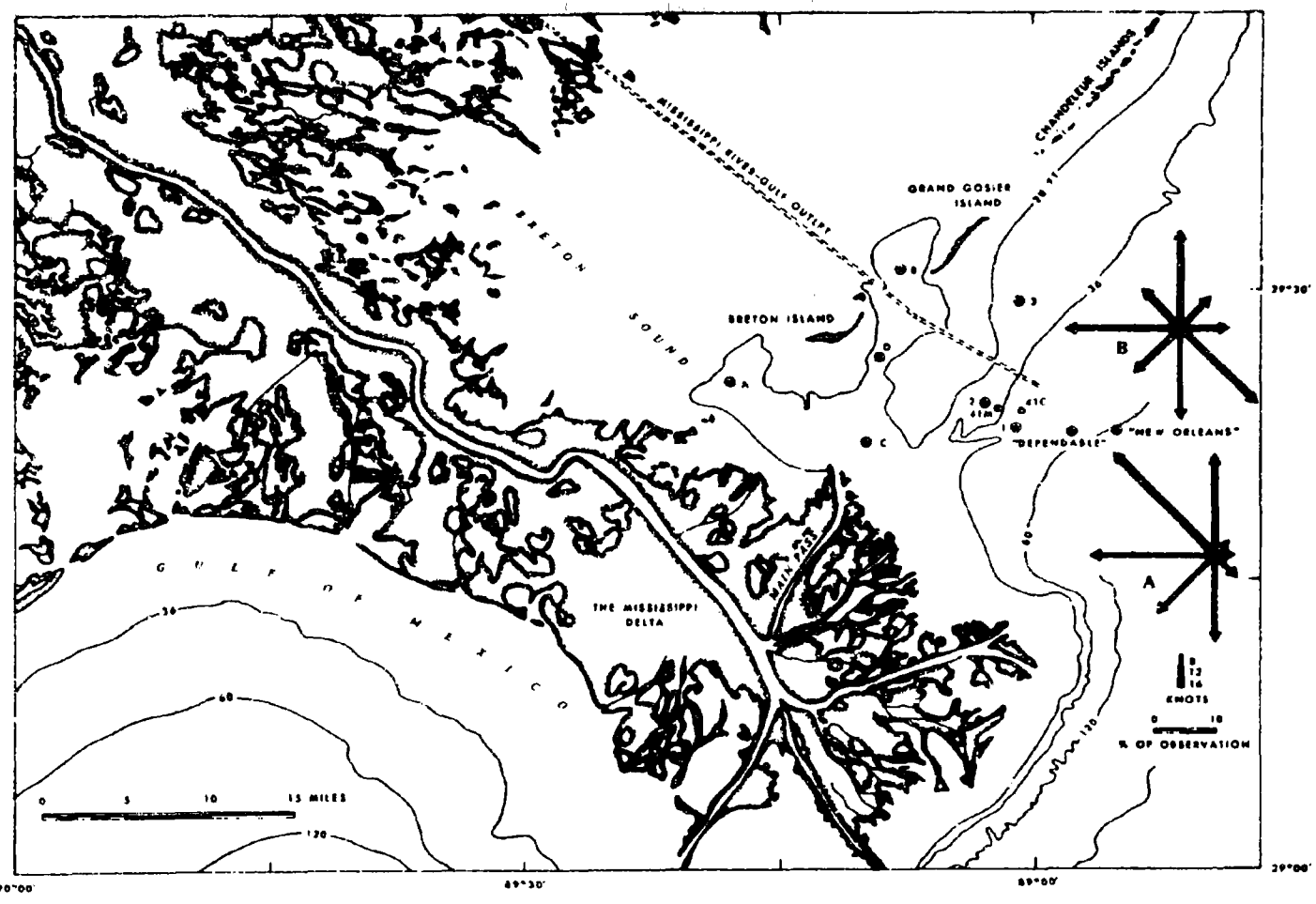


Figure 1. Location map with stations occupied in study. A is wind rose for long-term March observations. B is wind rose for March 1970 from lightship data.

tropic tides could be 1-2 knots and that at times of equatorial tides currents were much lower.

The general hydrography of the area is indicated on Figure 1 and is given in much greater detail on chart 1270 of the U.S. Coast and Geodetic Survey. An important alteration in the area since the time of Scruton's study was the dredging of the Mississippi River Gulf outlet channel to a controlled depth maintained at 36 feet, with deposition of spoil along the southwest side of the channel.

Orton (1964) gave wind data for subsquare 55 of Marsden square 81, in which the 41C platform lies. For the "average" March, on the basis of 5,331 observations, the winds are indicated on wind rose A of Figure 1. The strong northwestward and westward components seemingly would favor drift, insofar as it is wind controlled, toward the Mississippi Delta and the marshes surrounding Breton Sound. The Weather Bureau (1959) also has published data indicating that the frequency distribution of direction of wave approach for winter and spring months shows a predominance of waves coming from the east and southeast in the area of the 41C platform.

Tidal predictions given in Coast and Geodetic Survey (1970) tables for Breton Island for the month of March 1970 are shown in Figure 2.

Another very important part of the physical background necessary to an understanding of the situation is the influence of waters discharged by the Mississippi River. Figure 3 gives the stage height at New Orleans and discharge at Vicksburg, Mississippi, averaged over several years. March is typically a time of high stage and discharge, and 1970 was no exception. The discharged floodwaters are highly turbid and cool (10°C)

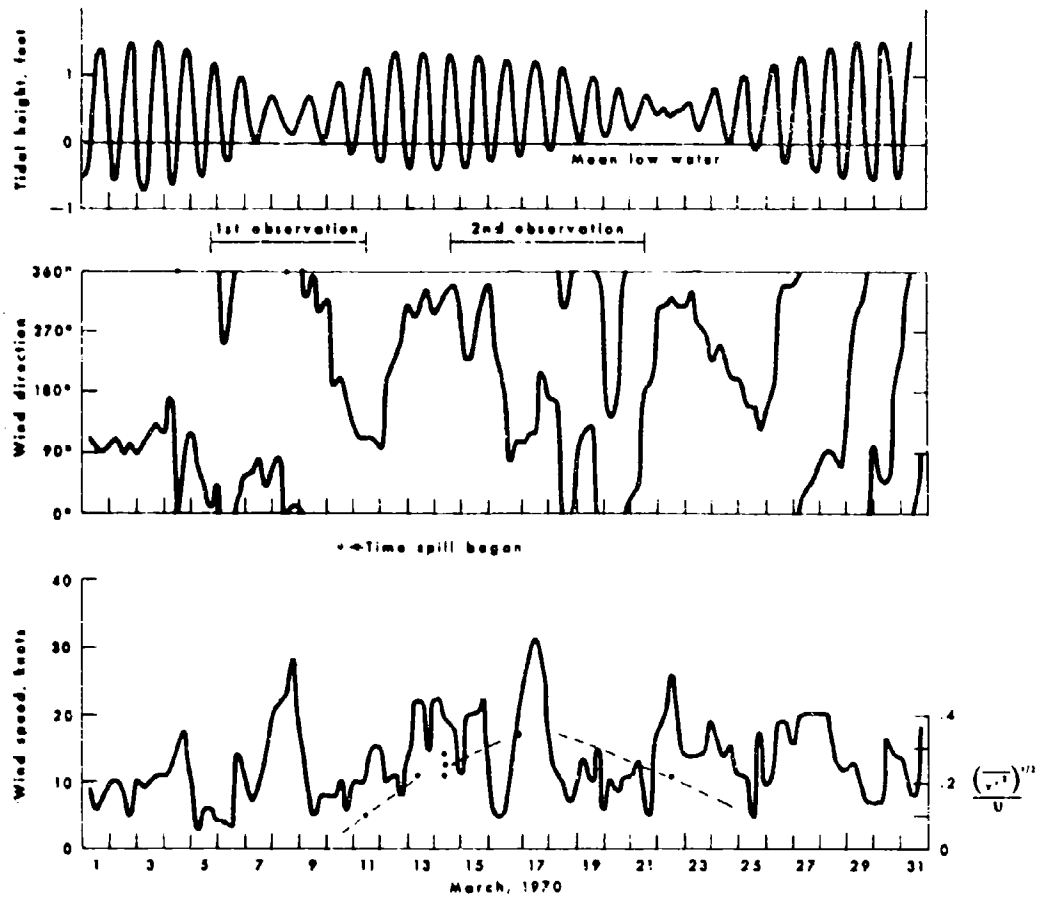


Figure 2. Tidal range for Breton Island and wind speed and direction observed at lightship during March 1970.

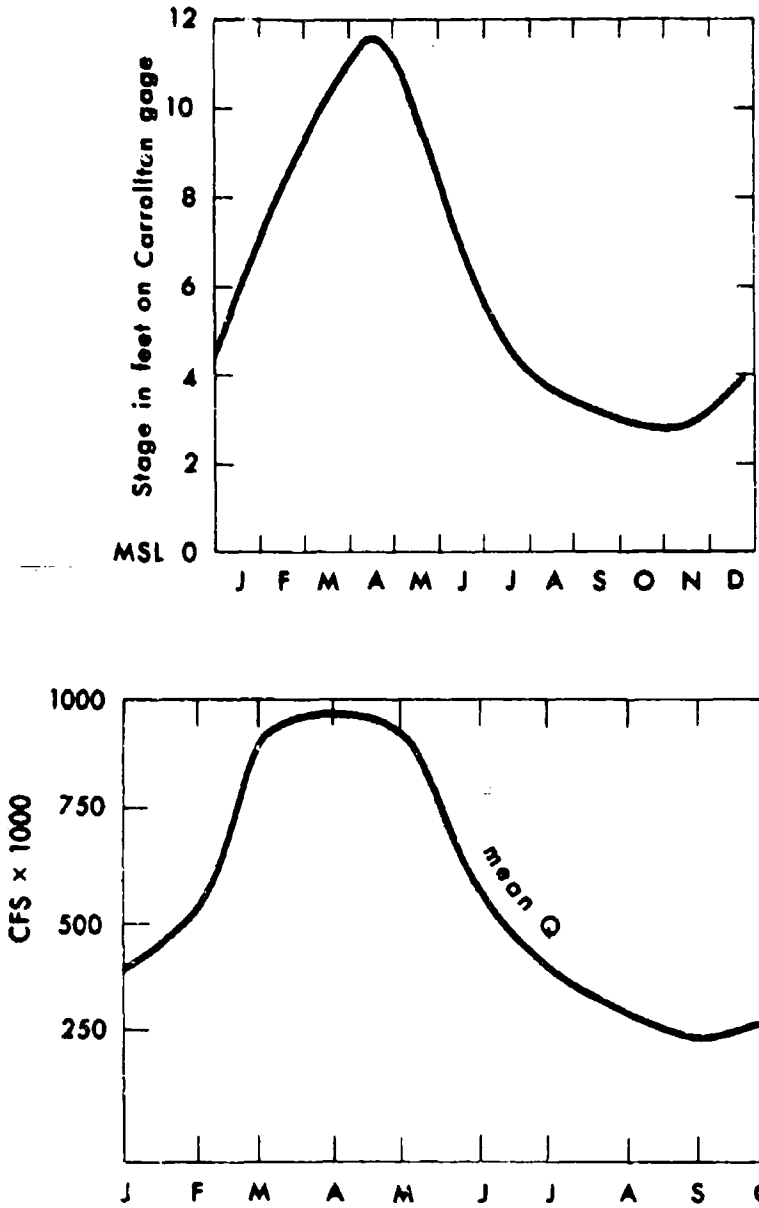


Figure 3. Stage height of Mississippi River at New Orleans and discharge at Vicksburg, long-term averages. (From F. Swaye, Ph.D. dissertation, L.S.U., 1970.)

and contrast sharply with the much less turbid and generally warmer (20°C) saline Gulf waters.

Except for the above-mentioned material, there was little background information useful for judging what might happen when oil began to spill from the Chevron platform. For this reason it was decided that, in light of the possibly dangerous situation that could develop, some basic oceanographic information should be collected before the fire was put out and during the spill. The Eighth District of the U.S. Coast Guard readily agreed to cooperate, and measurements were begun on March 5.

The most important consideration was current, particularly surface current. Temperature and salinity were found to be useful discriminators of the riverine and marine water masses which crossed the accident area. Wind records were also maintained to establish the relation these might have to surface currents. Currents at depth were monitored inasmuch as it seemed possible that a decision to use dispersants to emulsify the oil might lead to spread of oil throughout the water mass. Tides were measured directly since it was not certain how well the predicted curve would agree with the real situation. Wave height and wave period seemed useful indices that might affect diffusion of the drifting oil. Another category of observations was the direct delineation of the orientation and shape of the oil slicks in space and through time.

In all, observations were made from four different Coast Guard vessels at nine different anchorages for continuous periods ranging from 5 days to 6 hours. Slick observations were made from helicopters on a routine basis by Coast Guard personnel, usually twice a day in clear

weather. Overflights were made by several different groups using various conventional and more novel means of remote sensing to document the extent of oil slicks. These data have been made available to us by the U.S. Geological Survey and by Remote Sensing Inc., Houston, Texas. The National Aeronautics and Space Administration also made two overflights during which the C.S.I. group obtained ground truth observations. This material has not yet been made available; however, one of us was able to inspect briefly the imagery at the Manned Spacecraft Center in Houston. A tide and wave gage was suspended from Chevron's MP-41M rig, which is about 1 mile from the damaged structure. A bottom current installation was also made at an additional site, but this instrument has not yet been recovered.

Complete records of all temperature, salinity, and current profiles made from all nine stations are presented in the appendix. Graphical records of these and other observations are presented throughout the remainder of this report.

The 41C platform caught fire at 3 a.m. on Tuesday, February 10, 1970. While it was burning unchecked most of the escaping oil, estimated by Chevron at 1,000 barrels per day, was burned and did not reach the water surface. The work near the platform necessary for quenching the fire required pumping water onto the flame, however, and this tended to wash oil into the water, resulting in light slicks for about a month before the fire was out. The first attempt (March 8) to extinguish the flame was successful, but spontaneous reignition occurred after spillage of crude oil for 6 minutes. On March 10 the fire was successfully extinguished, and oil continued to spill for approximately 1 month before all wells were capped.

Our observations, except for those kept and made available to us by Coast Guard personnel, were confined to two periods, March 5-11 and March 14-20.

## MEASUREMENT TECHNIQUES

### Tides

Tides were recorded by a Hydro Products 521 model submerged wave and tide gage. This hydrostatic pressure-sensing unit is designed for bottom installation, but since there was little time to dive to emplace the instrument properly, it was simply suspended by a rope from the MP-41M platform in firm contact with the bottom. The instrument functioned well and gave data which agree very well with tides predicted for Pensacola (Fig. 4).

### Salinity-Temperature

Salinity and temperature were determined with a Beckman RS-5 induction salinometer. The induction electrode was mounted generally just above the current meter and raised and lowered to the various depths at which currents were monitored so that simultaneous temperature and salinity readings could be made. This instrument functioned well at all times. A few values above 37 parts per thousand are anomalous for this area of the Gulf of Mexico and probably indicate some instability in calibration or misreading of the instrument. Figure 5 is a record of salinity and temperature for the entire period of observations from the C.G.C. Dependable.

### Winds

Wind speed and direction were recorded at quarter-hour intervals by the men on watch on the U.S.C.G.C. Dependable during the whole period of our observations on board that vessel. Crewmen on watch on the cutters

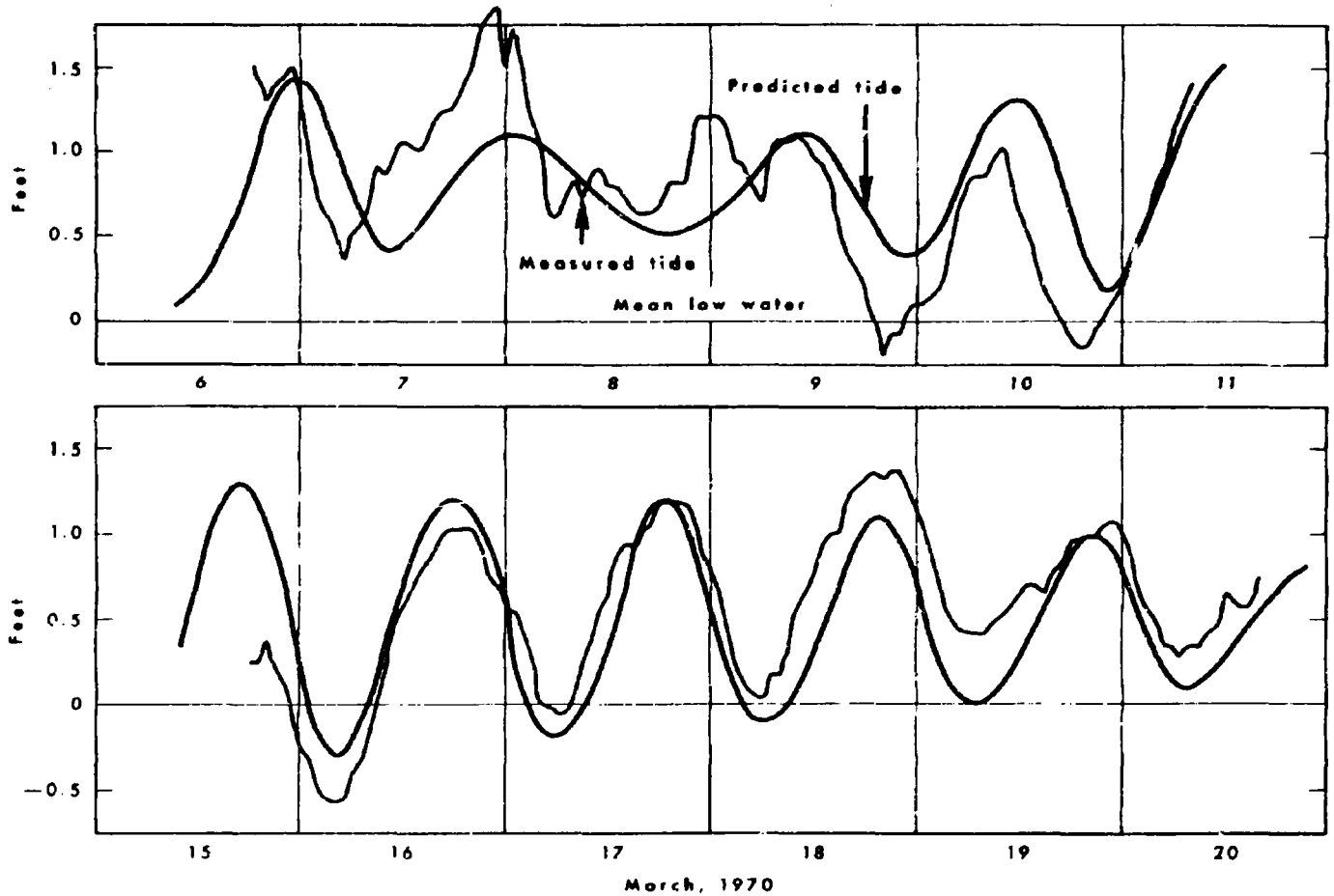


Figure 4. Observed and predicted tides.

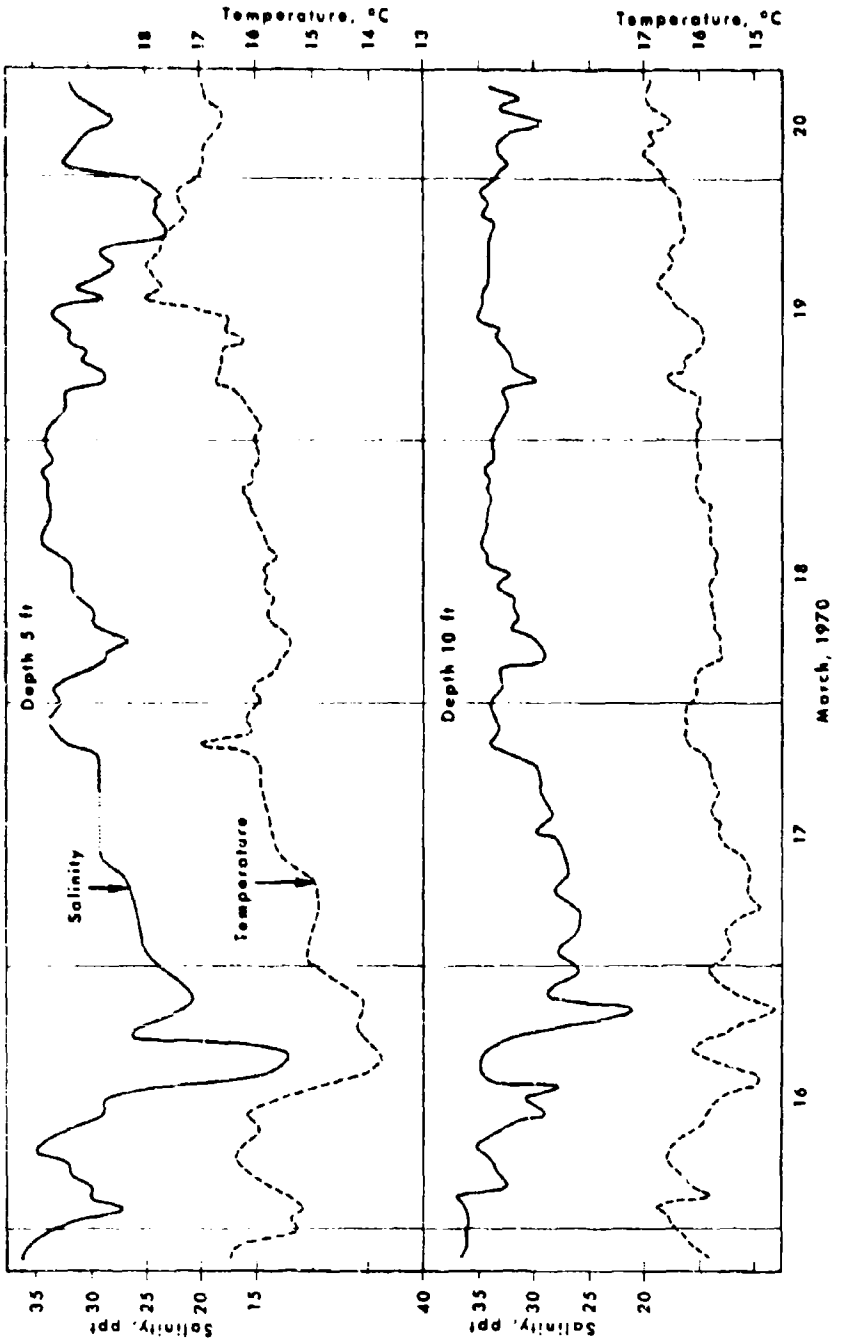


Figure 5. Salinity and temperature records from 5- and 10-foot depths at Dependable station.

Pt. Spencer and Pt. Estero also kept logs at various times of wind speed and direction at our request. The lightship New Orleans regularly records meteorologic data every 6 hours year-round and relays this information to the Weather Bureau. Figure 2 gives a plot of wind speed and one of wind direction for the entire month of March based on the lightship records. Figure 6 shows wind speed and direction recorded from March 15 to March 20 by the Dependable. On Figure 1 the lightship wind records for March are plotted as wind rose B (based on 115 observations) for direct comparison with the winds expected in an "average" March.

Currents

The most successful current monitoring was done with Marine Advisers Q-15 ducted current meters, which were raised and lowered by means of the ship's winches. Savonius rotor-type meters were employed with some success at fixed levels by suspending the instruments on cables from the cutter Reliance and from the lightship New Orleans.

The greatest difficulty in measuring currents in shallow coastal waters is the effect of the oscillatory orbital wave motions on the speed sensors. The Savonius rotor, for example, will spin up with the wave motions and can overestimate the steady current by a factor of three or four. A bidirectional ducted meter such as the Q-15, used extensively in this program, largely eliminates this error.

The chief problem in current monitoring from ships is the motion of the ship itself even when at anchor. In this study it was noted that whenever winds exceeded about 12 knots the vessels began to yaw from side to side, swinging on the anchor. This motion of the ship drags the current

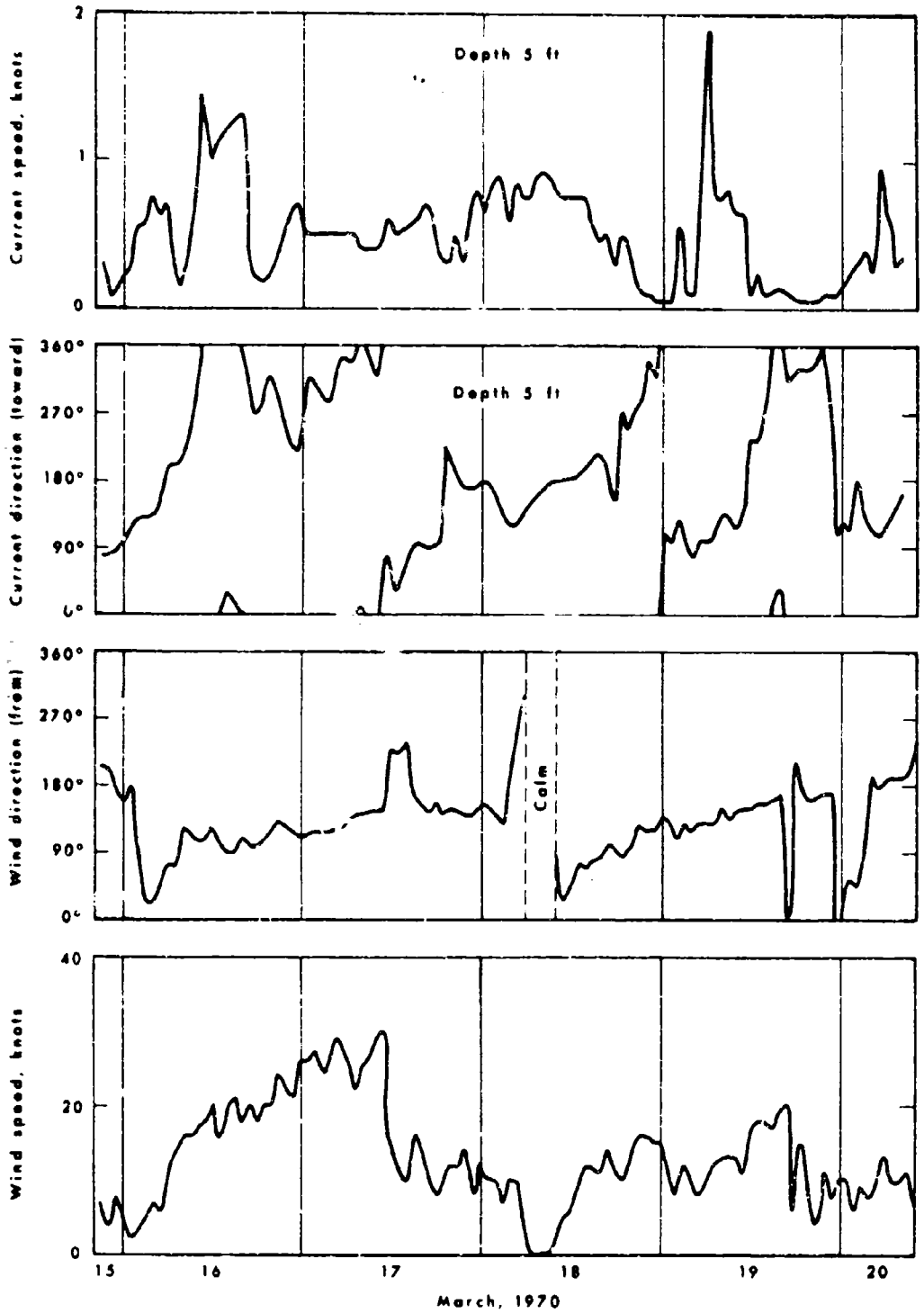


Figure 6. Current speed and direction at 5-foot depth and wind speed and direction at Dependable station.

meter and causes rhythmic oscillations of readout, giving errors that can be as much as .5 knot too high. This type of error is obvious on the record; all erroneous data have been deleted from consideration. Current observations from the Dependable are plotted on Figures 6 and 8.

The vertical motions of the ship are an additional problem which can give false impressions about currents. Both side-to-side swinging and vertical motion led to a generally unsatisfactory performance for the Savonius meters, and information from these is not used here. The ducted meters respond in a selective way directionally. For a detailed discussion of these types of error see Murray (1969).

Measuring currents very near to the surface with any type of suspended meter is difficult except in periods of calm sea states. The periods of high waves encountered in the study sometimes made it impossible to obtain current readings at 5 feet depth because of extreme swinging of the instrument as waves rocked the ships. Use of floating drogues or drift cards for surface current measures therefore seems preferable if adequate means of tracking are available.

Sometimes currents changed in speed very rapidly, as can be seen in Figure 6 at about 0700 CST, when current speed changed from .05 to 1.9 knots in a 2-hour period. This poses a sampling problem. The intervals for completion of a single profile were about 1 hour, meaning that readings at any given depth were repeated about once an hour. With such rapid changes taking place, this may not have been sufficient to record all peak speed periods. It would be preferable to have currents at a given depth monitored continuously.

Ideally, much more could have been done, and will be done as the "state of the art" for shallow-water current measuring instruments improves. It is tempting to think of moored strings of ducted current meters spaced at fixed depths and recording continuously. The moored deployment would eliminate many of the problems inherent in unsteady ships, the continuous recording would give better resolution, and the ducted instruments would give better directional response. Although this seems a greatly improved means of profiling, another approach will be necessary for continuous study of very-near-surface currents at times of varying sea state, a problem of critical importance in the movement of oil on water.

Waves

Wave height and wave period were recorded by the Hydro Products 521 model instrument previously described in the section on tides. As mentioned, this instrument was installed by suspending it from a platform. Its attachment to the platform probably added some noise to the data (particularly the wave period) owing to the effect of the structure on waves approaching from certain directions. Other than this, the records seemed excellent and are plotted in Figure 7 with wind speed for comparison.

Choppy seas are indicated by low period numbers. At 1200 CST on March 17, for instance, during a high wind, wave period reached a minimum of 3 seconds. Shortly after this the wind fell off abruptly and the record began to show a steady swell with period of about 7 seconds. The swell probably existed prior to this but was masked by the seas.

Slicks

The Coast Guard's routine Situation Reports gave direction and approximate width and length of the oil slicks when visibility conditions allowed

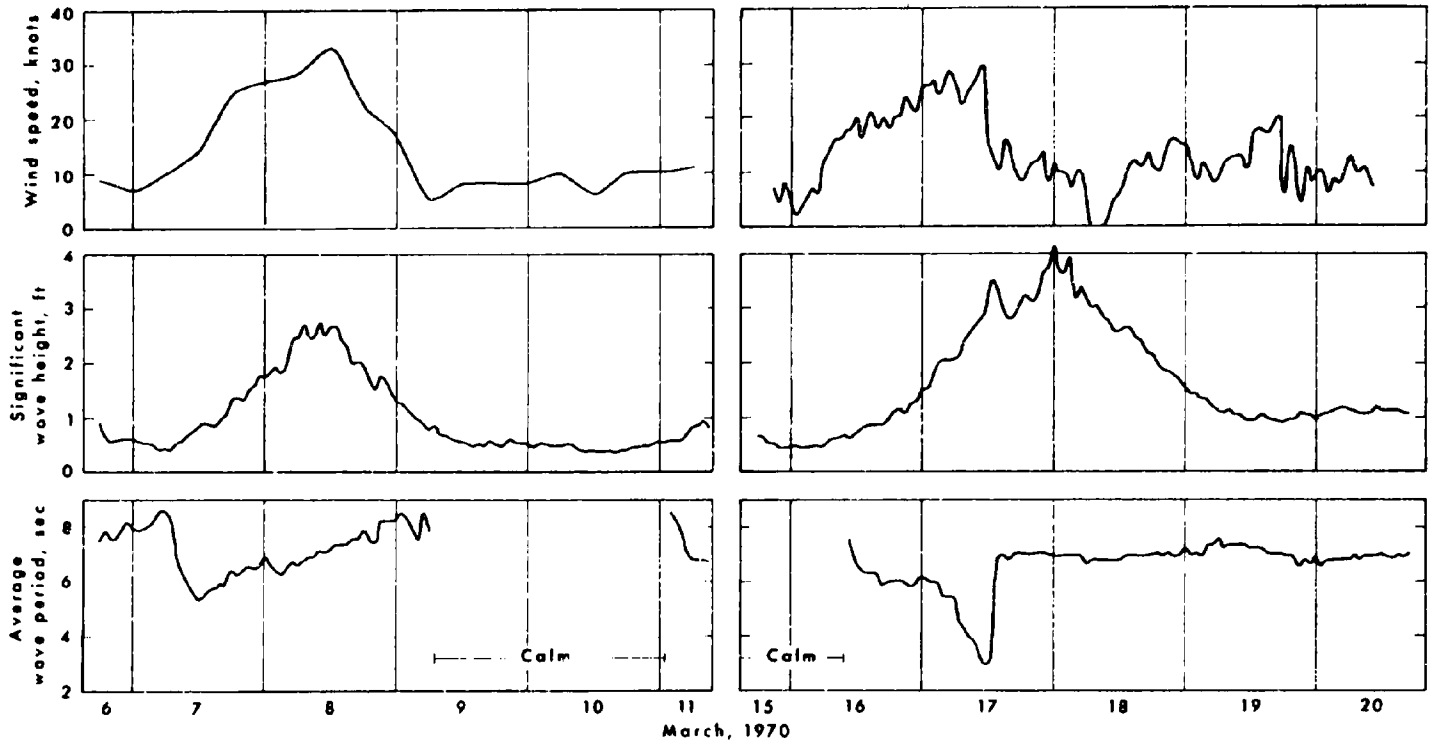


Figure 7. Wave height and wave period from 521 meter installed at Chevron platform MP-41M and wind speed for same intervals.

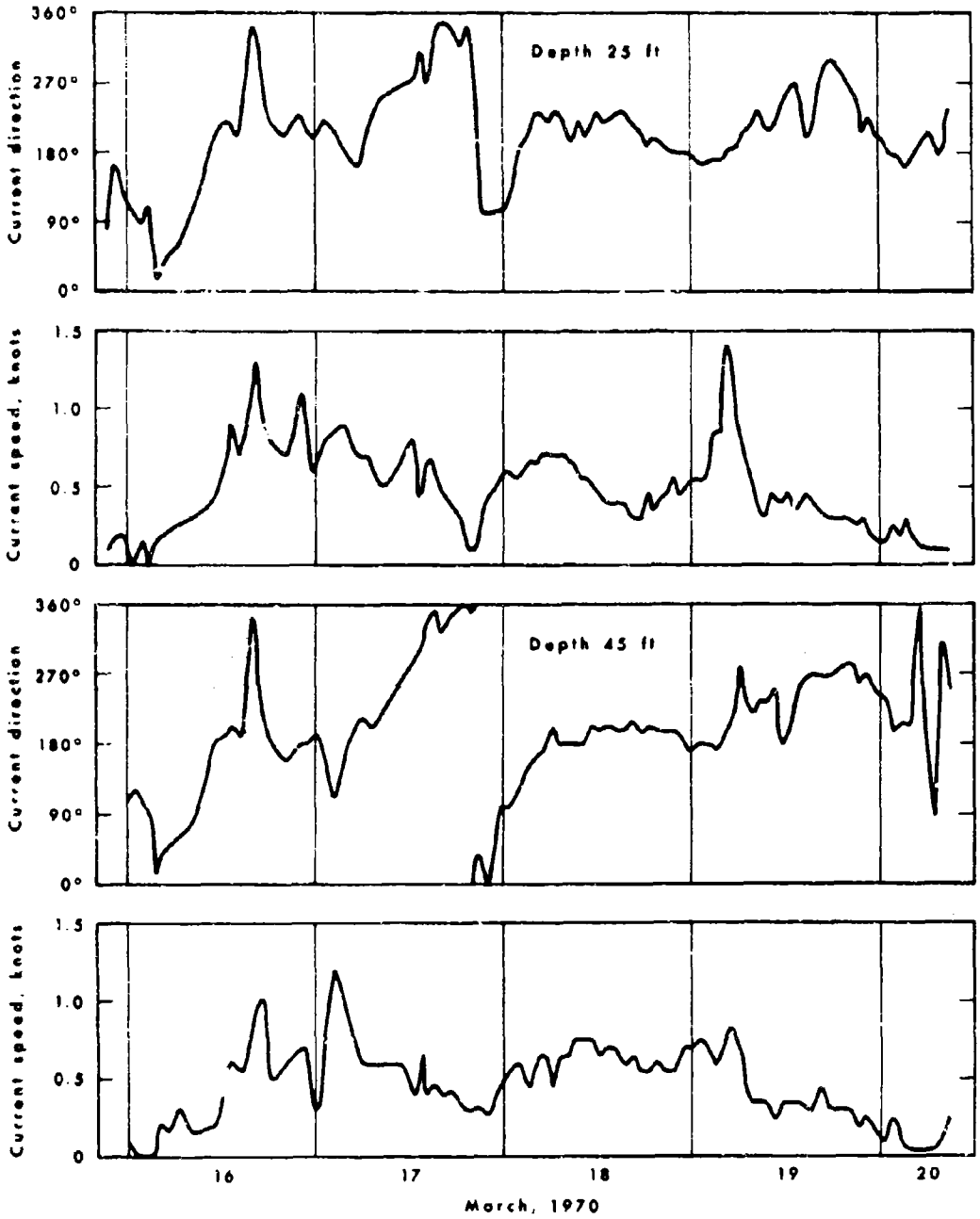


Figure 8. Current speed and direction at 25- and 45-foot depths at Dependable station.

observation from helicopters or other aircraft. Aerial remote sensing by photography and infrared scanners also recorded the distribution of oil on several occasions. The infrared (8-14μ) scanning device showed the form and xtent of the oil slick especially well. In these images the lighter films of oil, which formed the greater part of the area of the slick, generally appeared darker than the surrounding water. The heavier agglomerated masses of oil, which occurred in patches up to a centimeter in thickness, showed as very light areas on the scanner imagery.

## ANALYSIS AND INTERPRETATION OF DATA

During the 12 days at the site of the Chevron spill our research group collected a tremendous volume of data. This data was subsequently augmented by numerous photographs and imagery taken by several government agencies and private companies, the information in the Situation Reports, and assorted other data. Because of time limitations, in-depth analysis has been restricted to the characteristics of the currents; gross relationships between measured current, winds, and slick movements; and theoretical slick analysis. We have arranged most of the observational data in figures, and this section will be mainly a discussion of the salient features exhibited by the figures.

### Tides

On Figure 2 the most conspicuous feature of the tides predicted for March is the biweekly cycle of high-range tropical tides and low-range equatorial tides, which are characteristic of this area of the Gulf of Mexico. The maximum range for tropic tides is about 2.5 feet, and the range for equatorial tides may be only 0.1 foot or less. In restricted

waters strong winds can increase or diminish tidal range considerably. The tides are largely of diurnal character, but semi-diurnal components may be evident, particularly during equatorial tides.

Figure 4 shows the measured tides, with predicted curves plotted for comparison. Agreement between the two is excellent, indicating that the tide predictions at Pensacola are useful for the area of study. The interval of March 6-11 spans a period of equatorial tides and that of March 15-20 covers a period transitional from tropic to equatorial. The semi-diurnal components are evident for the period of March 8-9 and again in the period March 17-20.

Salinity and Temperature

Salinity and temperature profiles in the area of the 41C platform were quite variable in the upper portions, while temperature and salinity at depths below 15 feet were rather constant at about 16°C and 35 parts per thousand, respectively. At times the temperature profiles were virtually isothermal, but a distinct halocline generally existed between 5 and 15 feet beneath the surface. During periods of high winds and waves the halocline moved downward, reflecting deeper mixing (see, for instance, the salinity records from the Dependable for March 17 cited in the appendix).

In the zone above the halocline, salinity and temperature variations at a station were extreme and sudden. Figure 9 shows the situation which existed at the Dependable just prior to and during the first NASA overflight. A mass of highly turbid water moved past the Dependable at approximately 1330 CST, and temperatures quickly declined by 2° at the surface while salinity dropped from 24 to 13 parts per thousand. Figure 5 shows the record

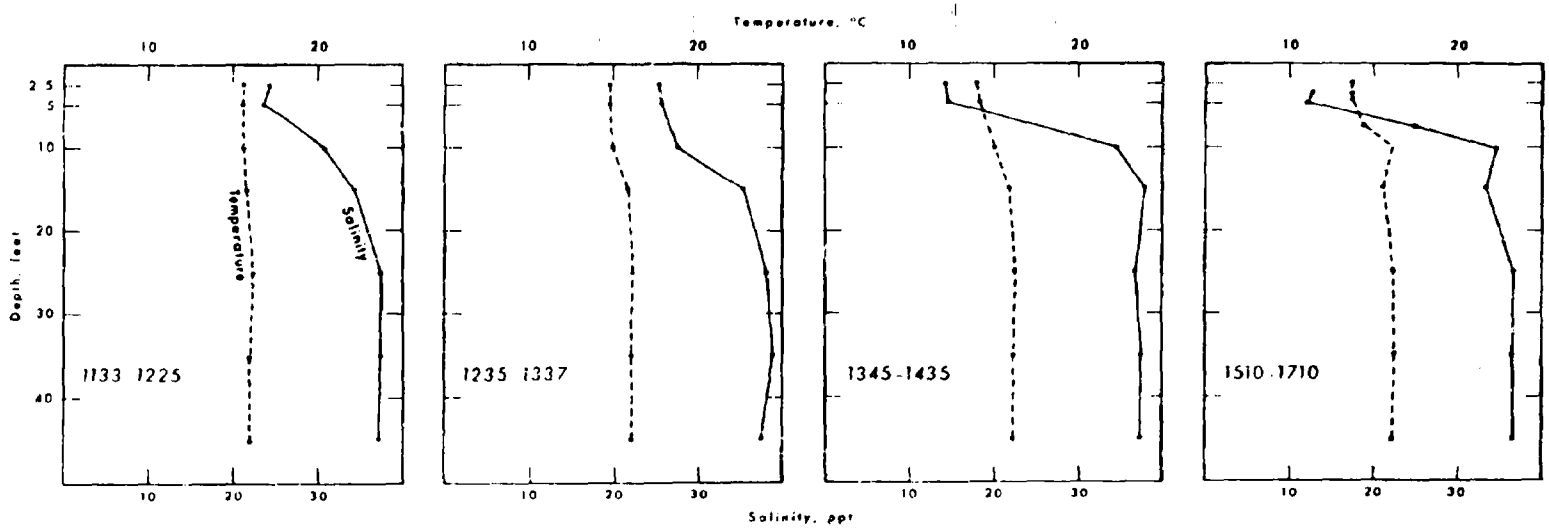


Figure 9. Salinity and temperature profiles, Dependable station, March 16, 1970.

of this event as well as that at the 10-foot depth, where declines of temperature and salinity are not as great. A similar passage of a freshwater body was recorded in the Pt. Spencer, station 1, observations on the night of March 5, when salinities declined abruptly from 27 to 18 parts per thousand, then slowly returned to normal levels (see appendix).

These low-salinity surficial water masses usually were clearly demarcated from higher salinity waters by a sharp "tide line" or interface. Such interfaces are familiar phenomena in the Mississippi Delta area. The interface is prominent not only because of the strong contrast in turbidity across it but also because frequently there are concentrations of floating debris along it. Oil likewise tended to hang up along it. Slicks of great width would contract to narrow bands along the interface and abruptly assume the same orientation as the interface.

The fact that oil tended to be stranded along this boundary, together with the fact that only a small amount of oil reached shore from this large spill and this only on Breton and Grand Gosier islands, suggests that coastal low-salinity water masses may have acted as a buffer zone, protecting the marshlands. River water discharged from the numerous passes of the flooding Mississippi must also create a hydraulic gradient leading to a net offshore displacement of surface waters.

Winds

Wind rose B of Figure 1, based on 115 observations, shows w as observed by the lightship New Orleans in March 1970. While the "average" March depicted in A shows a clear predominance of winds from the east, south, and southeast, the March 1970 record differs in the great frequency

of winds from the northwest. This was perhaps a fortunate circumstance in preventing spread of oil into the marshlands to the west and northwest.

The wind speeds and directions indicated in Figure 2 show the erratic nature of winds during March. The two periods of highest winds, on March 8 and March 17, occurred during the periods of observations and added variety as well as difficulty to the operations. These periods are discussed in the section on waves. Average wind speed for the whole month is approximately 12 knots.

Figure 6 shows winds recorded on the Dependable for March 15-20, during most of which time winds from the southeast prevailed.

Waves

Our data on significant wave height and average wave period near 41C, displayed in Figure 7, are restricted to the periods of on-site observations, March 6-11 and March 15-20. Significant wave height $H_{1/3}$ is the average of the highest one-third of the waves. The correlative wind speed in the figure shows that each observation period had a clearly defined storm pattern. During the lightest winds the wave height diminished to 0.2-0.3 foot, while the highest waves (~4.0 feet), early on March 18, were actually swell generated offshore. The expected close correlation between wind speed and wave height is obvious, but a close examination does reveal some interesting features.

During the first storm period the wind blew from the north, a direction in which the fetch is limited to about 10 nautical miles. According to Wiegel's (1962) empirical equation, the maximum possible wave height $H_{1/3}$ is given in a nondimensional form

$$\frac{g H_{1/3}}{U_w^2} = .00305 \left(\frac{g F}{U_w^2}\right)^{0.466}$$

where $U_w$ is the 10-meter wind speed and F is the fetch. This expression predicts a maximum of 4 feet for $H_{1/3}$, but the wind duration was not sufficient to generate this height of wave; the height reached only 2.7 feet. In addition, the fetch is too limited for any appreciable swell to develop, and this is demonstrated by the abrupt decrease in wave height in phase with the decay of the wind speed.

The second storm (March 16-18) blew from the southeast, the direction of maximum fetch into this area. The wind speed attained its maximum at 1200 hours on March 17, but the maximum observed wave height of 4.2 feet lagged by 12 hours because of the arrival of large swell from offshore.

The interaction of sea and swell is better illustrated by the wave period diagrams in Figure 7. During the first storm, as soon as the wind speed exceeded 10 knots the sea began to build and the wave period dropped abruptly to 5.3 seconds, reflecting the surface chop (wind waves), then gradually recovered up to 8 seconds with the arrival of swell. Again, in the second storm, the sea began to build when the wind exceeded 10 knots. The wave period dropped gradually as low as 3 seconds until 1200 hours March 17, when the wind speed suddenly dropped from 30 knots to 10 knots. This discontinuity is immediately reflected in the wave period, with a step-up in period from 3 seconds to 7 seconds as the sea quickly dissipated and the swell predominated.

Prior studies (Johnson and Hwang, 1961; Masch, 1961) have shown that the wave height and period can significantly affect the dispersal of fluid

properties such as amount of suspended solid waste or thermal maxima, and so by extension the surface oil concentration. It is unfortunate that with the excellent quality of the wave data during these two intervals there is practically no quantitative data on the oil slick with which to make comparison. The slick geometry at other times can, however, be related to the wave field indirectly through the wind speed--this is discussed in the section on diffusion theory.

Currents

A priori considerations and experience lead us to expect a mixture of current types in this area--tidal currents, wind-drift currents, slope currents from setup, setdown, and from Mississippi River outflow, and relative currents associated with freshwater-saltwater density gradients.

Near-Surface Currents.--The unreduced current speeds and directions from the 5-foot depth during March 15-20 are plotted on Figure 6, together with the wind speeds and directions. Owing mainly to exceptional logistical support, our most reliable current information comes from this period. The figure shows that the wind remained consistent from the southeastern quadrant but that the current direction rotated clockwise in three broad cycles. The periods were usually well over 24 hours; so these are not simple rotary tidal currents. The wind speed was generally greater than 10 knots and the current speed generally exceeded 0.6 knot.

A clear relationship between the wind and the 5-foot current existed during only one time interval. Between 1800 hours March 16 and 1100 hours March 17 the wind blew from the southeast at over 20 knots; at the same time the current flowed into the northwesterly quadrant at about 0.5 knot.

The Situation Reports disclose that the only severe pollution of beaches on the adjacent islands took place on the afternoon and evening of March 16 on Breton Island. Oil was carried onshore by the currents driven by the strong southeasterly winds.

Since the magnitude of tidal currents is approximately proportional to the tidal range, the diminishing current on March 19 probably reflects the oncoming equatorial tide of March 20.

The overall lack of correlation between the wind and the unreduced current observed at a depth of 5 feet suggests that the other current agents operating (tidal, relative, slope) are usually of the same magnitude or greater than the wind current contribution, effectively masking any relationships from all but a detailed analysis. It seems probable now that the 5-foot current does not reliably represent the surface current. It is unfortunate that the vertical ship motion and wave action prevented us from getting any detailed data closer to the surface than 5 feet.

Subsurface Currents.--Two further levels of the current observations during March 16-20 are shown in Figure 8. The general magnitude of the current speed differs little at the 25-foot level and the 45-foot level from that of the near-surface current. Speeds of 0.4 to 0.5 knot are most common at these depths. The current directions at the 25- and 45-foot levels, while remarkably similar to one another, differ sharply from the near-surface current directions in that they are reasonably steady. During most of this observation period these currents were moving toward the south-southwest. There is a possibility that these seaward-flowing currents were returning to the offshore water which was brought onshore by

the steady southeasterly wind. This seaward return flow effect at depth is quite clear on March 16 and 17, when the surface waters were moving onshore with the oil that washed onto Breton Island.

In summary, during the observation interval at the Dependable station, changes of current speed and direction below 10 feet are minimal. There is also a decided reduction in the tendency toward rotary flow in the lower layers.

Measurements (see appendix) from the C.G.C. Pt. Spencer in 40 feet of water on March 5 and 6 were made during the calmest period of the month; they clearly showed a clockwise rotating diurnal tidal current with minimum interference from wind currents. The current flowed initially south after high tide, turned westerly, and then flowed north about 13 hours after high tide. The average speed in the upper 10-foot layer was 1 knot; below this level the average speed was 0.5 knot. Directional turning of the lower layer lags slightly behind that of the upper layer.

Tidal Currents.--In order to isolate and examine the periodic tidal currents from the mixture of types comprising the observed current, harmonic analysis was carried out on the 5-foot level currents at the Dependable station March 16-19 and on the 5-, 15-, 25-, and 45-foot levels for March 18.

Harmonic analysis extracts the periodic components which can be accounted for by any set number of harmonics. The first two harmonics, namely the diurnal tidal current, with a period of 1 lunar day (24 hours, 50 minutes), and the semi-diurnal tidal current, with a period of 12 hours, 25 minutes, account for nearly 95 percent of the total periodic tidal current. As shown in Figure 10, we have used the first three harmonics in

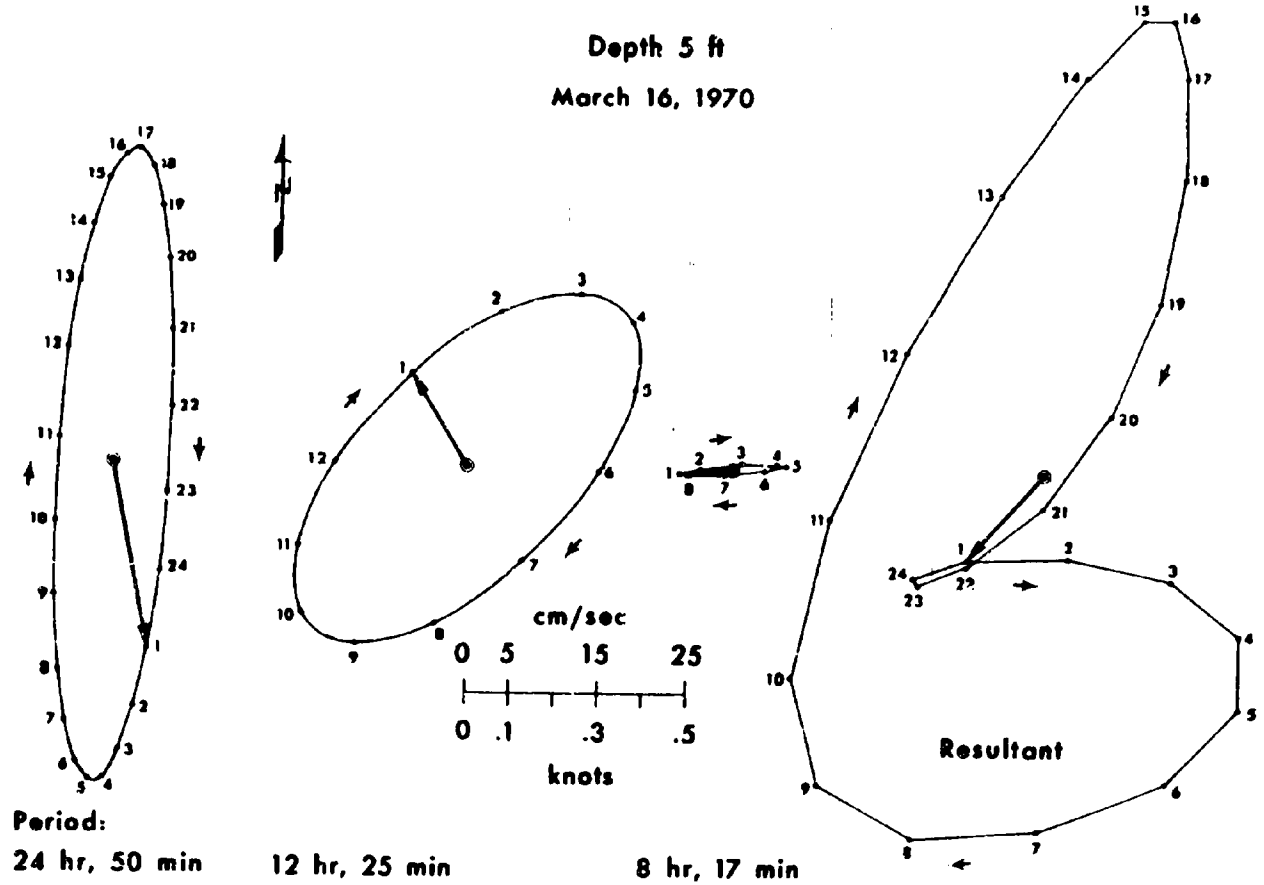


Figure 10. Tidal ellipses for first three harmonics and resultant tidal ellipse for 5-foot current.

our analysis. In this figure, which illustrates the method, the three diagrams to the left are the currents accounted for by the three harmonics individually--the irregular diagram on the right is the resultant current obtained by adding all the harmonics together. Such diagrams are called tidal ellipses; the current vector at any hour is given by an arrow drawn from the origin to the point labeled with that hour number. The length and direction of the arrow give the current speed and direction, respectively. On the graphs only the current vector at hour 1 is drawn. The smooth curve only serves as an envelope to connect the end points of the arrows. The semi-diurnal tide goes around its ellipse twice each day, etc. As the diurnal and semi-diurnal tide waves usually differ in magnitude, direction, and phase, the resultant tidal ellipse may be a rather complicated figure. As expected from our knowledge of the tides in the Gulf of Mexico, the diurnal tidal current is the most dominant. Because of the brevity of these records, it is not possible to assign an absolute time to the hourly notations on the tidal ellipses.

With the effects of steady currents removed, the tidal ellipses of Figure 11 show the day-to-day change in the tidal currents at the 5-foot level. The direction of rotation, as it should be in the northern hemisphere, is clockwise owing to Coriolis forces. There is an obvious decrease in the magnitude of the tidal current as time progresses because of the fact that we are nearly at equatorial tide on March 19 (the strength of the current is 1.0 knot on March 16 and only 0.6 knot on March 19). The orientation of the ellipse is generally in an onshore-offshore direction--the maximum currents, then, are onshore and offshore with the flood and

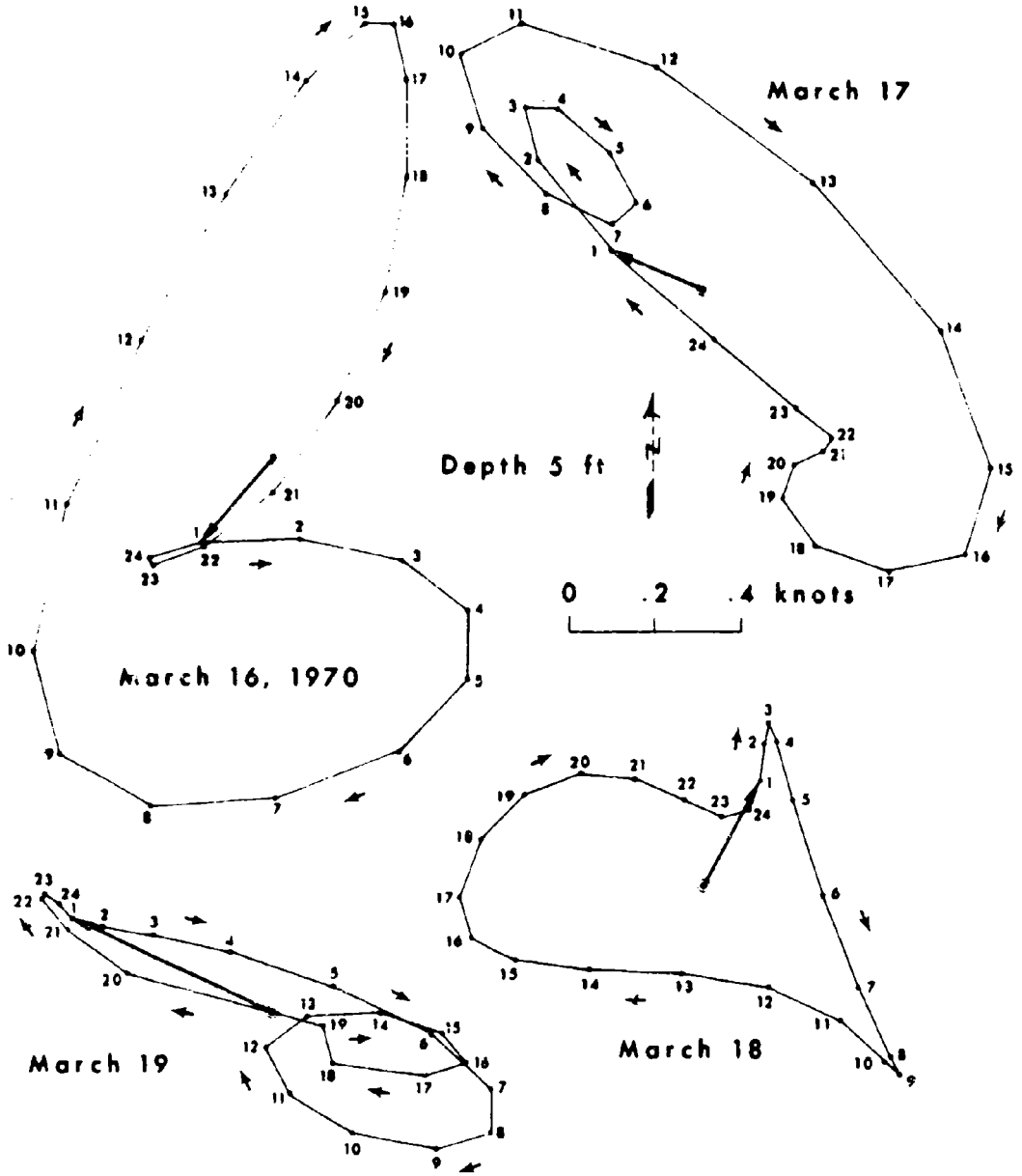


Figure 11. Resultant tidal ellipses for 4 days of current observations at Dependable station (5-foot depth).

ebb of the tide. This analysis has successfully removed a fairly typical tidal current from the rather confused data presented in Figure 6.

The changes in the tidal current ellipse as a function of depth are shown in Figure 12. Increasing frictional effects as the bottom is approached considerably distort the tidal current ellipse, resulting in occasional periods of counterclockwise rotation. Speeds are lower near the bottom and the higher speeds have a shorter duration.

It is apparent that oil purposely sunk into the bottom layers during equatorial tides would have the least aid from the tidal currents in dispersing.

Slicks

Figure 13, which is a plot of wind vectors against the slick vectors observed by helicopter visual surveillance, gives the distinct visual impression that there is a degree of correlation of wind direction and slick direction. A more detailed examination of the angle between simultaneous wind and current vectors is not possible owing to (1) uncertainties in the time of slick observations and (2) the fact that the only detailed wind data are restricted to the Dependable observations of March 15-20. It does seem clear from the figure, however, that after the wind has blown, say, a day from a given direction the slick aligns with the wind.

This relationship implies a good correlation between the movement of the upper foot of surface water and the wind. We have already shown that there is no clear relation between the current at the 5-foot level and the wind. Figure 14 shows the velocity profile predicted by Reid (1959) for a pure wind-drift current. There is a thin high-velocity

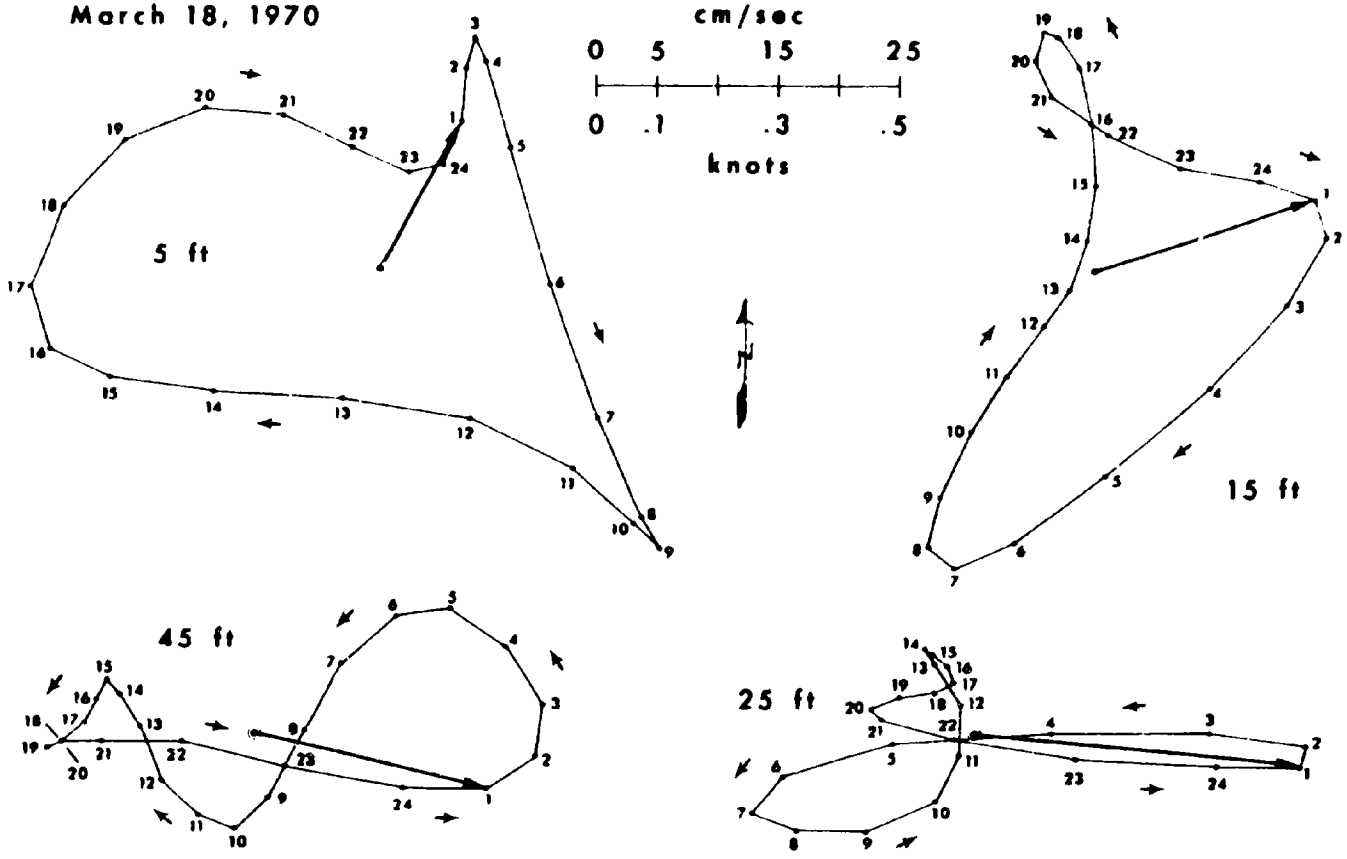


Figure 12. Resultant tidal ellipses at depths of 5, 15, 25, and 45 feet.

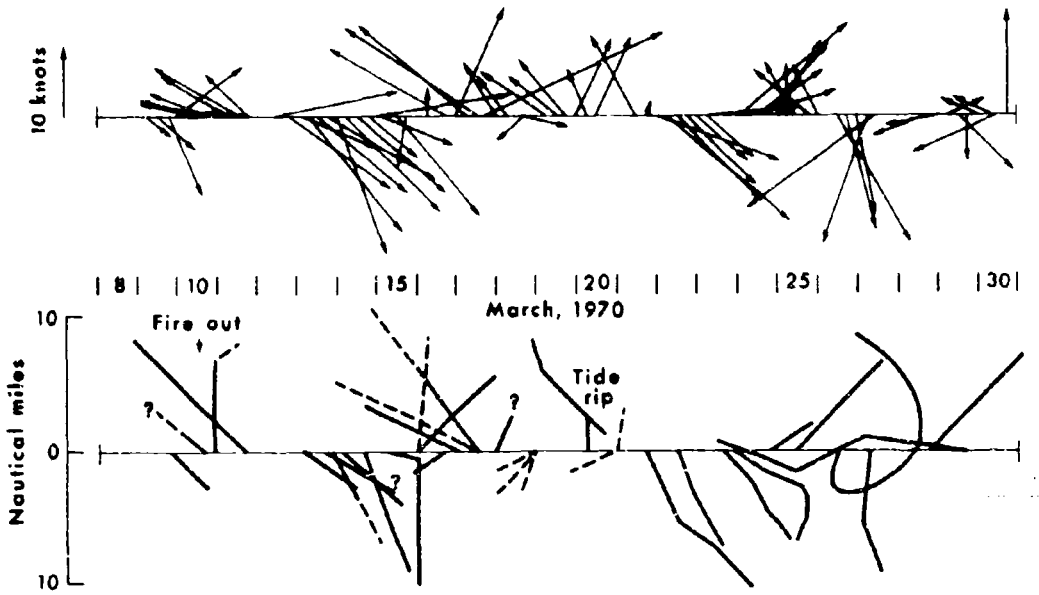


Figure 13. Wind vectors versus slick vectors.

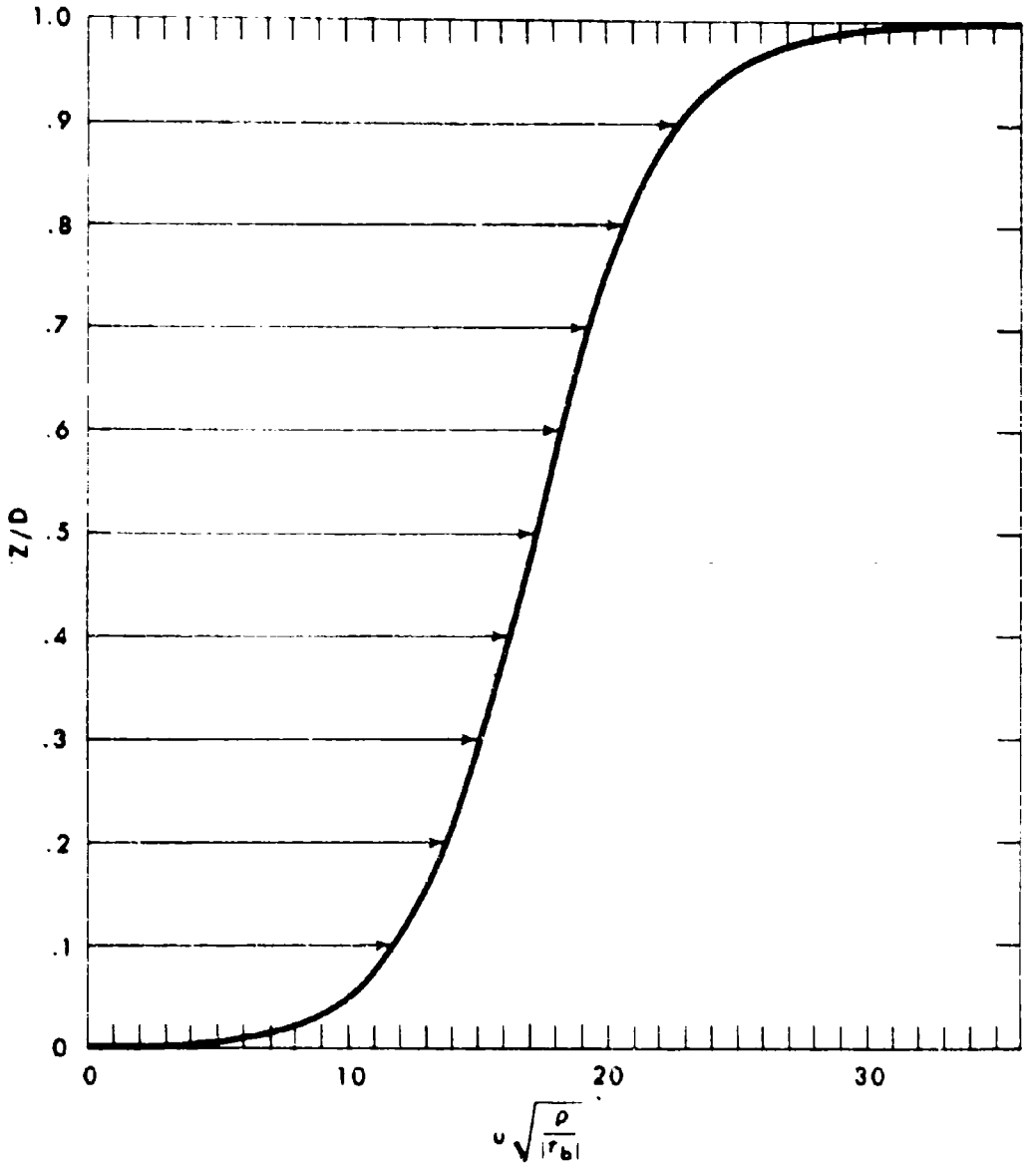


Figure 14. Non-dimensional vertical velocity profile for pure wind-drift current by Reid (1957). Z/D is relative depth, U is current speed, $\rho$ is fluid density, and $\tau_b$ is shear stress uniform throughout the fluid.

layer predicted near the surface; it is this type of situation which would allow the very-near-surface water to move with the wind while the underlying waters (say, at 5-foot depth) are only barely affected. Some other means of monitoring currents closer to the surface is necessary to clarify the problem.

At times of high winds with steady direction, oil did definitely move with the wind, as was discussed in the section on currents with respect to the strong winds of March 16-17, which pushed oil onto Breton Island. The U.S. Geological Survey photomosaics and color photographs of oil slicks which were provided to us showed five cases in which oil slicks extended with the wind (within 20 degrees), as indicated by plumes of spray from the fire boats hosing down the platform (Fig. 15). Two cases showed no clear indication of wind direction, and one showed a slick extending at about 90 degrees to the wind direction.

As mentioned previously, slick orientation often changed abruptly at interfacial lines. Slicks also changed strikingly in shape at interfacial lines, becoming narrow bands (Fig. 16) of thicker oil accumulation, with coalescing "rafts" or "mats" of oil up to 1 centimeter thick. This change in shape of the slick and the observed stranding of other floating objects along the interface suggest that the boundary is a locus of downwelling at which floating materials collect. The slicks seem literally to contract to lie along the interface as if "swept" into a linear accumulation. The narrow accumulations are also sometimes distorted in patterns suggestive of very large Kelvin-Helmholtz waves, which may form along the interface of fluids in motion relative to each other.

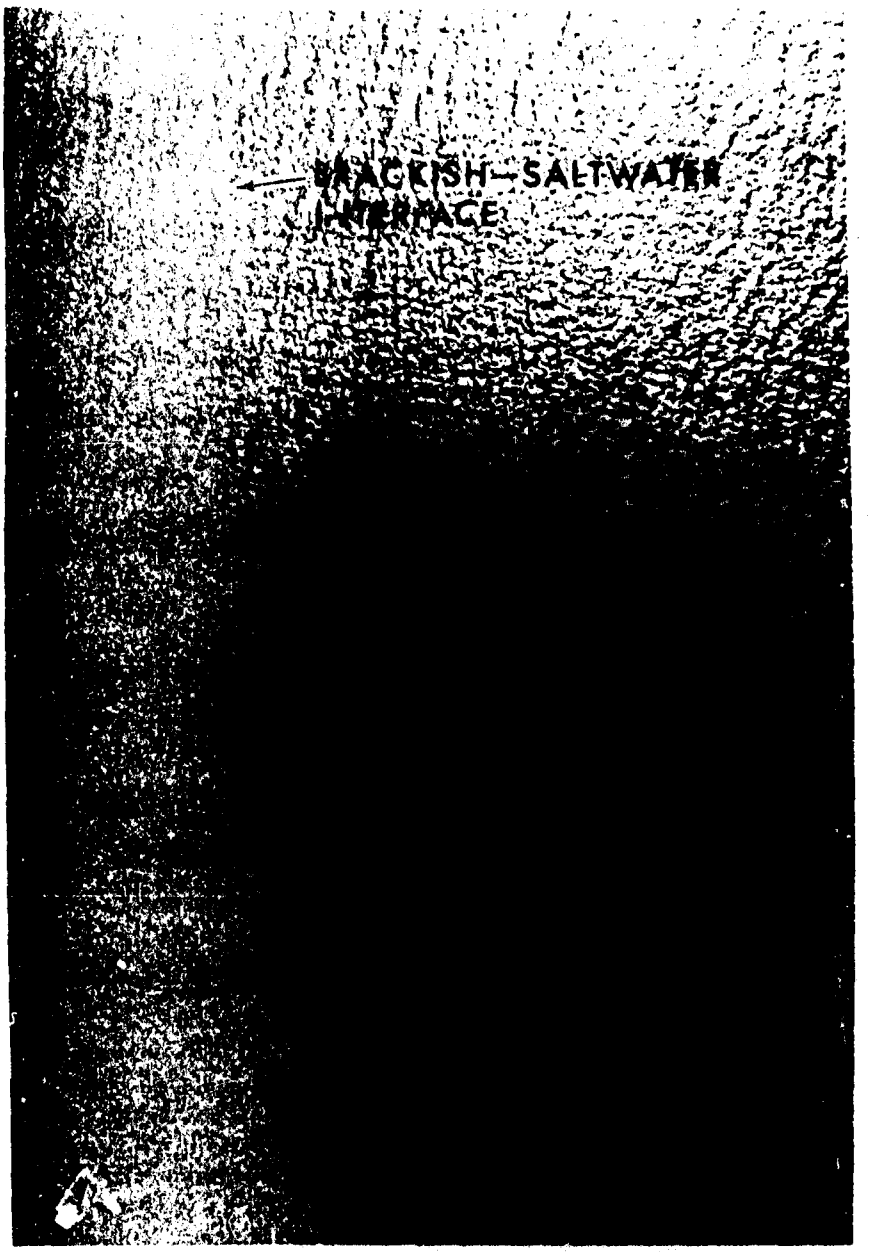


Figure 16. Narrow band of oil stranded along brackish water-saltwater interface. (Provided by U.S.G.S.)

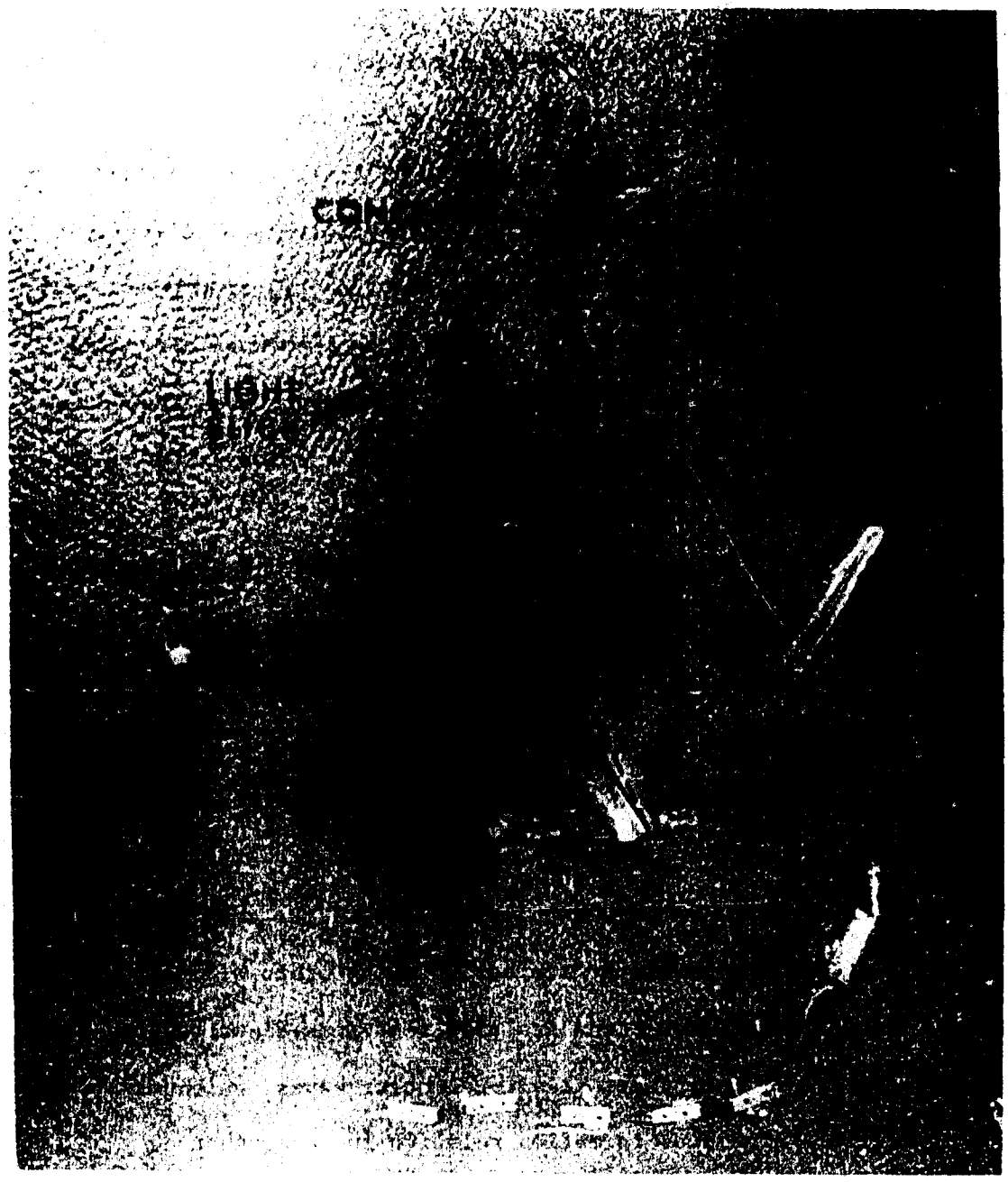

Figure 15. Photograph of slick, March 14, 1970. (Provided by U.S.G.S. Barge line was for trapping onshore-flowing oil. For direction and scale refer to Fig. 18.)

Where interfaces were not involved, slicks showed shapes that were straight or arcuate to varying degrees. The arcuate forms are indicative of currents, either tidal or wind generated, which rotated as the slick developed. Straight forms develop during periods of steady current direction.

The "mat" type of oil accumulation and the thin film slicks were the only types of floating oil noted. Some reports were heard at the time of thicker accumulations, but they were not substantiated by our observations.

The most useful images of oil slicks that were available for the study were those made by 8-14μ infrared scanning imagery. These showed the thin film as dark areas relative to the surrounding waters and the "rafts" of oil in thicker accumulations as bright areas. The same imagery showed excellent delineation of interfaces between different water masses as well. Sensitivity of this type of imagery at high altitude allowed sensing of the entire slick on a single image with adequate detail of size and shape. Future emergencies of this kind should be better documented by this type of sensing.

## THEORETICAL CONSIDERATIONS--SLICK PREDICTION

### Introduction

The mixing, dispersion, or diffusion of oil on the sea is undoubtedly a complicated process under field conditions because the process is largely controlled by changes in the weather and sea states. However, our understanding of the physical processes and ultimately of the spread of the oil can be greatly increased by application of the theory of turbulent diffusion. This approach has been successfully applied in the diffusion of atmospheric

pollutants and in studies of the spread of dye and other substances on lakes and on the sea.

Simple turbulent diffusion theory does not consider such effects as particle fallout, particle interaction, coagulation, or evaporation. Special terms may be added to the equations to account for these effects, however (see Yudine, 1959; McNown and Lin, 1952; and Sutton, 1953). Empirical determination of the diffusion coefficient K in the field during an oil spill should take these effects into account to some degree. The following development applies only to an oil slick dispersing in a laterally homogeneous water body. As shown in the previous section, horizontal density gradients and discontinuities will considerably distort the diffusion pattern.

Statistical Theory of Turbulence

In his pioneering paper of 1921 and again in a detailed treatise in 1935, G. I. Taylor developed the statistical theory of turbulence which laid the groundwork for most modern studies of diffusion problems in the atmosphere and ocean. By considering the one-dimensional spread of particles (or marked fluid parcels) from a continuous point source, Taylor developed the relation for the y direction

$$\sigma_y^2 = 2\,\overline{v'^2} \int_0^T \int_0^t R_y(\xi)\, d\xi dt \qquad (1)$$

where $\sigma_y^2$ is the variance of the fluid parcels around the source, $\overline{v'^2}$ is the square of the turbulence intensity, assumed to be constant over a period of several hours, $v' = v - \bar{v}$ as usual, $\xi$ and $t$ are time parameters, and

$R(\xi)$ is the Lagrangian autocorrelation function. For a detailed derivation of (1) see Haltiner and Martin (1959, p. 156). The Lagrangian autocorrelation function measures the relationship between the velocity of a parcel at one instant and the velocity of the same parcel at some subsequent instant.

$$R_y(\xi) = \frac{\overline{v'(t)\, v'(t-\xi)}}{\overline{v'^2}} \quad . \tag{2}$$

Hence for very short time lags $v'(t) \approx v'(t-\xi)$ and $R_y(\xi) \approx 1$. For long time lags there will be on the average no relation between $v'(t)$ and $v'(t-\xi)$; so $R_y(\xi) \approx 0$. Similar expressions for $R_x(\xi)$ and $R_z(\xi)$ extend the Taylor analysis to three dimensions.

After considering very short times, performing the double integration, and then taking the first derivative with respect to time of $\sigma_y$, equation (1) reduces to

$$\frac{d\sigma_y}{dt} = (\overline{v'^2})^{1/2} \quad . \tag{3}$$

In the case of long diffusion times $\int_0^t R_y(\xi)\, d\xi = t_y^*$ a constant, and equation (1) reduces to

$$\frac{d\sigma_y^2}{dt}\Big]_\infty = 2\, \overline{v'^2}\, t_y^* . \tag{4}$$

The subscript $\infty$ refers to the ultimate constant value this quantity will attain. If a uniform horizontal mean flow is passing the source moving in the positive x direction at a speed U assumed constant over a period of several hours, the relation $T = x/U$ can be used to transform the spread of

the material into the x-y plane; so (3) becomes (for short diffusion times)

$$\frac{d\sigma_y}{dx} = \frac{(\overline{v'^2})^{1/2}}{U} \tag{5}$$

and (4) becomes (for long diffusion times)

$$\left.\frac{d\sigma_y^2}{dx}\right]_\infty = \frac{2\,\overline{v'^2}\,\ell_y^*}{U^2} \tag{6}$$

where $\ell_y^*$ the Lagrangian eddy size = $U\,t_y^*$. Thus $\frac{d\sigma}{dx}$ for short times and $\frac{d\sigma^2}{dx}$ for long times are both constants. Figure 17 illustrates the three ensuing diffusion regimes: (a) the linear or short-term regime, where $\sigma_y \propto x$, (b) the long-term regime, where $\sigma_y \propto x^{1/2}$, and (c) the intermediate or transitional regime, where $\sigma_y \propto x^n$, $1/2 < n < 1$. For the purposes of the illustration the area occupied by the dispersing material can be outlined by assuming that the radius to the visible edge of the slick ($y = R$) can be identified initially with some constant multiple of the root-mean-square displacement $\sigma_y$. It will also be assumed that the visible radius corresponds to an equal concentration C contour. Pritchard (1966) has expressed objection to this assumption in dye studies of diffusion processes, but because of the technical difficulty of obtaining cross slick measurements of the concentration C the assumption is at present unavoidable. An expanding slick should, then, initially exhibit a linear growth of its radius, followed ultimately by a slow parabolic expansion. We can logically apply the one-dimensional Taylor equations to an expanding oil slick because (a) oil is generally constrained by buoyancy forces to the surface (no

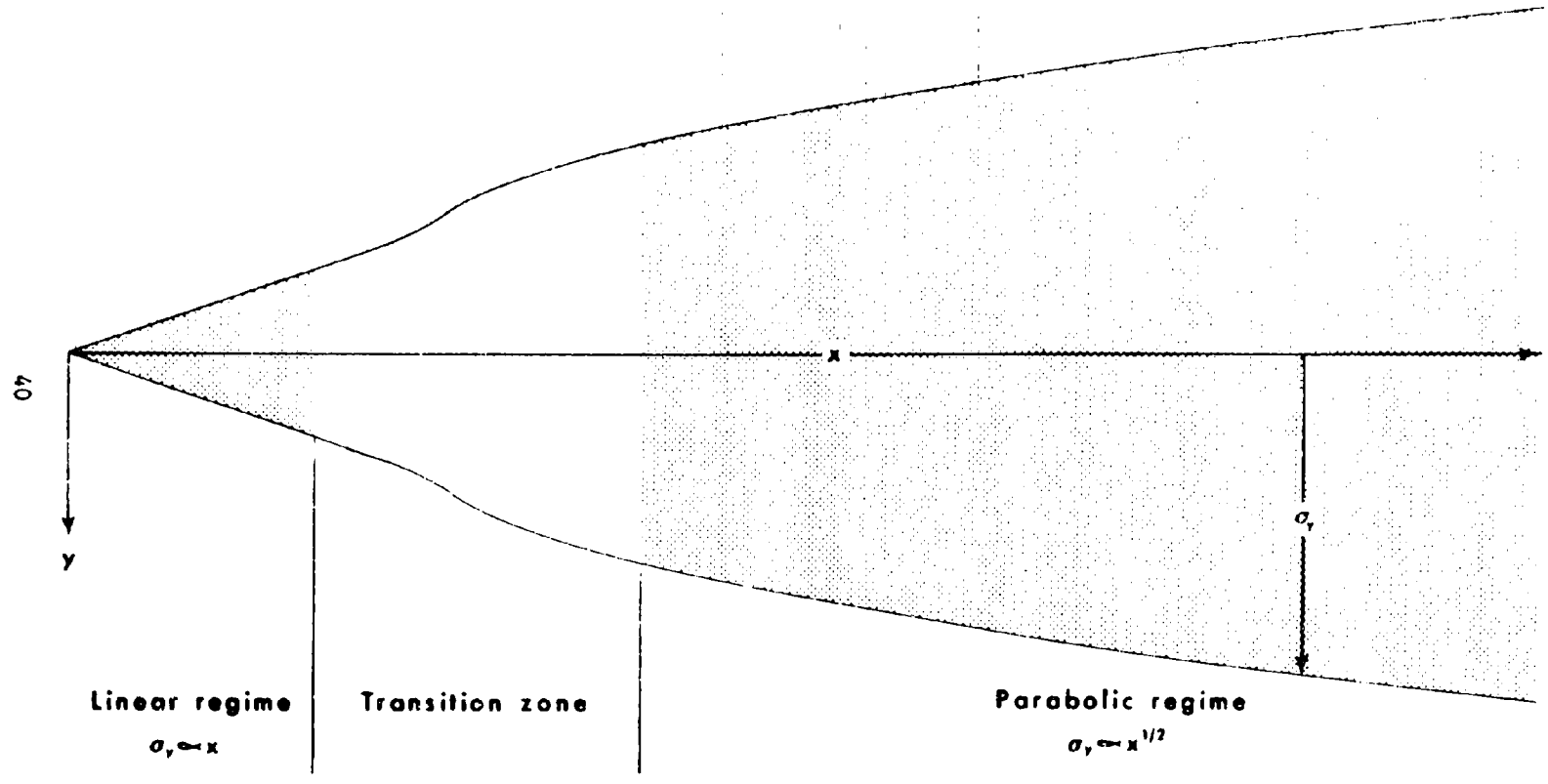


Figure 17. Linear, transitional, and parabolic diffusion regimes predicted by Taylor theory.

mixing in the vertical direction) and (b) the longitudinal diffusion of the oil particles in the direction of the mean horizontal velocity is negligible compared to the displacements in this direction by the mean current itself.

Taylor has further demonstrated that the diffusion coefficient $K_y$ can be expressed as

$$K_y = 1/2 \left[\frac{d\sigma_y^2}{dt}\right]_{\infty} = \frac{U}{2}\left[\frac{d\sigma_y^2}{dx}\right]_{\infty} \tag{7}$$

or, substituting (6),

$$K_y = \frac{\overline{v'^2}\, \ell_y^*}{U} . \tag{8}$$

Inspection of our own color and infrared color photographs, together with photographs and infrared imagery supplied to us by the U.S. Geological Survey and Remote Sensing Inc. of Houston, clearly and repeatedly shows the presence of the linear regime near the spilling well, 41C. This is exceptionally well shown in Figure 18. If we assume first that $\sigma_y = \alpha R$ (the root-mean-square displacement is directly proportional to the visible radius R) and as a first approximation that the proportionality constant $\alpha$ is near unity ($\sigma_y \simeq R$), we can use the photographs and imagery to obtain estimates of the relative turbulence intensity of the oil from (5) and the diffusion coefficient of the oil from (7).

Table 1 lists the source and values for the relative turbulence intensity $(\overline{v'^2})^{1/2}/U$ of the oil, measured as the tangent of one-half the angle of expansion $2\theta$ of the oil slick from the well.

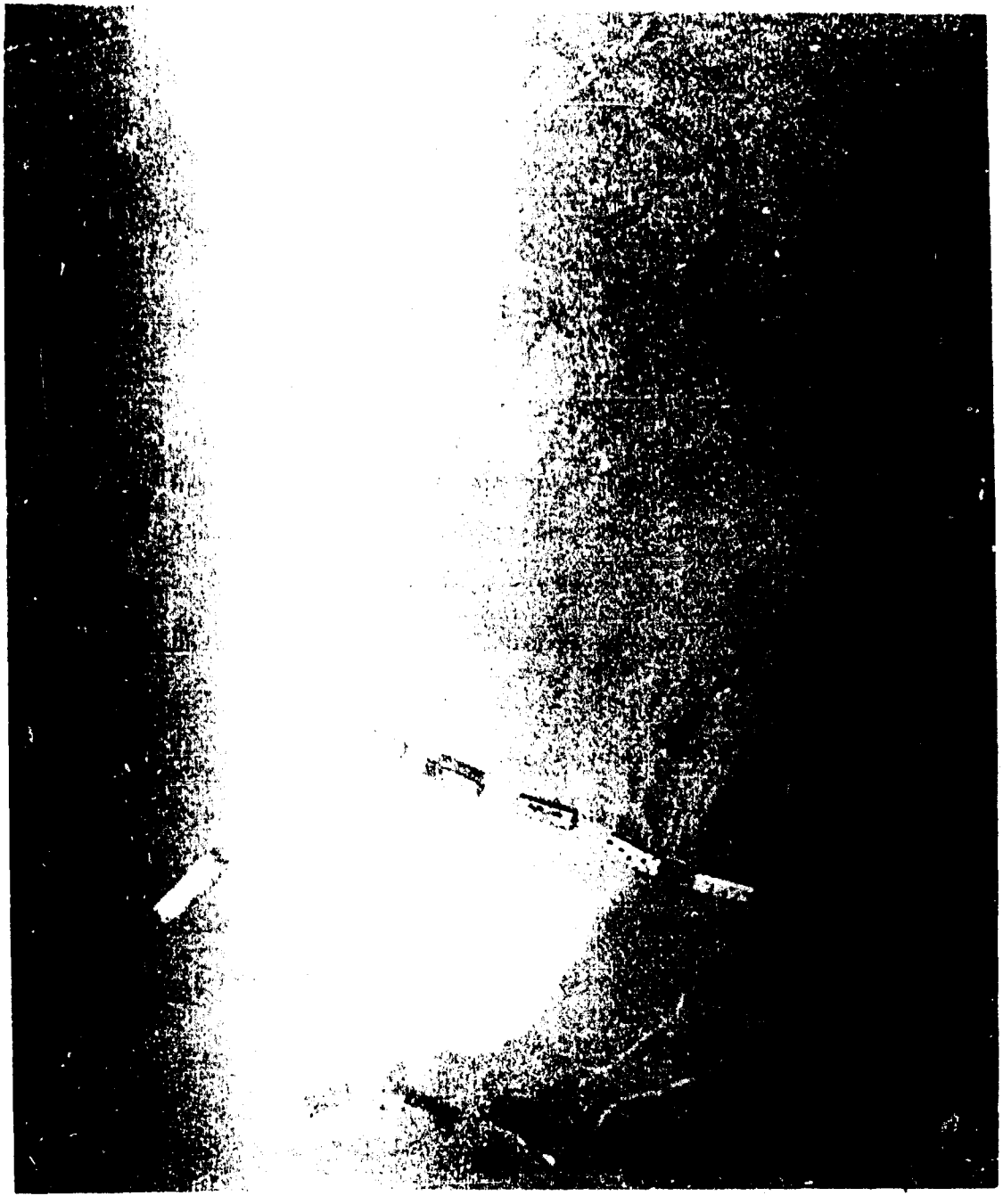

**Figure 18.** Photograph of slick illustrating initial linear expansion regime. (Provided by U.S. Long arm of barge line is about 1,920 feet.)

Table 1

Intensity of Turbulence Indicated by Oil

| Source | $\tan \theta = \overline{(v'^2)}^{1/2}/U$ |
|---|---|
| U.S.G.S. Infrared Color, undated | 0.41 |
| U.S.G.S. Color #0074, 3/14 | 0.25 |
| U.S.G.S. Color #0003, 3/16 | 0.33 |
| U.S.G.S. Color #0071, 3/14 | 0.28 |
| U.S.G.S. B & W Mosaic, 3/22 | 0.22 |
| U.S.G.S. B & W Mosaic, 3/13 | 0.22 |
| Remote Sensing Inc., 3/14 | 0.22 |
| Remote Sensing Inc., 3/11 | 0.10 |
| Average | 0.25 |

These results are encouraging, as it is well known (see, e.g., Kalinske and Pien, 1944; and Bowden, 1962) that the relative turbulence intensity in channel flow is in the range of 0.05 to 0.15. The effect of wave motions on the oil, especially breaking action, could certainly increase this value up to the observed average 0.25. Although the data points are few, a plot of tan $\theta$ against wind speed in Figure 2 does seem to indicate a higher relative turbulence intensity of oil at higher wind speeds (stronger wave action).

Unfortunately, there is only one set of imagery which shows a slick with sufficient length and contrast to permit the measurements of the parabolic regime and so the determination of a value for the diffusion coefficient $K_y$. This is the Remote Sensing Inc. infrared imagery (8-14

scanner) of March 11, 1230 hours CST. The plot of $\sigma_y^2$ against x is shown in Figure 19. As predicted by (6), the linear relationship is strong; the regression coefficient = 0.97. With $d\sigma_y^2/dx]_\infty$ now known, use of (7) leads to an estimate of the diffusion coefficient of oil K of $4 \times 10^5$ $cm^2/sec$ at that time. Since Figure 7 shows that wind speed and wave height were moderate on March 11, $4 \times 10^5$ $cm^2/sec$ is probably a low rather than a high estimate. Comparison with the few published measurements of horizontal eddy viscosity (the diffusion coefficient for momentum) is encouraging. Sverdrup, Johnson, and Fleming (1942) report values (p. 485) ranging from $2 \times 10^6$ $cm^2/sec$ in a small area with weak currents to $4 \times 10^8$ $cm^2/sec$ in strong currents. It is now generally understood that the diffusion coefficient is a function of the scale of the phenomena under investigation. As Orlob (1959) clearly points out, the boundary of the field (basin), among other parameters, will restrict the maximum eddy size $\ell_y^*$ that may develop; and since $K_y$ is related to $\ell_y^*$ by two other constants $K_y = (\overline{v'^2}\ \ell_y^*)/U$ (8), the diffusion coefficient in a bounded area should likewise approach a constant value.

It should be pointed out that the y coordinate of $\sigma_y$ as one moves in the positive direction (downslick) does not necessarily follow an equal concentration contour. The evidence in Figure 19 does, however, seem to indicate that this is approximately the case for some distance downslick, until the concentration level at a distance $\sigma_y$ from the average slick center line $C(y = \sigma_y)$ falls below the concentration level which is assumed to serve as a visible limit. In Figure 19 the discontinuity in the $\sigma_y^2$ versus x plot at $x \approx 30{,}000$ feet is interpreted as that point where first

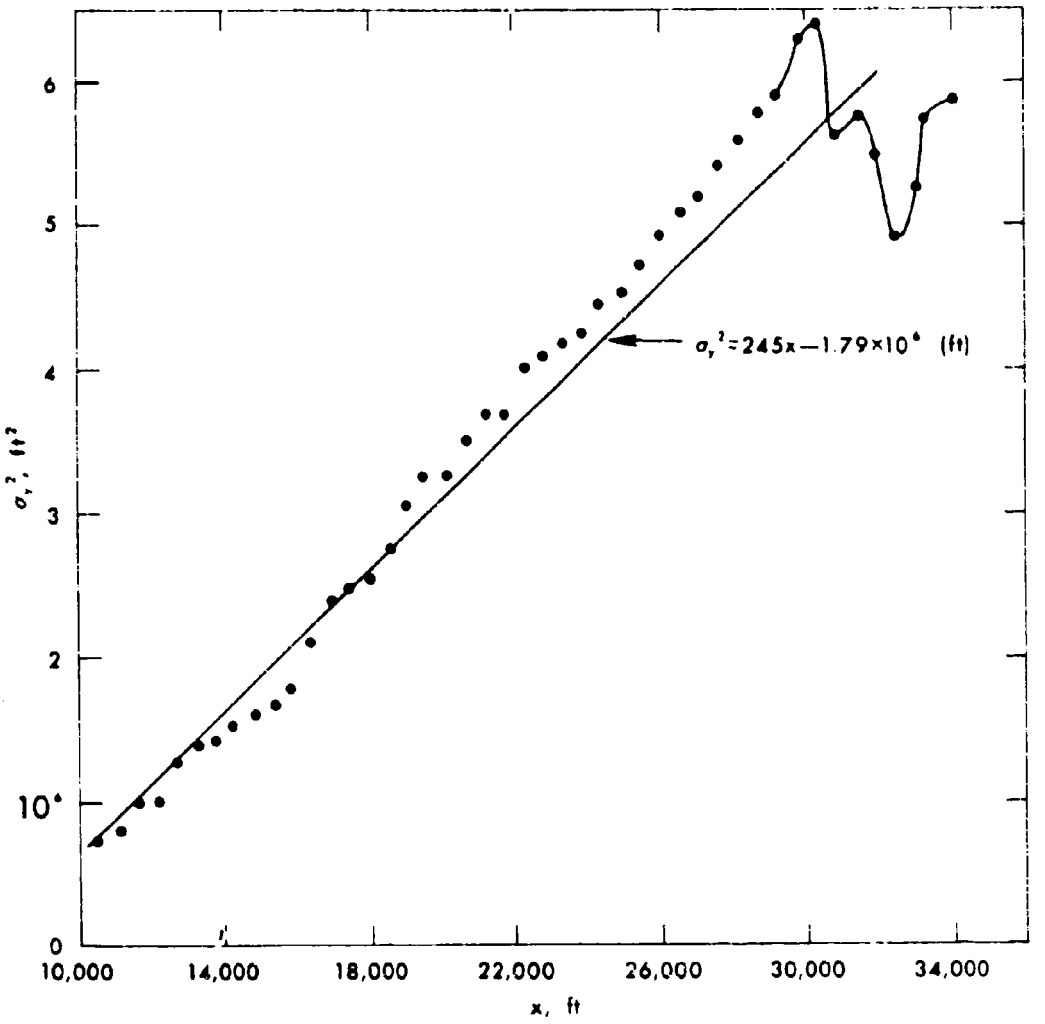


Figure 19. Plot of slick width variance ($\sigma^2$) against distance from source (x), illustrating linear relation that determines the diffusion coefficient.

$C(y = \sigma_y) < C(y = R)$.

Despite its power and apparent applicability to oil slicks, the Taylor theory cannot predict concentration contours or slick boundaries. For this we must turn to the classical diffusion equations.

General Diffusion Equations and Slick Prediction

Again regarding the spread of oil as a two-dimensional process in the x-y plane, with a near horizontal motion U in the postive x direction, the diffusion equation is

$$\frac{\partial C}{\partial t} + U \frac{\partial C}{\partial x} = \frac{\partial}{\partial x}\left(K_x \frac{\partial C}{\partial x}\right) + \frac{\partial}{\partial y}\left(K_y \frac{\partial C}{\partial y}\right) . \tag{9}$$

If the slick has come to steady state $\frac{\partial C}{\partial t} = 0$, and assuming (1) that the diffusion in bitropic $K_x = K_y = K$ and (2) that K has reached its constant value, (9) becomes

$$U \frac{\partial C}{\partial x} = K\left(\frac{\partial^2 C}{\partial x^2} + \frac{\partial^2 C}{\partial y^2}\right) . \tag{10}$$

For a derivation of the complete diffusion equation see Haltiner and Martin (1959, p. 265). The exact solution of (10) for a two-dimensional point source (infinite line source) in an infinite fluid is

$$C = \frac{Q\, e^{U\,x/2K}}{2\pi K} K_o\left(\frac{U\,r}{2K}\right) \tag{11}$$

where Q is the rate of emission of the source (g/sec), $K_o(\lambda)$ is, using standard notation, the modified Bessel function of 2nd Kind and Zero Order, and $r = (x^2 + y^2)^{1/2}$. For very reasonable values of U and K the first term

of the asymptotic expansion for $K_o(\lambda)$ (Abramowitz and Stegun, 1965, eq. 9.7.2; Roberts, 1923, p. 644) can be substituted in (11), yielding

$$C = \frac{Q\, e^{Ux/2K}}{2\pi K} \left( \frac{\pi}{Ur/K} \right)^{1/2} e^{-\frac{Ur}{2K}} . \qquad (12)$$

Therefore

$$C = \frac{Q\, e^{-\frac{Ur}{2K}(1 - \cos \phi)}}{2\,(\pi K\, U\, r)^{1/2}} \qquad (13)$$

where $\phi$ is measured in a clockwise direction from the positive x axis. Equation (13), then, is the expression we are seeking; it gives the distribution of the emitted oil as a function of distance and direction (r, $\phi$) from the source, the rate of emission at the source Q, the ambient current speed U, and the oil diffusion coefficient K. The value of Q (personal communication, Commander Dixon, U.S.C.G.) during the Chevron incident is taken as 1000 bbl/day = 1241 g/sec.

Furthermore, following Roberts (1923) it can easily be shown that the maximum half-width of a given concentration contour is

$$y_{max} = \frac{Q}{(2\pi e)^{1/2} UC} \qquad (14)$$

and by setting $\phi = 0$ in (13) the maximum extension downslick of a given concentration contour is

$$x_{max} = \frac{Q^2}{4\pi KUC^2} . \qquad (15)$$

It is not difficult conceptually to relate the oil concentration C in $g/cm^2$ to the slick thickness. There may, in fact, be a direct relationship

if the hydrostatic equation $p = \rho gh$ is used. If C is identified with p (as they have the same dimensions), then the slick thickness h is directly proportional to C.

$$h = \frac{C}{\rho g} . \tag{16}$$

This idea, however, needs much closer examination.

One difficulty in using (13) to predict slick boundaries is that it predicts small but finite oil concentrations at infinitely great distances from the emitting source. In meteorology it is routine (Sutton, 1953) to take 10 percent of the maximum concentration as a visible boundary contour. Unfortunately, $C \to \infty$ at the origin in (13); so we must take some concentration close to the origin as a control level. Inspection of the solution of (13) along the center line of the slick ($\phi = 0$) for $K = 4 \times 10^5$ cm$^2$/sec, $Q = 1241$ g/sec, and $U = 50$ cm/sec (1 knot) shows that the presence of the source at $r = 0$ is just beginning to affect the solution adversely in the vicinity of $r = 100$ meters. The control concentration for the Remote Sensing Inc. (RSI) slick of March 11, with $K = 4 \times 10^5$ cm$^2$/sec, $Q = 1241$ g/sec, and $U = 50$ cm/sec, is, using (13), $0.7828 \times 10^{-3}$ g/cm$^2$. The slick boundary $C_{y=R}$, then, is taken as $0.7828 \times 10^{-4}$ g/cm$^2$. If this latter value for the concentration at the boundary is used, (14) predicts one-half the slick width and (15) predicts the slick length. The predicted maximum width of the RSI March 11 slick is 1,534 meters, the observed maximum width is 1,507 meters; the corresponding predicted length is 9,995 meters, while the observed length is 14,710 meters. The slick width is predicted more accurately than the length, but the results indicate the basic soundness of our approach. Furthermore, the average of 23 observations on slick

length made by Coast Guard helicopter visual surveillance teams, reported in the Situation Reports and displayed in Figure 13, comes out to 12,600 meters, compared to our prediction of 9,995 meters.

An exact expression for the area of a slick is not easily obtained from the basic equations; so we have resorted to an elliptical approximation

$$A = \pi ab \tag{17}$$

where a the semi-major axis is one-half the slick length given by (15) and b the semi-minor axis is the half width given by (14). Therefore

$$A \approx \frac{Q^3}{8\sqrt{2\pi e}\, K\, U^2\, C_{y=R}^{\ 3}} \,. \tag{18}$$

Inspection of (14) shows that the slick width will increase directly with Q and decrease directly as U increases. It is noteworthy that (14) predicts that the slick width is independent of K. The slick length is more strongly dependent on Q, increasing as $Q^2$ and decreasing directly as U or K increases. The area given by (18) increases as $Q^3$ and decreases as $U^2$ and the first power of K.

The effect of varying U, with Q and K held constant, is shown in Figure 20. Low values of U produce a long, large slick; values of U approximately equal to those observed in the field during the Chevron incident (0.6-0.8 knot) produce relatively short and slender slicks much like those repeatedly observed in photographs and visually. The estimated time t required to reach a steady state is also shown in Figure 20. This is crudely approximated as the time required for oil to travel with the current out to

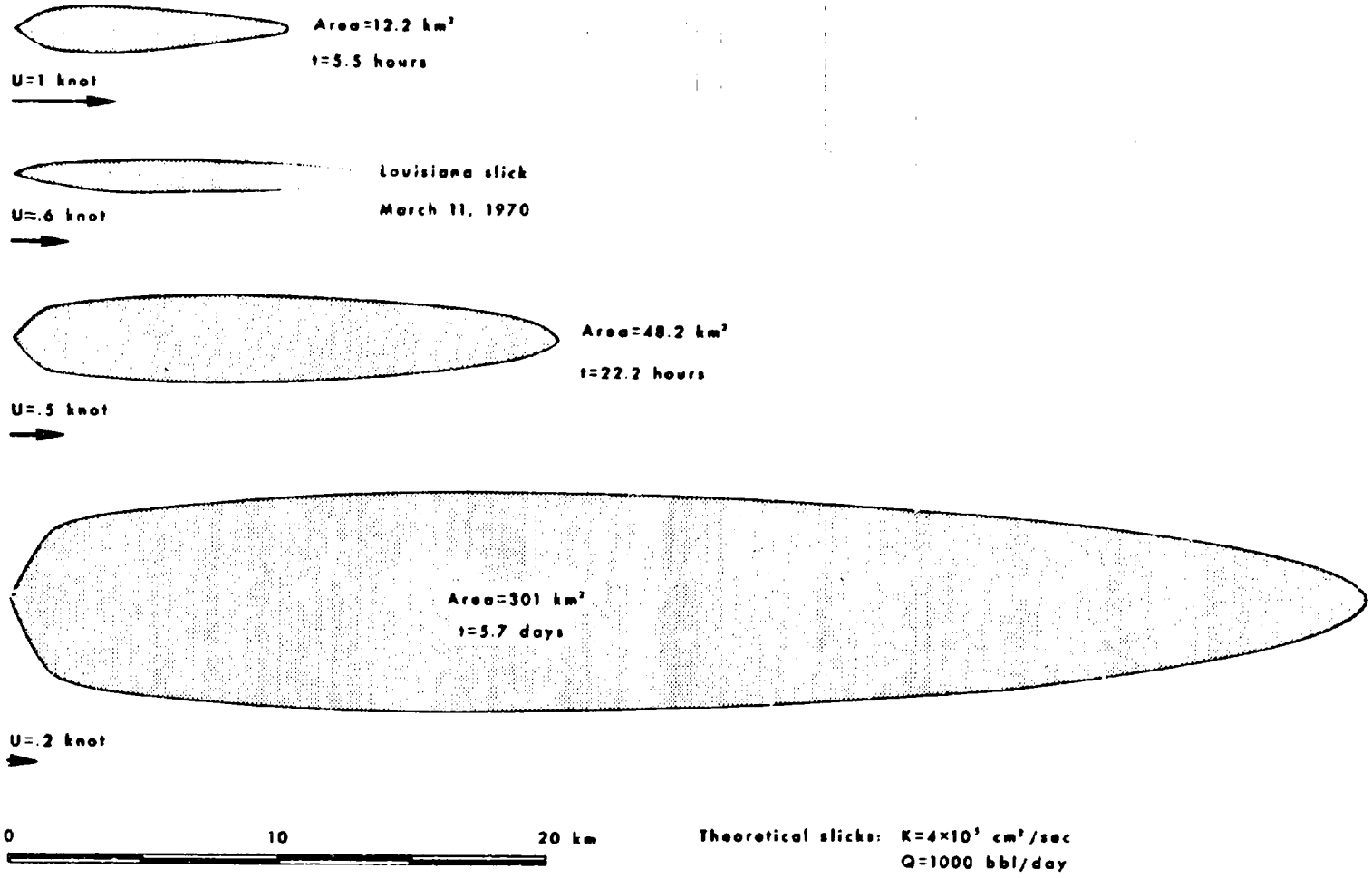




Figure 20. Comparison of observed slick against theoretical slicks, illustrating effect of decreasing current velocity on slick size.

the outermost slick boundary. A numerical solution of the time dependent differential equation should produce a considerably more accurate estimate.

The shape factor SF of the slick, defined as the ratio of slick width to slick length, is, combining (14) and (15),

$$SF = \frac{4\ (2\pi)^{1/2}\ K\ C_{y=R}}{Q\ e^{1/2}} \quad .$$

It is noteworthy that the relative shape of the slick is independent of the current speed, being controlled solely by (K/Q) for a given boundary concentration. Low values of (K/Q) produce elongate slicks; high values of (K/Q) produce more circular slicks. For the Chevron incident, using $K = 4 \times 10^5$ cm$^2$/sec, $C_{y=R} = .78 \times 10^{-4}$ g/cm$^2$, and Q = 1241 g/sec, the predicted value of the shape factor SF = 0.15. Table 2 lists the shape factors determined from slick geometries reconstructed from U.S. Coast Guard helicopter visual surveillance Situation Reports. Unfortunately, only data from the last week of the incident were of sufficient detail to be of use in this regard.

Table 2

Shape Factors During Chevron Incident

| Date | Time | Shape Factor |
|---|---|---|
| 3/26 | 0011 Z | 0.50 |
| 3/26 | 1756 Z | 0.19 |
| 3/29 | 0140 Z | 0.22 |
| 3/29 | 1905 Z | 0.07 |
| 3/30 | 1521 Z | 0.17 |
| 3/30 | 1940 Z | 0.16 |
| 3/31 | 2030 Z | 0.32 |
| Average | | 0.23 |

The approximate agreement of the average SF with the predicted value of 0.15 suggests that the value of K on the average should be closer to $6 \times 10^5$ than to $4 \times 10^5$ $cm^2/sec$ for the last week of March.

Figures 21 through 27 present in more detail and in graphic form most of the results we have discussed up to now. Figures 21, 22, 23, and 24 show slick area as a function of Q, K, and U, whereas Figures 25, 26, and 27 show slick width and slick length as functions of these same three variables. In further studies along these lines an effort should be made to incorporate these parameters into a single nondimensional diagram or nomogram.

Although this two-dimensional diffusion approach seems to present a good approximation of gross slick geometries, it is really based on the concentration value at the slick boundary, for which we made only a rough estimate (10 percent of C at $r = 100$ m, $\phi = 0$). In future work this point must be examined in much greater detail.

## SUMMARY

Observations prior to and during the long period of continuous oil spillage from a Chevron production platform near the Mississippi Delta permit certain generalizations to be made about movement of oil in coastal shallow water bodies. An understanding of the situation seemed to require information on currents, winds, tides, waves, and orientations and shapes of spreading oil masses. Salinity and temperature structure of the surrounding waters seemed useful for indicating the riverine and marine influences expected in the delta. Information was gathered on all of these in the hope that understanding could be gained of the principal agents which control rates and direction of motion of oil on water.

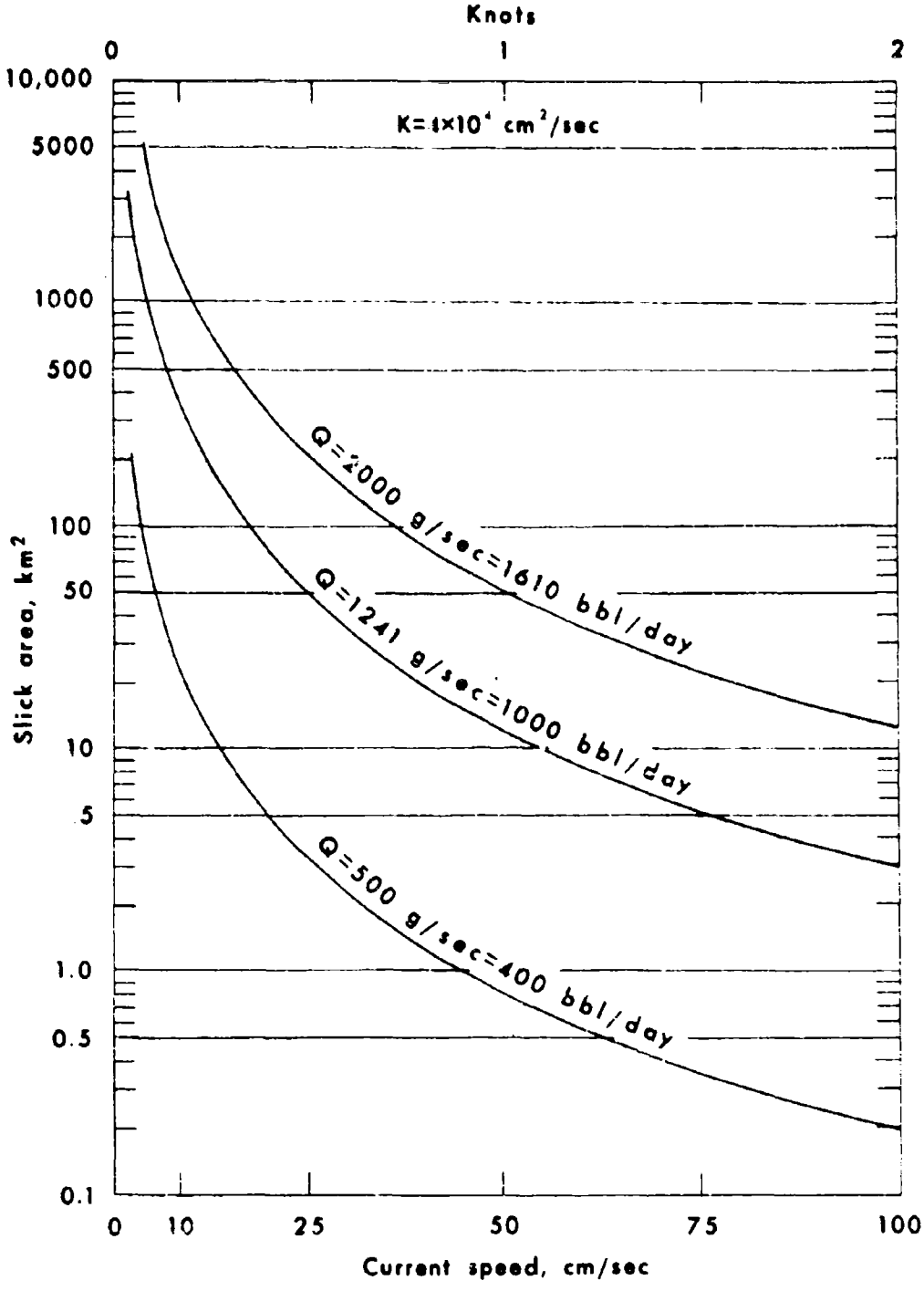


Figure 21. Slick area (A) as a function of current speed (U) for various rates of oil discharge (Q).

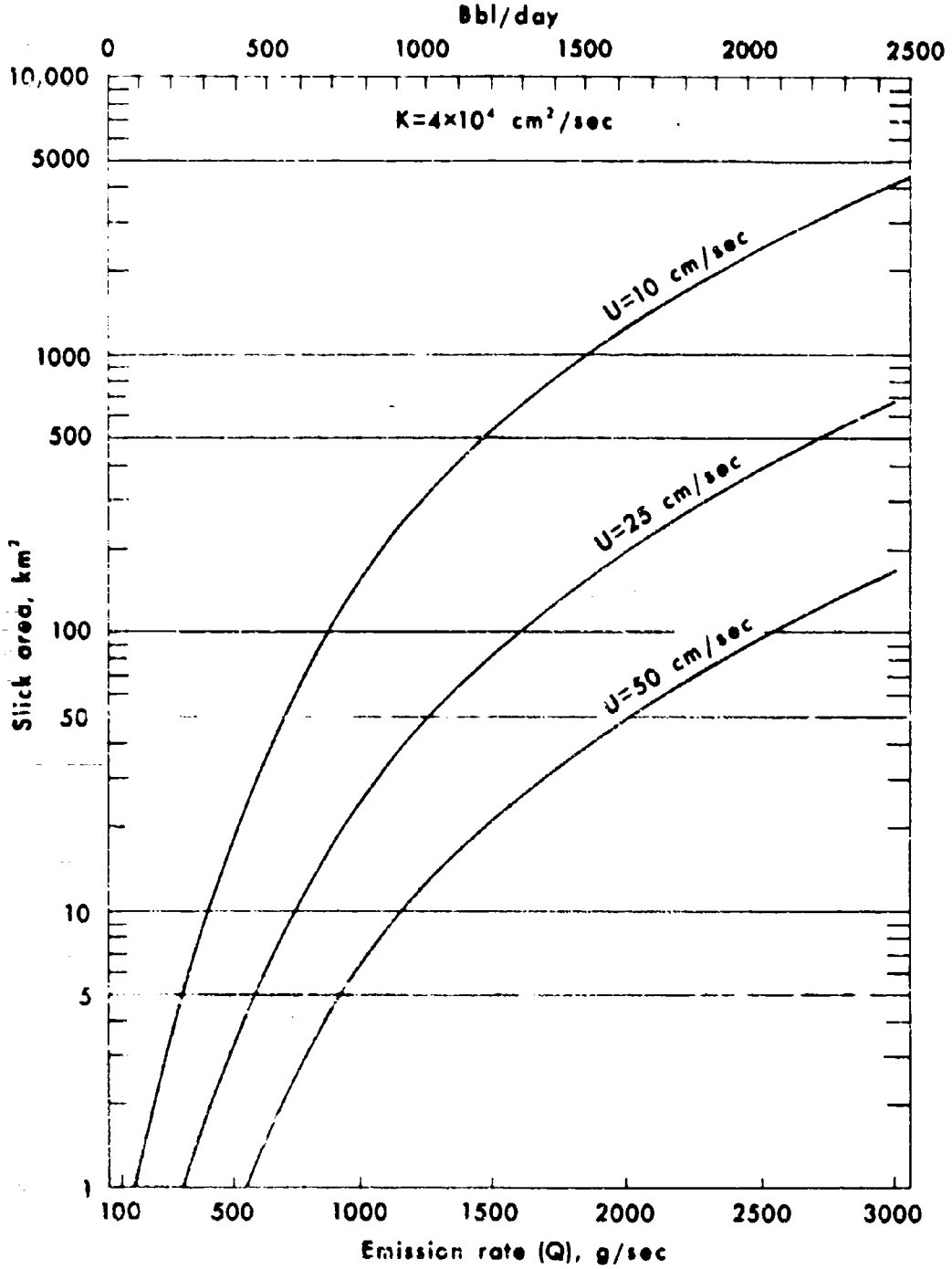


Figure 22. Slick area (A) as a function of oil discharge (Q) for various values of current speed (U).

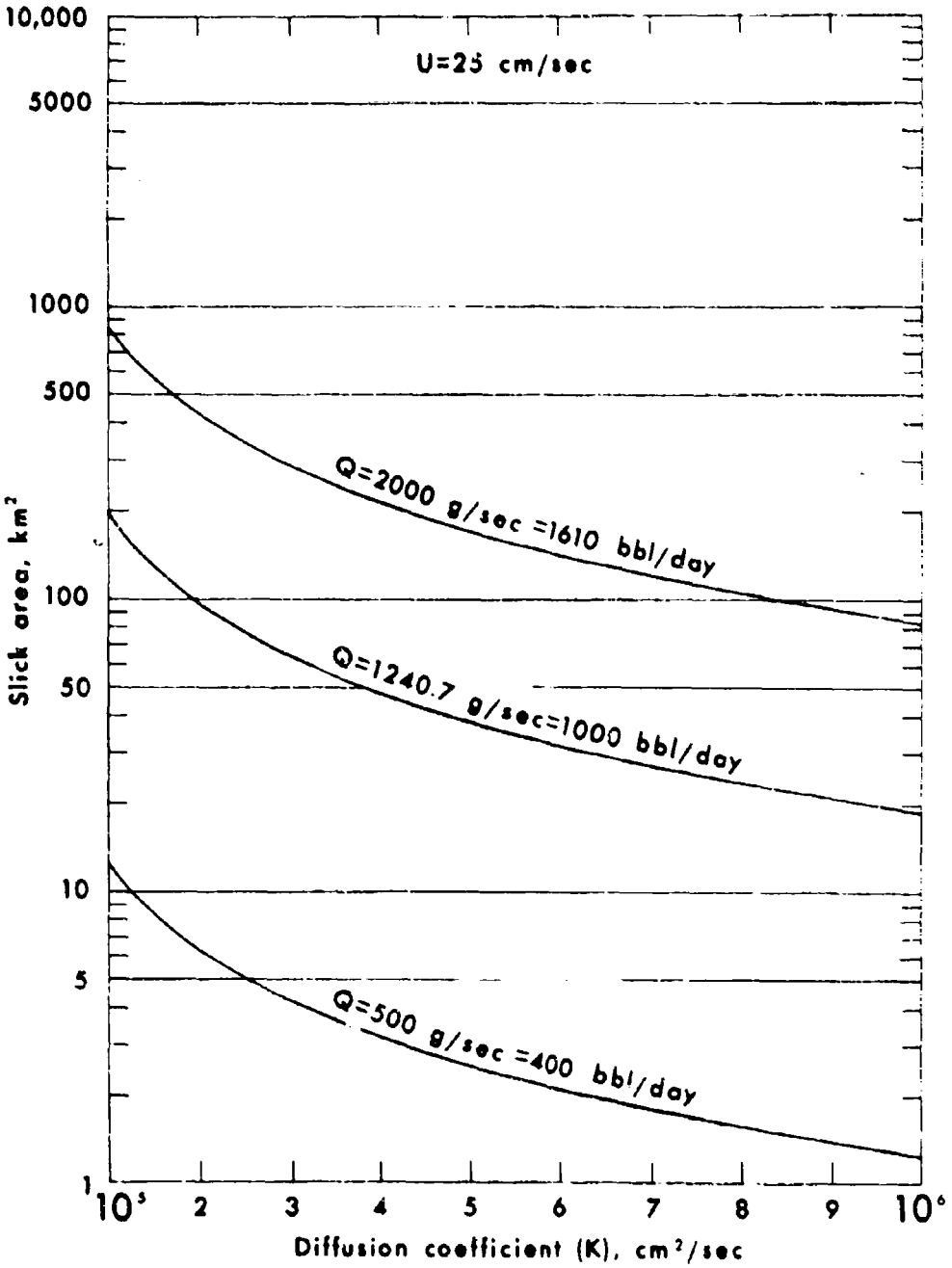


Figure 23. Slick area (A) as a function of diffusion coefficient (K) for various values of discharge (Q).

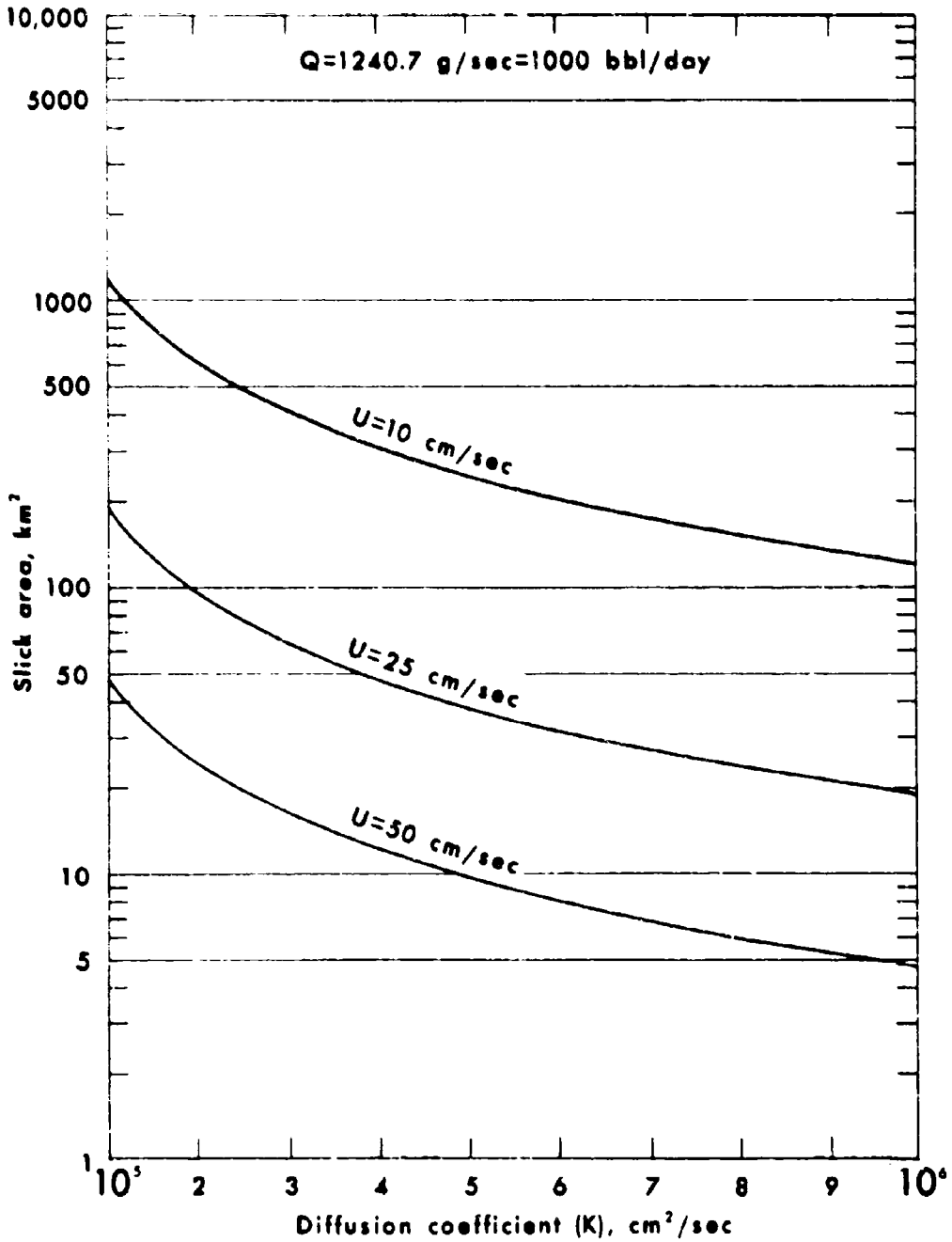


Figure 24. Slick area (A) as a function of diffusion coefficient (K) for various values of current speed (U).

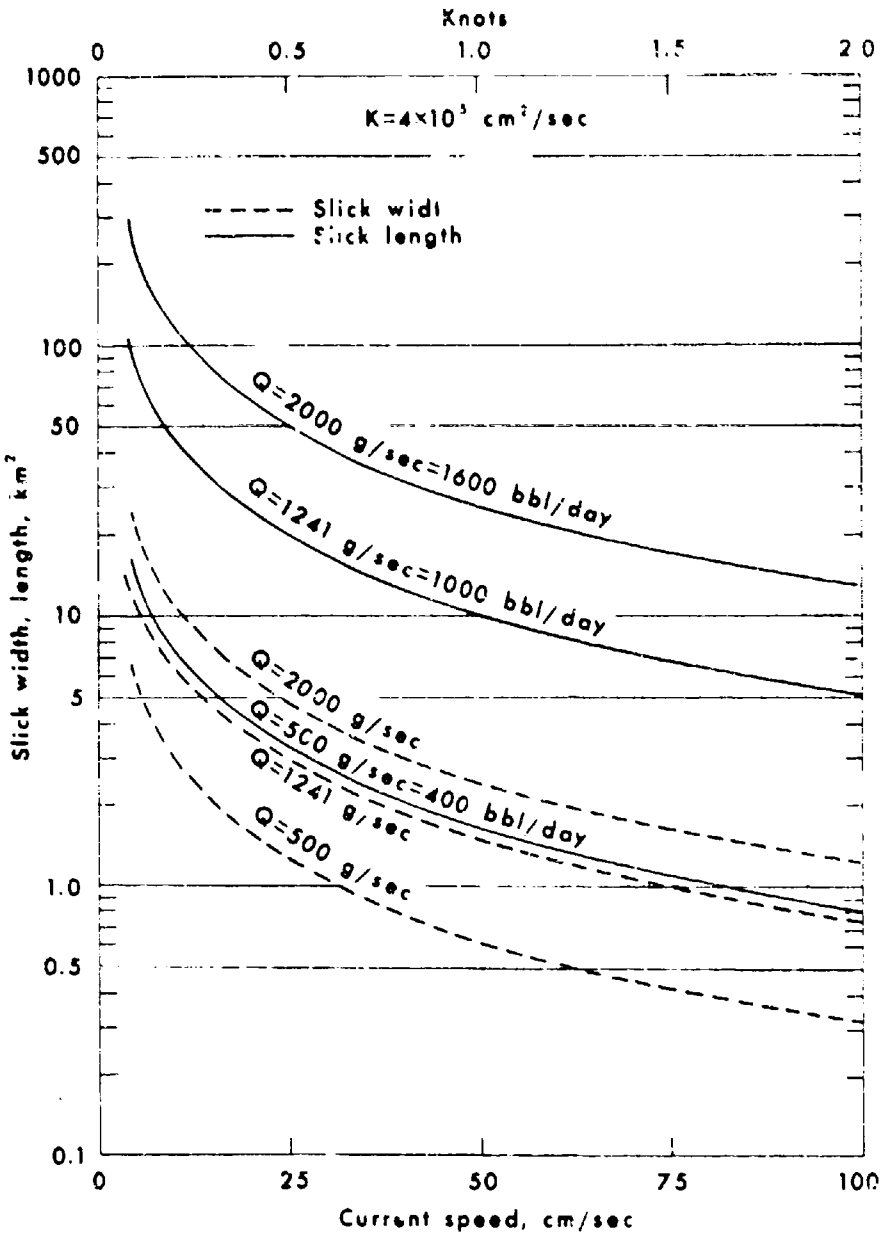


Figure 25. Slick width (W) and slick length (L) as a function of current speed (U) for various values of discharge rate (Q).

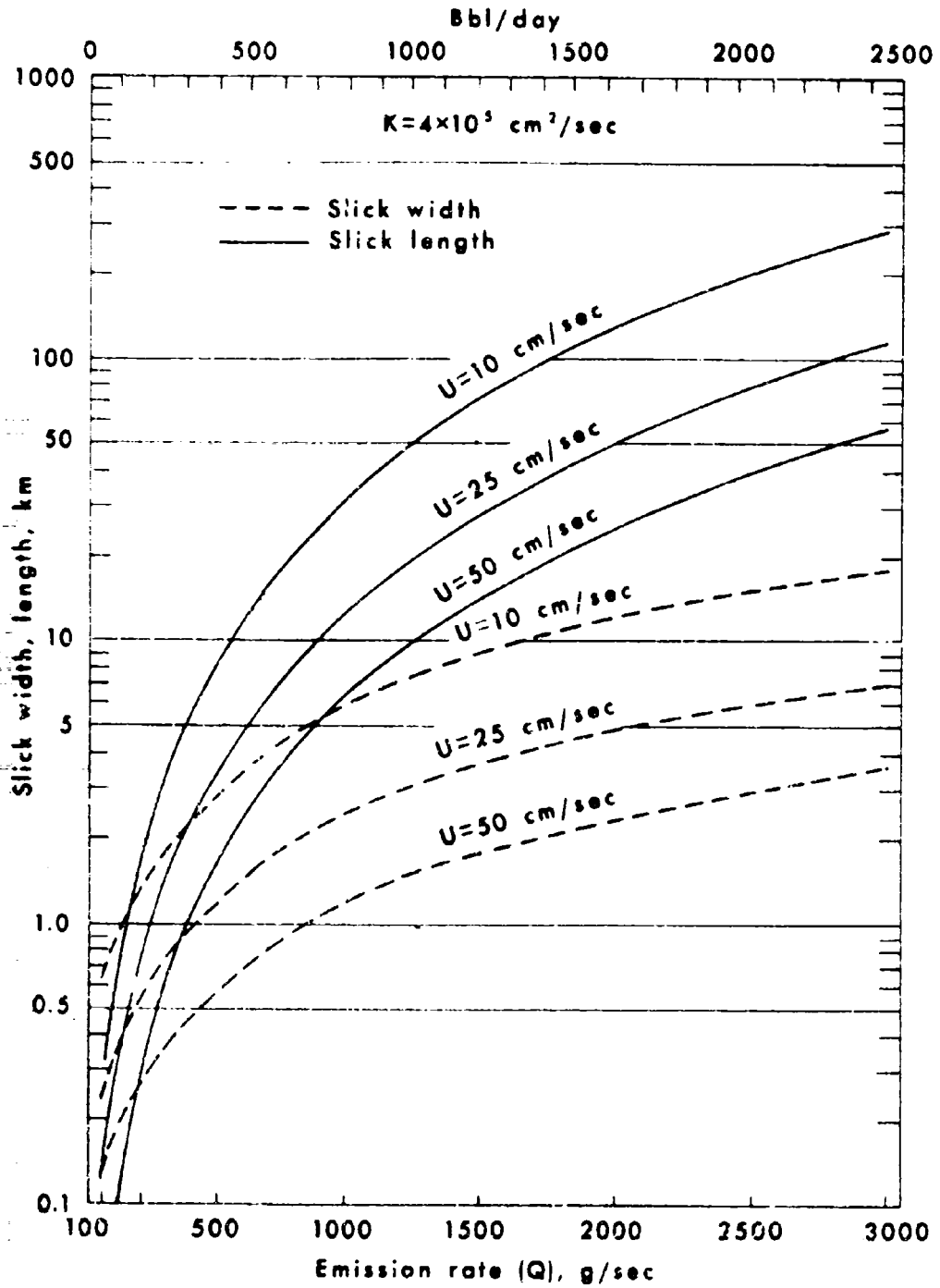


Figure 26. Slick width (W) and slick length (L) as a function of rate of discharge (Q) for various values of current speed (U).

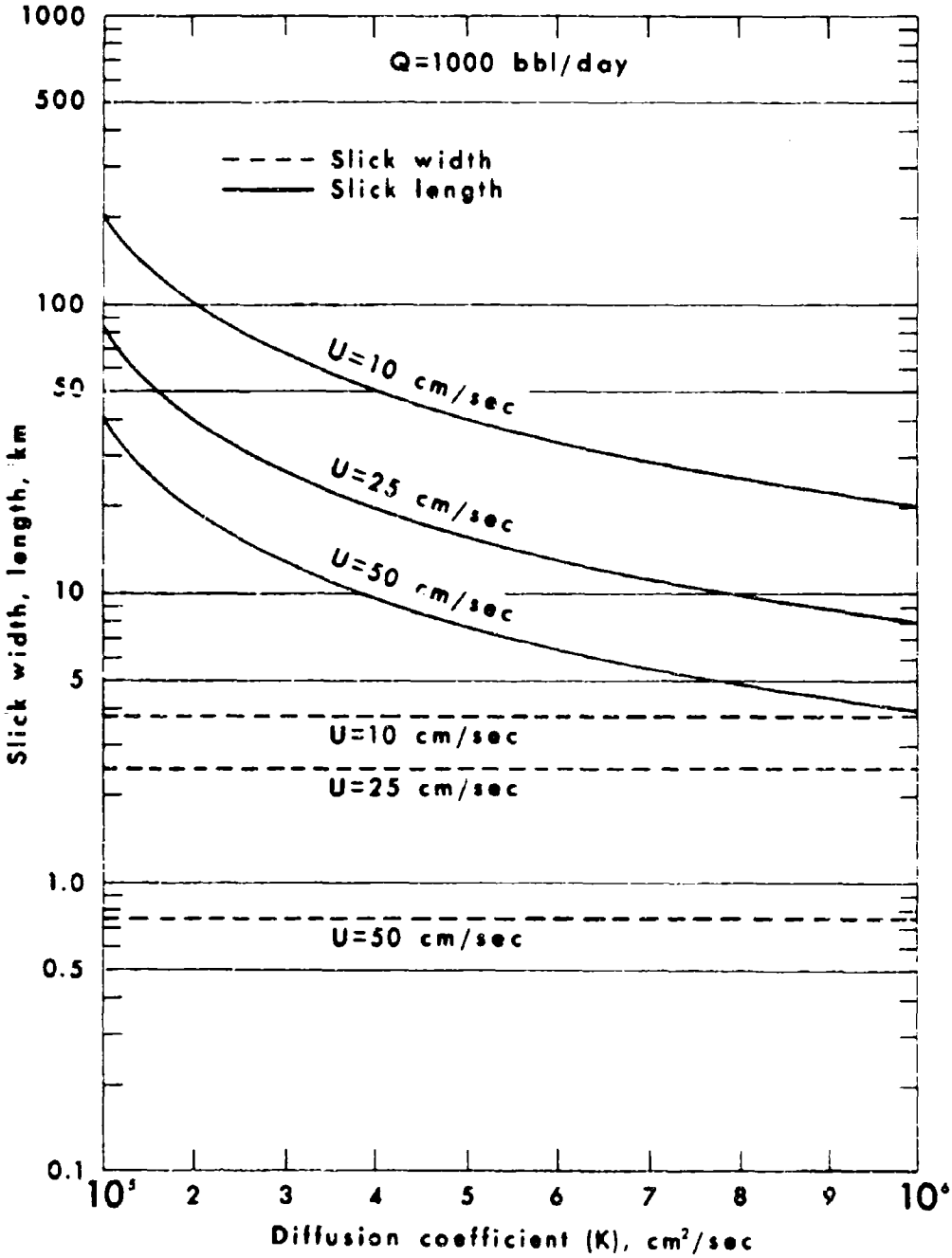


Figure 27. Slick width (W) and slick length (L) as a function of diffusion coefficient (K) for various values of current speed (U).

Winds during March were somewhat more varied than would be expected from long-term records. Strong winds to the southeast, which are usually rather infrequent in March, were probably important in reducing the amount of oil reaching shore.

At least once each week winds were sufficiently strong to generate waves of 2 to 4 feet, significant wave height. Two such periods of wave buildup and decay were documented by our instrumentation. There is no doubt that the stirring and mixing caused by these waves played a significant role in the continued breakup and diffusion of the oil slicks.

Salinity and temperature in the upper 15 feet of the water column showed rapid and strong variation. These were related to masses of turbid lower salinity water deriving from the river mouths. Interfaces between the river-derived and marine water masses were usually sharp and acted as barriers to movement of oil by other agents. The large amount of water being discharged from the Mississippi during March was one of the more important deterrents to movement of oil into the marshes because of this barrier effect, plus the escape of discharged river water out to sea.

Observations on the local tides indicated that they agreed very well with those predicted at Pensacola. The current observations, on the other hand, showed a complicated pattern; although tidal components were strong, their interaction with wind-drift currents and slope currents masked any clear relationship between the tide and the current or the wind and the current. Harmonic analysis of the currents did isolate typical current ellipses which had strong diurnal and semi-diurnal components (0.5-1.0 knot). This analysis further showed that the amplitude of the tidal current decreased

with decreasing tidal range (as the time of equatorial tides approached) and increased with distance from the bottom.

A general association of slick movement with wind direction is indicated from aerial photographs and from Coast Guard Situation Reports. Oil washed ashore on Breton Island on March 16 and 17 in a period of strong winds blowing from the well to the island. This was the main period when oil reached shore. The indicated association of slick movement with wind is in contrast with the lack of correlation between the wind and the current at the 5-foot level. One possible explanation suggested by theory is that the slick was embedded in a thin, high-velocity surface driven by the wind stress.

Slick shapes and orientations were often controlled by long (up to several miles) lines or zones separating brackish water masses from those of normal Gulf salinity. There apparently was no horizontal component of motion across these interfaces, as oil and other material frequently accumulated along them. These discontinuities often formed a natural barrier, preventing oil from moving onto the shore.

A theoretical analysis was undertaken to ascertain the effects of the rate of oil discharge, the ambient current speed, and the rate of oil diffusion on the area, width, and length of an ideal slick. Typical values for the Chevron incident predict an equilibrium or steady-state slick length of about 10 kilometers in length and 1.5 kilometers in width. These values agree very well with the on-site observations. Other results on the theoretical analysis are as follows: (1) For a given oil spill

incident the current speed largely determines the size a slick will reach; (2) the ratio of the diffusion coefficient to the rate of oil discharge controls the shape of the slick; (3) high discharges will provide elongate slicks; and (4) the consistently high current speeds during the Chevron incident kept the slick size to a minimum and greatly enhanced the rate of diffusion of the oil.

## CONCLUSIONS

1. In the waters surrounding the Chevron MP-41C platform it is apparent that wind stress tends to drive a thin layer of surface water before the wind. This is indicated by the frequent agreement of slick orientation with wind direction.

2. Detailed measurements of currents at 5-foot depth did not show agreement with slick orientations or wind directions except for periods of higher wind speeds.

3. Harmonic analysis removed significant diurnal and semi-diurnal components from the current records. The remaining non-periodic components largely reflect a combination of wind-generated currents and slope currents from setup, setdown, and river discharge.

4. Tidal currents showed a strong dependence on the range of tide, with the speed dropping by a factor of 2 or 3 from tropic tide periods to equatorial tide periods. Dispersion of oil could be expected to diminish accordingly.

5. Currents at depth showed a greater importance of non-periodic components; and, although rotational effects were still evident, the deeper currents frequently ran counter to the near-surface currents. The trajectory of chemically dispersed oil could therefore not be predicted from

surface observations.

6. The sharp boundaries associated with lower salinity water masses moving through the area were sites of oil stranding and accumulation.

7. Theoretical analysis indicates a strong effect of current speed on slick size. The high speeds of the Chevron incident rapidly diffused the oil and kept slick sizes to a minimum. Slick size and shape also varied as a function of rate of oil discharged and the coefficient of diffusion, which was empirically determined to be $4 \times 10^5$ $cm^2/sec$ for the Chevron case.

ACKNOWLEDGMENTS

Our gratitude is expressed to the Geography Programs, Office of Naval Research, and to the U.S. Coast Guard for enabling us to carry out this study. In particular, our thanks go to Miss Evelyn L. Pruitt, ONR; Admiral Ross P. Bullard, Eighth Coast Guard District Commander; Lieutenant Commander David H. Dickson, Jr., Chief, Intelligence and Law Enforcement Branch (Eighth District); Captain Lewis W. Tibbits, Jr., Chief of Staff, Eighth U.S. Coast Guard District; Lieutenant Commander Roy L. Foote, Operations, Eighth District; and Lieutenant Commander Stephen L. Richmond of Operations, New Orleans Group.

We are grateful for the assistance of the officers and crews of the U.S.C.G. cutters Dependable, Reliance, Pt. Spencer, and Pt. Estero. Special thanks go to BMCM Rufus R. McGiness and BMCM Clyde M. Bowden.

Photographic coverage of the oil slicks was provided by the U.S. Geological Survey through the assistance of Messrs. William A. Radlinski and Charles J. Rovinove. Mr. Jerry Wermund of Remote Sensing Inc., Houston, Texas, provided excellent infrared scanner imagery of the slicks.

The capability of the Coastal Studies Institute, which permitted a rapid response to this emergency situation, was created by the long-term support of the Institute by the Office of Naval Research, Geography Programs, under Contract No. N00014-69-A-0211-0003, Project No. NR 388 002.

Mr. Norwood Rector, Mr. Stan Sandifer, Miss Sharon Dunn, and Mr. William E. Hart of the Coastal Studies Institute contributed long hours beyond the call of duty to assure successful completion of the project.

# APPENDIX

| Station | Date | Profile | Depth | Salinity | Temperature | Current Speed | Direction | Time |
|---|---|---|---|---|---|---|---|---|
| Pt. Spencer Station 1 | 3/5 | 1 | 2.5 | 31.5 | 16.2 | 1.0 | 162 | 2245 |
| | | | 5 | 31.1 | 16.3 | .70 | 154 | 2235 |
| | | | 10 | 32.7 | 16.3 | .50 | 162 | 2220 |
| | | | 15 | 34.0 | 16.5 | .15 | 234 | 2215 |
| | | | 20 | 34.7 | 16.3 | .10 | 360 | 2200 |
| | | | 25 | 34.9 | 15.9 | .10 | 360 | 2150 |
| | | | 35 | 35.7 | 15.5 | .20 | 360 | 2125 |
| | | 2 | 2.5 | 27.4 | 16.45 | 1.2 | 180 | 2355 |
| | | | 5 | 30.7 | 16.6 | .75 | 180 | 2348 |
| | | | 10 | 32.3 | 16.4 | .55 | 216 | 2342 |
| | | | 15 | 34.5 | 16.3 | .40 | 216 | 2334 |
| | | | 20 | 34.4 | 16.5 | .25 | 198 | 2325 |
| | | | 25 | 35.2 | 15.9 | .15 | 234 | 2315 |
| | | | 30 | 35.0 | 15.7 | .20 | 225 | 2305 |
| | | | 33 | 35.4 | 15.8 | .15 | 306 | 2255 |
| | 3/6 | 3 | 2.5 | 22.49 | 15.88 | 1.4 | 171 | 0103 |
| | | | 5 | 27.15 | 16.18 | .75 | 180 | 0056 |
| | | | 10 | 32.50 | 16.18 | .55 | 144 | 0044 |
| | | | 15 | 34.08 | 16.76 | .45 | 216 | 0035 |
| | | | 20 | 34.42 | 16.30 | .30 | 198 | 0028 |
| | | | 25 | 35.51 | 15.68 | .20 | 198 | 0018 |
| | | | 30 | 35.65 | 15.88 | .18 | 180 | 0015 |
| | | | 36 | 35.51 | 15.65 | | | 0007 |
| | | 4 | 2.5 | 18.30 | 15.85 | .75 | 216 | 0225 |
| | | | 5 | 20.0 | 16.00 | .75 | 221 | 0215 |
| | | | 10 | 32.29 | 16.05 | .75 | 180 | 0203 |
| | | | 15 | 34.19 | 16.25 | .50 | 216 | 0153 |
| | | | 20 | 34.34 | 16.58 | .38 | 234 | 0147 |
| | | | 25 | 35.20 | 15.82 | .25 | 216 | 0141 |
| | | | 30 | 35.50 | 15.60 | .30 | 198 | 0127 |
| | | | 35 | 35.64 | 15.62 | .23 | 162 | 0124 |

| Station | Date | Profile | Depth | Salinity | Temperature | Current Speed | Direction | Time |
|---|---|---|---|---|---|---|---|---|
| | | 5 | 2.5 | 21.46 | 16.15 | 1.5 | 261 | 0345 |
| | | | 5 | 21.41 | 16.01 | 1.0 | 252 | 0335 |
| | | | 10 | 32.03 | 15.82 | .65 | 252 | 0325 |
| | | | 15 | 32.43 | 15.83 | .45 | 216 | 0312 |
| | | | 20 | 34.15 | 16.48 | .35 | 198 | 0304 |
| | | | 25 | 35.03 | 16.15 | .30 | 180 | 0253 |
| | | | 30 | 35.32 | 15.62 | .30 | 162 | 0247 |
| | | | 35 | 35.75 | 15.50 | .20 | 108 | 0240 |
| | | 6 | 2.5 | 29.12 | 16.13 | .75 | 288 | 0510 |
| | | | 5 | 28.75 | 16.00 | .75 | 252 | 0500 |
| | | | 10 | 28.71 | 15.98 | .65 | 198 | 0445 |
| | | | 15 | 31.48 | 15.90 | .45 | 180 | 0435 |
| | | | 20 | 33.58 | 16.02 | .35 | 144 | 0425 |
| | | | 25 | 34.86 | 15.86 | .2 | 180 | 0420 |
| | | | 30 | 35.27 | 15.48 | .15 | 144 | 0410 |
| | | | 35 | 35.50 | 15.68 | .05 | 108 | 0355 |
| | | 7 | 2.5 | 30.97 | 15.90 | .75 | 360 | 0620 |
| | | | 5 | 30.95 | 15.88 | .75 | 360 | 0610 |
| | | | 10 | 30.84 | 16.05 | .60 | 270 | 0600 |
| | | | 15 | 32.63 | 15.67 | .10 | 198 | 0550 |
| | | | 20 | 33.57 | 15.74 | .05 | 144 | 0535 |
| | | | 25 | 34.91 | 15.70 | .05 | 117 | 0525 |
| | | | 30 | 35.25 | 15.82 | .05 | 90 | 0520 |
| | | 8 | 2.5 | 31.22 | 16.17 | 1.0 | 360 | 0725 |
| | | | 5 | 31.22 | 16.01 | .95 | 360 | 0718 |
| | | | 10 | 31.12 | 16.05 | .85 | 328 | 0713 |
| | | | 15 | 31.22 | 16.08 | .65 | 288 | 0705 |
| | | | 20 | 31.88 | 16.0 | .20 | 216 | 0655 |
| | | | 25 | 34.55 | 15.88 | .15 | 108 | 0646 |
| | | | 30 | 35.01 | 15.55 | .15 | 72 | 0635 |

| Station | Date | Profile | Depth | Salinity | Temperature | Current Speed | Direction | Time |
|---|---|---|---|---|---|---|---|---|
| | | 9 | 10 | 31.67 | 16.10 | .75 | 360 | 0812 |
| | | | 15 | 31.82 | 16.09 | .60 | 328 | |
| | | | 20 | 33.0 | 15.79 | .20 | 25 | 0757 |
| | | | 25 | 34.2 | 15.6 | .20 | 198 | 0745 |
| | | | 30 | 35.08 | 15.5 | .15 | 144 | 0740 |
| | | 10 | 5 | 32.85 | 16.24 | .70 | 288 | 0955 |
| | | | 10 | 33.21 | 16.25 | .60 | 288 | 0947 |
| | | | 15 | 32.97 | 16.11 | .45 | 252 | 0938 |
| | | | 20 | 33.52 | 15.74 | .15 | 252 | 0932 |
| | | | 25 | 34.05 | 15.40 | .25 | 198 | 0925 |
| | | | 30 | 34.4 | 15.59 | .20 | 180 | 0915 |
| | | 11 | 5 | 33.24 | 16.26 | .75 | 288 | 1041 |
| | | | 10 | 33.25 | 16.22 | .75 | 270 | 1035 |
| | | | 15 | 33.24 | 16.28 | .55 | 198 | 1027 |
| | | | 20 | 33.20 | 16.11 | .25 | 180 | 1018 |
| | | | 25 | 34.07 | 15.58 | .05 | 180 | 1010 |
| | | | 30 | 35.18 | 15.47 | .05 | 252 | 1004 |
| Pt. Spencer Station 2 | 3/10 | 1 | 2 | 8.18 | 13.70 | | | 0640 |
| | | | 5 | 26.58 | 15.04 | 1.0 | 18 | 0634 |
| | | | 10 | 33.45 | 14.92 | 1.25 | 40 | 0640 |
| | | | 15 | 34.57 | 15.04 | .80 | 18 | 0645 |
| | | | 17.5 | 35.36 | 15.40 | | | 0655 |
| | | | 20 | 36.01 | 15.76 | .50 | 18 | 0708 |
| | | | 25 | 35.96 | 15.96 | .50 | 360 | 0715 |
| | | | 27.5 | 35.98 | 15.82 | .45 | 360 | 0720 |
| | | | 28.5 | 35.93 | 15.85 | .40 | 360 | 0725 |
| | | | 30 | 35.99 | 15.83 | .35 | 360 | 0728 |
| | | 2 | 2.5 | 7.23 | 14.06 | .75 | 360 | 0835 |
| | | | 3.0 | 16.77 | 15.26 | | | 0843 |

| Station | Date | Profile | Depth | Salinity | Temperature | Current Speed | Direction | Time |
|---|---|---|---|---|---|---|---|---|
| | | | 5.0 | 33.27 | 15.57 | 1.25 | 30 | 0830 |
| | | | 10 | 34.42 | 14.78 | 1.0 | 36 | 0820 |
| | | | 15 | 35.45 | 15.56 | .85 | 36 | 0813 |
| | | | 20 | 35.92 | 15.82 | .6 | 360 | 0807 |
| | | | 25 | 36.03 | 15.87 | .5 | 360 | 0800 |
| | | 3 | 2.5 | 16.55 | 14.93 | .75 | 360 | 0935 |
| | | | 5 | 33.17 | 15.45 | 1.0 | 36 | 0934 |
| | | | 10 | 34.27 | 15.38 | .80 | 36 | 0920 |
| | | | 15 | 35.40 | 15.60 | .75 | 18 | 0903 |
| | | | 20 | 35.83 | 15.82 | .60 | 360 | 0847 |
| | | | 25 | 35.99 | 15.85 | .55 | 360 | 0853 |
| | | | 30 | 36.18 | 15.83 | .35 | 360 | 0847 |
| | | 4 | 2.5 | 10.60 | 15.33 | 1.0 | 360 | 1030 |
| | | | 5 | 31.27 | 15.36 | 1.1 | 15 | 1040 |
| | | | 10 | 35.35 | 15.34 | .8 | 15 | 1045 |
| | | | 15 | 35.68 | 15.82 | .65 | 18 | 1050 |
| | | | 20 | 36.09 | 16.14 | .55 | 360 | 1105 |
| | | | 25 | 36.15 | 16.10 | .60 | 360 | 1117 |
| | | | 30 | 35.92 | 15.91 | .40 | 360 | 1135 |
| | | 5 | 2.5 | 13.73 | 16.17 | 1.6 | 360 | 1145 |
| | | | 5 | 16.85 | 15.75 | 1.2 | 360 | 1135 |
| | | | 10 | 34.55 | 15.22 | .70 | 36 | 1127 |
| | | | 15 | 35.62 | 15.84 | .50 | 360 | 1117 |
| | | | 20 | 36.01 | 16.02 | .35 | 360 | 1107 |
| | | | 25 | 36.16 | 15.94 | .30 | 360 | 1058 |
| | | | 30 | 36.07 | 15.97 | .35 | 15 | 1050 |
| Pt. Spencer | 3/10 | 1 | 2.5 | 26.84 | 16.62 | 1.0 | NNE | 1423 |
| Station 3 | | | 5 | 26.86 | 16.58 | .8 | 015 | |
| | | | 10 | 28.4 | 16.36 | | | 1403 |
| | | | 15 | 33.61 | 15.21 | | | 1410 |
| | | | 20 | 34.24 | 15.21 | | | |

| Station | Date | Profile | Depth | Salinity | Temperature | Current Speed | Direction | Time |
|---|---|---|---|---|---|---|---|---|
| | | | 25 | 34.59 | 15.21 | .3 | 070 | 1447 |
| | | | 27.5 | 34.67 | 15.19 | .24 | 036 | 1451 |
| | | 2 | 2.5 | 26.0 | 16.81 | 1.1 | NE | 1512 |
| | | | 5 | 26.19 | 16.81 | .8 | NE | 1520 |
| | | | 10 | 31.53 | 16.21 | .7 | E | 1554 |
| | | | 15 | 34.45 | 15.46 | .33 | 90 | 1604 |
| | | | 20 | | | .33 | 70 | |
| | | | 25 | 34.43 | 15.07 | .2 | ENE | 1614 |
| | | 3 | 2.5 | 28.97 | 16.73 | .75 | SE | 1638 |
| | | | 5 | 27.62 | 16.60 | .7 | ESE | 1653 |
| | | | 10 | 29.54 | 16.67 | .9 | 72 | 1708 |
| | | | 15 | 33.56 | 15.84 | .4 | 108 | 1721 |
| | | | 20 | 34.25 | 15.35 | .35 | 108 | 1734 |
| | | | 25 | 35.10 | 15.26 | .25 | 56 | 1745 |
| | | | 27 | 34.09 | 15.35 | .15 | | 1751 |
| | | 4 | 2.5 | 21.5 | 16.26 | .7 | S | 1837 |
| | | | 5 | 27.75 | 16.40 | .5 | SE | 1847 |
| | | | 10 | 31.46 | 16.32 | .65 | SW | 1852 |
| | | | 15 | 31.02 | 16.04 | .5 | SW | 1914 |
| | | | 20 | 32.73 | 16.04 | .1 | E | 1924 |
| | | 5 | 5 | 24.23 | 16.38 | .36 | SW | 2037 |
| | | | 10 | 31.46 | 16.12 | .84 | SW | 2104 |
| | | | 15 | 31.09 | 16.38 | .46 | W | 2120 |
| | | | 20 | 33.58 | 15.75 | .10 | NW | 2124 |
| | | | 25 | 35.00 | 15.48 | .20 | NW | 2140 |
| | | 6 | 5 | 26.9 | 15.8 | .72 | W | 2150 |
| | | | 10 | 30.71 | 16.21 | .64 | WNW | 2202 |
| | | | 15 | 33.01 | 15.57 | .47 | NW | 2210 |
| | | | 20 | 34.05 | 15.34 | .38 | NW | 2220 |
| | | | 25 | 34.45 | 15.10 | .5 | NW | 2240 |

| Station | Date | Profile | Depth | Salinity | Temperature | Current Speed | Direction | Time |
|---|---|---|---|---|---|---|---|---|
| | | 7 | 5 | 26.00 | 16.43 | .64 | NW | 2243 |
| | | | 10 | 30.19 | 15.85 | .68 | NW | 2248 |
| | | | 15 | 33.48 | 15.82 | .72 | NW | 2314 |
| | | | 20 | 34.10 | 15.43 | .40 | NW | 2315 |
| | | | 25 | 35.0 | 15.57 | .24 | NW | 2321 |
| | 3/11 | 8 | 5 | 26.91 | 16.07 | .8 | NW | 0000 |
| | | | 10 | 33.27 | 16.55 | .6 | NW | 0006 |
| | | | 15 | 33.90 | 15.11 | .6 | NW | 0015 |
| | | | 20 | 35.0 | 15.0 | .6 | NW | 0030 |
| | | | 25 | 35.27 | 16.25 | .56 | NW | 0040 |
| | | 9 | 5 | 27.89 | 16.39 | | | 0045 |
| | | | 10 | 33.04 | 15.25 | .6 | NW | |
| | | | 15 | | | 1.0 | NW | |
| | | | 20 | | | .4 | NW | 0153 |
| | | 10 | 5 | 29.14 | 16.34 | .8 | NW | 0212 |
| | | | 10 | 34.50 | 15.29 | .8 | NW | 0220 |
| | | | 15 | 34.65 | 15.28 | .8 | W | 0225 |
| | | | 20 | 35.00 | 15.35 | .8 | WNW | 0230 |
| | | | 25 | 35.35 | 15.32 | .45 | W | 0250 |
| | | 11 | 5 | 28.85 | 16.10 | .8 | NW | 0312 |
| | | | 10 | 34.5 | 15.11 | 1.0 | NW | 0320 |
| | | | 15 | 34.56 | 15.25 | .8 | NW | 0330 |
| | | | 20 | 34.70 | 15.05 | .75 | NW | 0335 |
| Reliance | 3/8 | 1 | 5 | 33.87 | 15.10 | .42 | 270 | 2337 |
| | | | 10 | 33.90 | 15.05 | .40 | 270 | 2332 |
| | | | 15 | 33.92 | 15.05 | .35 | 270 | 2328 |
| | | | 25 | 33.97 | 15.06 | .25 | 252 | 2325 |
| | | | 45 | 33.97 | 15.10 | .20 | 216 | 2310 |

| Station | Date | Profile | Depth | Salinity | Temperature | Current Speed | Direction | Time |
|---|---|---|---|---|---|---|---|---|
| | 3/9 | 2 | 5 | 33.90 | 14.90 | .40 | 270 | 0003 |
| | | | 10 | 33.89 | 15.01 | .35 | 270 | 0009 |
| | | | 15 | 33.96 | 15.00 | .30 | 270 | 0018 |
| | | | 25 | 33.95 | 14.95 | .20 | 252 | 0030 |
| | | | 35 | 33.96 | 14.92 | .30 | 234 | 0036 |
| | | | 44 | 33.71 | 15.00 | .25 | 360 | 0043 |
| | | 3 | 5 | 33.96 | 14.88 | .20 | 234 | 0115 |
| | | | 10 | 33.88 | 15.00 | .30 | 340 | 0124 |
| | | | 15 | 33.60 | 15.02 | .25 | 360 | 0130 |
| | | | 25 | 33.61 | 14.81 | .20 | 324 | 0142 |
| | | | 35 | 34.05 | 14.89 | .25 | 234 | 0152 |
| | | | 44 | 36.24 | 14.93 | .25 | 270 | 0157 |
| | | 4 | 5 | 36.43 | 14.93 | .15 | 234 | 0205 |
| | | | 10 | 33.67 | 14.78 | .20 | 234 | 0209 |
| | | | 15 | 33.70 | 14.80 | .15 | 234 | 0215 |
| | | | 25 | 34.16 | 14.86 | .15 | 252 | 0225 |
| | | | 35 | 34.03 | 14.90 | .15 | 270 | 0232 |
| | | | 44 | 34.42 | 14.85 | .25 | 270 | 0239 |
| | | 5 | 5 | 34.45 | 14.84 | .15 | 360 | 0247 |
| | | | 10 | 34.40 | 14.85 | .20 | 360 | 0255 |
| | | | 15 | 34.30 | 14.84 | .20 | 360 | 0315 |
| | | | 25 | 34.53 | 14.79 | .15 | 360 | 0325 |
| | | | 35 | 34.35 | 14.80 | .20 | 360 | 0333 |
| | | | 44 | 34.35 | 14.85 | .15 | 360 | 0341 |
| | | 6 | 5 | 34.70 | 14.75 | .15 | 360 | 0347 |
| | | | 10 | 34.56 | 14.80 | .20 | 360 | 0357 |
| | | | 15 | 34.53 | 14.80 | .15 | 360 | 0405 |
| | | | 25 | 34.35 | 14.73 | .15 | 270 | 0410 |
| | | | 35 | 34.10 | 14.66 | .10 | 360 | 0419 |
| | | | 44 | 34.51 | 14.72 | .05 | 252 | 0428 |

| Station | Date | Profile | Depth | Salinity | Temperature | Current Speed | Direction | Time |
|---|---|---|---|---|---|---|---|---|
| | | 8 | 5 | 34.05 | 14.72 | .08 | 360 | 0600 |
| | | | 10 | 34.03 | 14.80 | .10 | 360 | 0610 |
| | | | 15 | 34.02 | 14.82 | .05 | 360 | 0622 |
| | | | 25 | 34.11 | 14.73 | 0.0 | 180 | 0643 |
| | | | 35 | 34.0 | 14.79 | 0.0 | 360 | 0706 |
| | | | 44 | 34.05 | 14.85 | .20 | 328 | 0718 |
| | | 9 | 5 | 33.86 | 14.82 | 0.0 | 72 | 0842 |
| | | | 10 | 33.95 | 14.66 | 0.0 | 360 | 0821 |
| | | | 15 | 33.74 | 14.70 | 0.05 | 360 | 0812 |
| | | | 25 | 33.92 | 14.75 | 0.0 | 360 | 0804 |
| | | | 35 | 33.85 | 14.72 | 0.0 | 342 | 0755 |
| | | | 44 | 34.14 | 14.82 | .25 | 342 | 0735 |
| Pt. Estero Station A | 3/16 | 1 | 2 | 27.33 | 14.77 | | 115 | 2153 |
| | | | 5 | 27.48 | 14.57 | .38 | 115 | |
| | | | 10 | 27.67 | 14.59 | .34 | 115 | |
| | | | 15 | 27.50 | 14.67 | .25 | 130 | |
| | | 2 | 2 | 25.45 | 14.25 | .18 | 70 | 2329 |
| | | | 5 | 25.68 | 14.56 | .24 | 90 | |
| | | | 10 | 27.15 | 14.38 | .22 | 140 | |
| | | | 15 | 27.28 | 14.43 | .43 | 180 | |
| | 3/17 | 3 | 2 | 21.75 | 13.92 | .17 | 30 | 0054 |
| | | | 5 | 21.75 | 13.90 | .12 | 70 | |
| | | | 10 | 23.40 | 14.15 | .58 | 110 | |
| | | | 15 | 23.68 | 14.33 | .56 | 105 | |
| | | 4 | 2 | 22.95 | 13.93 | .27 | 90 | 0220 |
| | | | 5 | 22.90 | 13.90 | .33 | 90 | |
| | | | 10 | 23.68 | 13.95 | .65 | 100 | |
| | | | 15 | 25.48 | 14.11 | .80 | 155 | |

| Station | Date | Profile | Depth | Salinity | Temperature | Current Speed | Direction | Time |
|---|---|---|---|---|---|---|---|---|
| | | 5 | 2 | 21.86 | 13.54 | .15 | 110 | 0345 |
| | | | 5 | 20.97 | 13.72 | .25 | 120 | |
| | | | 10 | 24.96 | 14.05 | .62 | 110 | |
| | | | 15 | 25.23 | 13.90 | .74 | 110 | |
| | | 6 | 2 | 22.19 | 13.52 | .23 | 140 | 0514 |
| | | | 5 | 21.69 | 13.60 | .26 | 100 | |
| | | | 10 | 22.78 | 13.80 | .55 | 110 | |
| | | | 15 | 24.73 | 13.91 | .75 | 105 | |
| | | 7 | 2 | 21.28 | 13.65 | .20 | 130 | 0645 |
| | | | 5 | 21.74 | 13.60 | .29 | 120 | |
| | | | 10 | 22.90 | 13.76 | .50 | 130 | |
| | | | 15 | 25.38 | 14.02 | .57 | 130 | |
| | | 8 | 2 | 31.24 | 13.68 | .18 | 90 | 0815 |
| | | | 5 | 21.60 | 13.70 | .14 | 90 | |
| | | | 10 | 21.60 | 13.70 | .27 | 140 | |
| | | | 15 | 24.78 | 14.02 | .34 | 140 | |
| | | 9 | 2 | 24.64 | 14.00 | .40 | 360 | 1000 |
| | | | 5 | 22.83 | 14.03 | .50 | 300 | |
| | | | 10 | 22.82 | 14.07 | .65 | 280 | |
| | | | 15 | 23.86 | 14.16 | .45 | 280 | |
| | | 10 | 2 | 23.78 | 14.16 | .70 | 340 | 1130 |
| | | | 5 | 24.75 | 14.20 | .80 | 340 | |
| | | | 10 | 23.95 | 14.20 | .38 | 340 | |
| | | | 15 | 23.95 | 14.28 | .36 | 270 | |
| | | 11 | 2 | 24.00 | 14.20 | .52 | 360 | 1255 |
| | | | 5 | 22.30 | 14.00 | .55 | 350 | |

| Station | Date | Profile | Depth | Salinity | Temperature | Current Speed | Direction | Time |
|---|---|---|---|---|---|---|---|---|
| | | | 10 | 22.20 | 13.90 | 37 | 330 | |
| | | | 15 | 22.12 | 13.91 | .46 | 340 | |
| | | 12 | 2 | 21.46 | 14.20 | .37 | | 1450 |
| | | | 5 | 21.46 | 13.97 | .46 | 360 | |
| | | | 10 | 21.42 | 13.80 | .32 | 340 | |
| | | | 15 | 22.36 | 13.87 | | 340 | |
| | | 13 | 2 | 20.70 | 14.21 | .26 | 300 | 2057 |
| | | | 5 | 20.54 | 14.20 | .58 | 290 | |
| | | | 10 | 27.45 | 14.66 | .33 | 330 | |
| | | | 15 | 27.30 | 14.67 | .19 | 360 | |
| | | 14 | 2 | 17.30 | 13.85 | .22 | 280 | 2210 |
| | | | 5 | 22.85 | 14.10 | .34 | 250 | |
| | | | 10 | 23.45 | 14.52 | .24 | 330 | |
| | | | 15 | 29.00 | 14.62 | .12 | 330 | |
| | | 15 | 2 | 09.30 | 13.80 | .10 | 110 | 2320 |
| | | | 5 | 19.80 | 14.15 | .25 | 180 | |
| | | | 10 | 26.70 | 14.55 | .10 | 300 | |
| | | | 15 | 28.23 | 14.76 | .10 | 90 | |
| | 3/18 | 16 | 2 | 13.80 | 13.20 | .28 | 90 | 0024 |
| | | | 5 | 18.32 | 13.95 | .36 | 160 | |
| | | | 10 | 27.95 | 14.74 | .26 | 120 | |
| | | | 15 | 27.90 | 14.75 | .38 | 120 | |
| | | 17 | 2 | 18.53 | 14.20 | .58 | 110 | 0132 |
| | | | 5 | 20.89 | 14.32 | .44 | 130 | |
| | | | 10 | 25.95 | 14.60 | .52 | 120 | |
| | | | 15 | 27.55 | 14.60 | .51 | 90 | |

| Station | Date | Profile | Depth | Salinity | Temperature | Current Speed | Direction | Time |
|---|---|---|---|---|---|---|---|---|
| | | 18 | 2 | 19.84 | 14.42 | .78 | 90 | 0237 |
| | | | 5 | 21.35 | 14.20 | .68 | 120 | |
| | | | 10 | 26.78 | 14.37 | .76 | 120 | |
| | | | 15 | 26.43 | 14.25 | .47 | 105 | |
| | | 19 | 2 | 21.08 | 14.18 | .93 | 100 | 0350 |
| | | | 5 | 21.45 | 14.22 | .86 | 95 | |
| | | | 10 | 24.60 | 14.45 | .68 | 120 | |
| | | | 15 | 26.36 | 14.23 | .45 | 95 | |
| | | 20 | 2 | 21.54 | 14.17 | .90 | 90 | 0522 |
| | | | 5 | 22.49 | 14.08 | .80 | 110 | |
| | | | 10 | 22.75 | 14.00 | .65 | 125 | |
| | | | 15 | 26.12 | 14.33 | .38 | 90 | |
| | | 21 | 2 | 21.80 | 14.21 | .77 | 120 | 0655 |
| | | | 5 | 22.38 | 14.13 | .63 | 110 | |
| | | | 10 | 23.34 | 14.11 | .43 | 140 | |
| | | | 15 | 26.25 | 14.19 | .20 | 60 | |
| | | 22 | 2 | 21.52 | 14.18 | .45 | 105 | 0751 |
| | | | 5 | 22.37 | 14.13 | .28 | 105 | |
| | | | 10 | 25.12 | 14.07 | .12 | 175 | |
| | | | 15 | 25.96 | 14.16 | .06 | 205 | |
| | | 23 | 2 | 21.94 | 14.35 | .27 | 110 | 0920 |
| | | | 5 | 22.35 | 14.24 | .00 | 185 | |
| | | | 10 | 23.52 | 14.28 | .17 | 235 | |
| | | | 15 | | | .16 | 260 | |
| | | 24 | 2 | 21.45 | 14.35 | .27 | 160 | 1007 |
| | | | 5 | 22.93 | 14.33 | .43 | 180 | |
| | | | 10 | 20.25 | 14.41 | .23 | 250 | |
| | | | 15 | 21.40 | 14.46 | .18 | 280 | |

| Station | Date | Profile | Depth | Salinity | Temperature | Current Speed | Direction | Time |
|---|---|---|---|---|---|---|---|---|
| | | 25 | 2 | 2.05 | 15.55 | .17 | 250 | 1110 |
| | | | 5 | 22.63 | 14.55 | .33 | 220 | |
| | | | 10 | 17.96 | 14.51 | .36 | 270 | |
| | | | 15 | 26.40 | 14.55 | .30 | 280 | |
| | | 26 | 2 | 6.50 | 16.76 | .28 | 240 | 1225 |
| | | | 5 | 22.40 | 14.70 | .40 | 250 | |
| | | | 10 | 22.90 | 14.50 | .32 | 270 | |
| | | | 15 | 25.85 | 14.55 | .33 | 260 | |
| Pt. Estero Station B | 3/15 | 1 | 5 | 27.70 | 14.01 | .60 | 230 | |
| | | | 10 | 28.70 | 14.56 | .52 | 225 | |
| | | | 15 | 29.77 | 14.27 | .63 | 225 | |
| | | | 20 | 29.98 | 14.08 | .74 | 225 | |
| | | | 25 | 31.48 | 14.80 | .35 | 216 | 2300 |
| | | 2 | 5 | 27.45 | 13.63 | .77 | 125 | |
| | | | 10 | 27.50 | 13.54 | .63 | 135 | |
| | | | 15 | 29.96 | 14.59 | | 135 | |
| | | | 20 | 29.46 | 14.61 | .76 | 135 | |
| | 3/16 | | 25 | 29.70 | 14.66 | .44 | 145 | 0005 |
| | | 3 | 5 | 28.07 | 13.61 | .93 | 130 | |
| | | | 10 | 28.10 | 13.57 | .87 | 140 | |
| | | | 15 | 28.26 | 13.86 | .78 | 135 | |
| | | | 20 | 29.33 | 14.45 | .45 | 130 | |
| | | | 25 | 30.71 | 14.84 | .16 | 100 | 0120 |
| | | 4 | 5 | 28.18 | 13.73 | .86 | 100 | |
| | | | 10 | 28.45 | 13.83 | .81 | 105 | |
| | | | 15 | 28.85 | 14.05 | .42 | 112 | |
| | | | 20 | 29.95 | 14.50 | .34 | 115 | |
| | | | 25 | 30.09 | 14.33 | .00 | 135 | 0232 |

| Station | Date | Profile | Depth | Salinity | Temperature | Current Speed | Direction | Time |
|---|---|---|---|---|---|---|---|---|
| | | 5 | 5 | 28.75 | 13.77 | .72 | 102 | |
| | | | 10 | 28.75 | 13.74 | .63 | 105 | |
| | | | 15 | 29.42 | 14.15 | .33 | 118 | |
| | | | 20 | 29.89 | 14.25 | .04 | 110 | |
| | | | 25 | 29.92 | 14.35 | .10 | 73 | 0355 |
| | | 6 | 5 | 26.60 | 13.61 | .43 | 75 | |
| | | | 10 | 28.98 | 13.65 | .37 | 75 | |
| | | | 15 | 29.01 | 13.77 | .34 | 275 | |
| | | | 20 | 29.45 | 14.19 | .36 | 100 | |
| | | | 25 | 30.12 | 14.55 | .26 | 345 | 0518 |
| | | 7 | 5 | 29.28 | 13.59 | .49 | 280 | |
| | | | 10 | 29.32 | 13.52 | .45 | 255 | |
| | | | 15 | 29.24 | 13.55 | .20 | 345 | |
| | | | 20 | 30.22 | 14.50 | .33 | 30 | |
| | | | 25 | 31.92 | 15.04 | .15 | 65 | 0650 |
| | | 8 | 5 | 29.33 | 13.52 | .36 | 0 | |
| | | | 10 | 29.27 | 13.73 | .34 | 0 | |
| | | | 15 | 29.65 | 13.72 | .30 | 15 | |
| | | | 20 | 32.47 | 14.89 | .45 | 10 | |
| | | | 25 | 33.30 | 15.20 | .42 | 20 | 0805 |
| | | 9 | 5 | 29.49 | 13.87 | .35 | 15 | |
| | | | 10 | 30.17 | 14.54 | .60 | 25 | |
| | | | 15 | 33.98 | 15.26 | .48 | 20 | |
| | | | 20 | 34.03 | 14.39 | .46 | 15 | |
| | | | 25 | 34.21 | 15.37 | .34 | 15 | 0840 |
| | | 10 | 5 | 30.40 | 14.23 | .36 | 0 | |
| | | | 10 | 31.92 | 14.58 | .77 | 0 | |
| | | | 15 | 33.87 | 15.14 | .63 | 0 | |
| | | | 20 | 33.76 | 15.17 | .35 | 0 | |
| | | | 25 | 33.69 | 15.18 | .21 | 0 | 1110 |

| Station | Date | Profile | Depth | Salinity | Temperature | Current Speed | Direction | Time |
|---|---|---|---|---|---|---|---|---|
| | | 11 | 5 | 30.51 | 14.23 | .53 | 0 | |
| | | | 10 | 31.24 | 14.47 | .63 | 0 | 1145 |
| Pt. Estero Station C | 3/20 | 1 | 2 | 16.45 | 14.25 | .58 | 90 | |
| | | | 5 | 28.53 | 15.22 | .31 | 80 | |
| | | | 10 | 33.52 | 15.15 | .12 | 60 | |
| | | | 15 | 33.90 | 15.46 | .13 | 280 | 0156 |
| | | 2 | 2 | 9.60 | 13.86 | 2.2 | 110 | |
| | | | 5 | 29.60 | 15.05 | .56 | 100 | |
| | | | 10 | 33.45 | 15.05 | .23 | 100 | |
| | | | 15 | 34.08 | 15.20 | .06 | 160 | 0300 |
| | | 3 | 2 | 15.50 | 15.94 | 2.2 | 120 | |
| | | | 5 | 29.18 | 15.25 | .64 | 110 | |
| | | | 10 | 32.57 | 14.90 | .25 | 110 | |
| | | | 15 | 33.85 | 15.49 | .07 | 130 | 0400 |
| | | 4 | 2 | 15.45 | 17.40 | 1.75 | 130 | |
| | | | 5 | 31.20 | 15.18 | .63 | 130 | |
| | | | 10 | 33.20 | 15.23 | .20 | 120 | |
| | | | 15 | 34.40 | 15.73 | .04 | 120 | 0454 |
| | | 5 | 2 | 18.32 | 16.75 | .80 | 120 | |
| | | | 5 | 26.00 | 15.75 | .58 | 130 | |
| | | | 10 | 33.62 | 15.51 | .16 | 140 | |
| | | | 15 | 33.55 | 15.56 | .03 | 150 | 0550 |
| | | 6 | 2 | 17.46 | 16.23 | .77 | 110 | |
| | | | 5 | | | .42 | 126 | |
| | | | 10 | 32.75 | 15.18 | .18 | 126 | |
| | | | 15 | 33.72 | 15.30 | .23 | 320 | 0640 |
| | | 7 | 2 | 21.25 | 15.45 | .60 | 115 | |
| | | | 5 | 27.70 | 15.64 | .37 | 150 | |
| | | | 10 | 31.70 | 15.20 | .14 | 345 | |
| | | | 15 | 33.48 | 15.42 | .38 | 345 | |
| | | | 17.5 | 33.54 | 15.22 | .42 | 345 | 0826 |

| Station | Date | Profile | Depth | Salinity | Temperature | Current Speed | Direction | Time |
|---|---|---|---|---|---|---|---|---|
| | | 8 | 2 | 21.15 | 15.44 | .38 | 170 | |
| | | | 5 | 21.50 | 15.85 | .50 | 190 | |
| | | | 10 | 31.01 | 15.35 | .02 | 325 | |
| | | | 15 | 33.04 | 15.08 | .26 | 330 | |
| | | | 17.5 | 33.23 | 15.29 | .36 | 340 | 1000 |
| Pt. Estero Station D | 3/18 | 1 | 5 | 27.45 | 15.35 | .25 | 40 | |
| | | | 10 | 29.68 | 15.00 | .33 | 340 | |
| | | | 15 | 31.30 | 15.11 | .30 | 50 | 2059 |
| | | 2 | 5 | 27.45 | 15.35 | .25 | 40 | |
| | | | 10 | 29.55 | 15.19 | .37 | 50 | |
| | | | 25 | 30.85 | 15.05 | .41 | 90 | 2220 |
| | | 3 | 5 | 27.75 | 15.35 | .25 | 90 | |
| | | | 10 | 29.50 | 15.18 | .43 | 180 | |
| | | | 25 | 28.70 | 15.60 | .36 | 180 | 2334 |
| | 3/19 | 4 | 2 | 24.80 | 15.21 | .10 | 45 | |
| | | | 5 | 24.70 | 15.65 | .00 | 55 | |
| | | | 10 | 27.23 | 15.35 | .38 | 190 | |
| | | | 25 | 31.75 | 14.83 | .36 | 200 | 0140 |
| | | 5 | 2 | 23.40 | 16.10 | .45 | 110 | |
| | | | 5 | 23.58 | 15.26 | .50 | 145 | |
| | | | 10 | 27.72 | 15.16 | 1.00 | 150 | |
| | | | 25 | 31.58 | 14.94 | .40 | 180 | 0314 |
| | | 6 | 2 | 17.70 | 15.46 | .57 | 90 | |
| | | | 5 | 23.86 | 15.22 | .78 | 125 | |
| | | | 10 | 30.78 | 14.76 | .82 | 165 | |
| | | | 25 | 31.58 | 14.85 | 1.00 | 165 | 0500 |

| Station | Date | Profile | Depth | Salinity | Temperature | Current Speed | Direction | Time |
|---|---|---|---|---|---|---|---|---|
| | | 7 | 2 | 22.03 | 15.18 | .05 | 160 | |
| | | | 5 | 26.91 | 15.18 | .65 | 170 | |
| | | | 10 | 30.71 | 15.02 | .65 | 185 | |
| | | | 25 | 31.17 | 15.08 | .38 | 200 | 0647 |
| | | 8 | 2 | 16.76 | 15.25 | .26 | 200 | |
| | | | 5 | 26.61 | 15.11 | .63 | 210 | |
| | | | 10 | 29.86 | 14.96 | .57 | 250 | |
| | | | 25 | 30.45 | 15.07 | .32 | 260 | 0730 |
| Dependable | 3/15 | 1 | 2.5 | 22.54 | 13.49 | 1.50 | 70 | 2115 |
| | | | 5 | 36.15 | 16.45 | 0.30 | 80 | 2120 |
| | | | 10 | 36.53 | 15.85 | 0.15 | 100 | 2125 |
| | | | 15 | 36.61 | 15.84 | 0.18 | 110 | 2130 |
| | | | 25 | 36.28 | 15.77 | 0.10 | 80 | 2135 |
| | | | 35 | 36.94 | 15.84 | | | 2142 |
| | | | 45 | 37.06 | 15.72 | | | 2150 |
| | | 2 | 2.5 | 21.80 | 13.45 | | | 2218 |
| | | | 5 | 35.81 | 16.38 | 0.06 | 80 | 2220 |
| | | | 10 | 36.06 | 16.18 | 0.25 | 95 | 2227 |
| | | | 15 | 36.11 | 15.90 | 0.17 | 125 | 2231 |
| | | | 25 | 36.32 | 15.80 | 0.18 | 160 | 2237 |
| | | | 35 | 36.34 | 15.78 | 0.13 | 170 | 2240 |
| | | | 45 | 36.44 | 15.76 | | | 2245 |
| | | 3 | 2.5 | 22.42 | 13.89 | 0.25 | 90 | 2247 |
| | | | 5 | 34.00 | 15.28 | 0.20 | 90 | 2350 |
| | 3/16 | | 10 | 36.00 | 16.46 | 0.34 | 110 | 0000 |
| | | | 15 | 36.18 | 15.91 | 0.22 | 120 | 0006 |
| | | | 25 | 36.44 | 15.77 | 0.18 | 125 | 0013 |
| | | | 35 | 36.48 | 15.84 | 0.14 | 110 | 0018 |
| | | | 45 | 36.48 | 15.76 | 0.08 | 110 | 0023 |

| Station | Date | Profile | Depth | Salinity | Temperature | Current Speed | Direction | Time |
|---|---|---|---|---|---|---|---|---|
| | | 4 | 2.5 | 21.54 | 13.93 | | 110 | 0040 |
| | | | 5 | 31.46 | 15.42 | 0.38 | 110 | 0045 |
| | | | 10 | 35.94 | 16.53 | 0.24 | 120 | 0052 |
| | | | 15 | 36.17 | 15.93 | 0.15 | 130 | 0057 |
| | | | 25 | 36.41 | 15.84 | 0.00 | 100 | 0105 |
| | | | 35 | 36.50 | 15.82 | 0.07 | 180 | 0109 |
| | | | 45 | 36.71 | 15.83 | 0.00 | 120 | 0115 |
| | | 5 | 2.5 | 24.15 | 14.12 | 1.0 | 130 | 0140 |
| | | | 5 | 26.84 | 15.16 | 0.55 | 120 | 0146 |
| | | | 10 | 36.17 | 16.79 | 0.3 | 130 | 0152 |
| | | | 15 | 36.47 | 16.12 | 0.15 | 150 | 0158 |
| | | | 25 | 36.29 | 15.91 | 0.15 | 90 | 0204 |
| | | | 35 | 36.51 | 15.90 | 0.12 | 90 | 0210 |
| | | | 45 | 36.54 | 15.79 | 0.0 | 100 | 0216 |
| | | 6 | 2.5 | 28.8 | 15.4 | 0.58 | 130 | 0240 |
| | | | 5 | 30.12 | 15.48 | 0.58 | 130 | 0250 |
| | | | 10 | 32.23 | 15.83 | 0.05 | 150 | 0256 |
| | | | 15 | 36.22 | 16.68 | 0.0 | 160 | 0302 |
| | | | 25 | 36.31 | 15.82 | 0.0 | 110 | 0308 |
| | | | 35 | 36.30 | 15.85 | 0.0 | 100 | 0314 |
| | | | 45 | 36.45 | 15.85 | 0.0 | 85 | 0320 |
| | | 7 | 2.5 | 26.54 | 15.15 | 0.85 | 120 | 0335 |
| | | | 5 | 29.83 | 15.77 | 0.75 | 130 | 0341 |
| | | | 10 | 32.32 | 16.16 | 0.34 | 100 | 0345 |
| | | | 15 | 33.16 | 16.55 | 0.28 | 45 | 0351 |
| | | | 25 | 36.30 | 16.00 | 0.15 | 15 | 0357 |
| | | | 35 | 36.40 | 15.9 | 0.28 | 30 | 0403 |
| | | | 45 | 36.31 | 15.9 | 0.22 | 35 | 0410 |

| Station | Date | Profile | Depth | Salinity | Temperature | Current Speed | Direction | Time |
|---|---|---|---|---|---|---|---|---|
| | | 8 | 2.5 | error | | 0.58 | 140 | 0440 |
| | | | 5 | 31.62 | 16.14 | 0.64 | 150 | 0450 |
| | | | 10 | 33.23 | 16.34 | 0.25 | 150 | 0458 |
| | | | 15 | 34.68 | 16.38 | 0.22 | 130 | 0504 |
| | | | 25 | 36.36 | 15.94 | 0.20 | 45 | 0510 |
| | | | 35 | 36.50 | 15.84 | 0.21 | 45 | 0520 |
| | | | 45 | 36.56 | 15.76 | 0.17 | 50 | 0528 |
| | | 9 | 2.5 | 29.28 | 14.69 | 0.62 | 160 | 0541 |
| | | | 5 | 31.91 | 16.34 | 0.70 | 200 | 0600 |
| | | | 10 | 33.79 | 16.58 | 0.35 | 90 | 0608 |
| | | | 15 | 36.31 | 16.64 | 0.35 | 90 | 0618 |
| | | | 25 | 37.60 | 15.92 | 0.25 | 55 | 0628 |
| | | | 35 | 36.96 | 16.01 | 0.25 | 55 | 0636 |
| | | | 45 | 36.77 | 15.89 | 0.30 | 65 | 0645 |
| | | 10 | 2.5 | 26.09 | 14.08 | 0.70 | 190 | 0700 |
| | | | 5 | 34.76 | 16.30 | 0.15 | 200 | 0712 |
| | | | 10 | 35.06 | 16.51 | 0.10 | 110 | 0725 |
| | | | 15 | 36.21 | 16.31 | 0.16 | 80 | 0733 |
| | | | 25 | 36.58 | 15.92 | | | 0745 |
| | | | 35 | 36.50 | 15.90 | 0.15 | 72 | 0750 |
| | | | 45 | 36.62 | 15.89 | 0.15 | 75 | 0800 |
| | | 11 | 2.5 | 28.23 | 15.08 | 1.20 | 290 | 0900 |
| | | | 5 | 32.47 | 15.96 | 0.60 | 270 | 0908 |
| | | | 10 | 32.62 | 15.94 | 0.20 | 180 | 0916 |
| | | | 15 | | | | | |
| | | 12 | 2.5 | 30.11 | 15.14 | 1.40 | 360 | 1016 |
| | | | 5 | 28.83 | 15.18 | 1.45 | 360 | 1019 |
| | | | 10 | 29.03 | 15.87 | 1.40 | 360 | 1030 |
| | | | 15 | 35.63 | 16.31 | 0.20 | 270 | 1040 |
| | | | 25 | 36.80 | 16.13 | 0.38 | 180 | 1050 |
| | | | 35 | 37.16 | 16.00 | 0.35 | 180 | 1100 |
| | | | 45 | 37.15 | 16.11 | 0.20 | 180 | 1110 |

| Station | Date | Profile | Depth | Salinity | Temperature | Current Speed | Direction | Time |
|---|---|---|---|---|---|---|---|---|
| | | 13 | 2.5 | 29.65 | 15.70 | 1.00 | 360 | 1133 |
| | | | 5 | 28.84 | 15.58 | 1.00 | 360 | 1143 |
| | | | 10 | 30.81 | 15.60 | 0.60 | 335 | 1154 |
| | | | 15 | 34.03 | 15.77 | 0.35 | 255 | 1203 |
| | | | 25 | 37.31 | 16.01 | 0.60 | 216 | 1212 |
| | | | 35 | 37.17 | 15.96 | 0.50 | 200 | 1216 |
| | | | 45 | 37.14 | 15.97 | 0.45 | 185 | 1225 |
| | | 14 | 2.5 | 25.3 | 14.9 | 1.3 | 360 | 1235 |
| | | | 5 | 25.85 | 14.9 | 1.15 | 360 | 1247 |
| | | | 10 | 27.8 | 15.0 | 0.4 | 345 | 1253 |
| | | | 15 | 35.4 | 15.8 | 0.45 | 245 | 1305 |
| | | | 25 | 38.0 | 16.1 | 0.9 | 220 | 1315 |
| | | | 35 | 38.8 | 16.0 | 0.6 | 225 | 1323 |
| | | | 45 | 37.4 | 16.0 | 0.6 | 200 | 1337 |
| | | 15 | 2.5 | 14.07 | 14.00 | 1.3 | 20 | 1345 |
| | | | 5 | 14.78 | 14.13 | 1.2 | 30 | 1355 |
| | | | 10 | 34.7-35.3 | 15.0-16.2 | 0.5 | 270 | 1400 |
| | | | 15 | 37.82 | 15.92 | 0.46 | 240 | 1410 |
| | | | 25 | 36.71 | 16.21 | 0.70 | 200 | 1418 |
| | | | 35 | 37.15 | 16.13 | 0.60 | 200 | 1425 |
| | | | 45 | 37.05 | 16.08 | 0.55 | 190 | 1435 |
| | | 16 | 2.5 | 11.94 | 13.88 | 1.30 | 355 | 1510 |
| | | | 5 | 12.08 | 13.77 | 1.30 | 360 | 1543 |
| | | | 10 | 34.80 | 16.12 | 1.3 | 360 | 1612 |
| | | | 15 | 33.30 | 15.58 | 1.4 | 360 | 1617 |
| | | | 25 | 36.60 | 16.14 | 1.3 | 340 | 1626 |
| | | | 35 | 36.50 | 16.22 | 1.4 | 20 | 1704 |
| | | | 45 | 36.49 | 16.14 | 1.0 | 340 | 1710 |

| Station | Date | Profile | Depth | Salinity | Temperature | Current Speed | Direction | Time |
|---|---|---|---|---|---|---|---|---|
| | | 17 | 2.5 | 14.56 | 13.68 | 0.60 | 360 | 1720 |
| | | | 5 | 26.04 | 14.12 | 0.20 | 270 | 1742 |
| | | | 10 | 30.51 | 15.47 | 0.30 | 270 | 1755 |
| | | | 15 | 33.63 | 15.79 | 0.70 | 225 | 1805 |
| | | | 25 | 35.00 | 16.18 | 0.80 | 225 | 1810 |
| | | | 35 | 36.25 | 16.24 | 0.70 | 160 | 1825 |
| | | | 45 | 36.24 | 16.28 | 0.50 | 180 | 1845 |
| | | 18 | 2.5 | 19.90 | 13.94 | | | 1910 |
| | | | 5 | 19.90 | 13.92 | 0.2 | 320 | 1930 |
| | | | 10 | 21.28 | 14.65 | 0.5 | 250 | 1958 |
| | | | 15 | 30.05 | 15.85 | 0.8 | 250 | 2003 |
| | | | 25 | 35.75 | 16.19 | 0.70 | 200 | 2015 |
| | | | 35 | 35.70 | 16.25 | 0.64 | 180 | 2025 |
| | | | 45 | 35.76 | 16.22 | 0.60 | 160 | 2032 |
| | | 19 | | | | 0.2 | | |
| | | | 5 | 20.82 | 14.10 | | | 2058 |
| | | | 10 | 28.88 | 15.42 | 0.4 | 270 | 2130 |
| | | | 15 | 31.08 | 16 08 | 1.0 | 250 | 2200 |
| | | | 25 | 32.00 | 16.20 | 1.1 | 225 | 2210 |
| | | | 35 | 35.14 | 16.16 | 1.0 | 180 | 2117 |
| | | | 45 | 35.20 | 16.25 | 0.7 | 180 | 2250 |
| | | 20 | | | | | | |
| | | | 5 | | | 0.1 | 270 | 2300 |
| | | | 10 | 26.00 | 15.81 | 0.7 | 220 | 2322 |
| | | | 15 | 27.78 | 15.89 | 0.8 | 205 | 2338 |
| | | | 25 | 34.40 | 15.35 | 0.6 | 198 | 2352 |
| | | | 35 | 34.35 | 15.92 | 1.1 | 200 | 2356 |
| | 3/17 | | 45 | 34.58 | 15.92 | 0.3 | 190 | 0006 |
| | | 21 | 2.5 | | | | | |
| | | | 5 | 24.80 | 15.1 | 0.7 | 320 | 0040 |
| | | | 10 | 27.6 | 15.5 | 0.5 | 350 | 0050 |
| | | | 15 | 24.0 | 15.04 | 0.6 | 230 | 0105 |
| | | | 25 | 31.8 | 16.07 | 0.8 | 220 | 0120 |
| | | | 35 | | | 1.0 | 200 | 0200 |
| | | | 45 | 38.7 | 15.66 | 1.2 | 110 | 0230 |

| Station | Date | Profile | Depth | Salinity | Temperature | Current Speed | Direction | Time |
|---|---|---|---|---|---|---|---|---|
| | | 22 | | | | | | |
| | | | 5 | 25.4 | 15.04 | 0.6 | 360 | 0255 |
| | | | 10 | 26.2 | 15.52 | 0.5 | 285 | 0313 |
| | | | 15 | 27.2 | 15.30 | 1.2 | 200 | 0332 |
| | | | 25 | 32.92 | 15.80 | 0.9 | 190 | 0350 |
| | | | 35 | 33.26 | 15.63 | 1.0 | 185 | 0410 |
| | | | 45 | 33.70 | 15.60 | 0.8 | 185 | 0420 |
| | | 23 | | | | | | |
| | | | 5 | 25.9 | 14.90 | 0.8 | 345 | 0500 |
| | | | 10 | 25.92 | 14.95 | 0.5 | 345 | 0515 |
| | | | 15 | 26.3 | 14.97 | 0.8 | 285 | 0525 |
| | | | 25 | 32.88 | 15.76 | 0.7 | 160 | 0535 |
| | | | 35 | 33.05 | 15.72 | 0.8 | 200 | 0545 |
| | | | 45 | 33.34 | 15.61 | 0.6 | 210 | 0555 |
| | | 24 | | | | | | |
| | | | 5 | 25.87 | 14.70 | 0.5 | 360 | 0630 |
| | | | 10 | 28.07 | 15.13 | 0.5 | 340 | 0638 |
| | | | 15 | 27.5 | 15.56 | 0.8 | 260 | 0645 |
| | | | 25 | 33.00 | 15.68 | 0.7 | 210 | 0655 |
| | | | 35 | 33.08 | 15.61 | 0.7 | 200 | 0702 |
| | | | 45 | 33.68 | 15.64 | 0.6 | 200 | 0712 |
| | | 25 | | | | | | |
| | | | 5 | 26.58 | 14.95 | 0.40 | 10 | 0745 |
| | | | 10 | 26.79 | 15.07 | 0.40 | 290 | 0810 |
| | | | 15 | 28.42 | 15.12 | 0.30 | 10 | 0823 |
| | | | 25 | 32.54 | 16.00 | 0.50 | 250 | |
| | | 26 | | | | | | |
| | | | 5 | 28.89 | 15.55 | 0.40 | 320 | 0957 |
| | | | 10 | 27.27 | 15.28 | 0.70 | 350 | 1011 |
| | | | 15 | 27.88 | 15.45 | 0.70 | 280 | 1034 |
| | | | 25 | 31.50 | 15.89 | 0.60 | 265 | 1043 |
| | | | 35 | 33.98 | 15.74 | 0.80 | 260 | 1055 |
| | | | 45 | 34.46 | 15.98 | 0.60 | 265 | 1107 |

| Station | Date | Profile | Depth | Salinity | Temperature | Current Speed | Direction | Time |
|---|---|---|---|---|---|---|---|---|
| | | 27 | | | | | | |
| | | | 5 | | | 0.6 | 80 | |
| | | | 10 | 27.60 | 15.62 | 0.6 | 340 | 1124 |
| | | | 15 | 28.89 | 15.58 | 0.8 | 265 | 1132 |
| | | | 25 | 32.95 | 15.77 | | | 1138 |
| | | | 35 | 34.10 | 15.97 | 0.7 | 280 | 1154 |
| | | | 45 | 34.68 | 16.28 | 0.5 | 280 | 1201 |
| | | 28 | | | | | | |
| | | | 10 | 29.41 | 15.65 | 0.50 | 30 | 1210 |
| | | | 15 | 29.15 | 15.66 | 0.25 | 330 | 1222 |
| | | | 25 | 32.91 | 15.84 | 0.80 | 270 | 1232 |
| | | | 35 | 34.85 | 16.0 | 0.65 | 285 | 1241 |
| | | | 45 | 34.85 | 16.08 | 0.40 | 290 | 1248 |
| | | 29 | 10 | 28.83 | 15.60 | 0.6 | 70 | 1300 |
| | | | 15 | 30.20 | 15.62 | 0.15 | 60 | 1307 |
| | | | 25 | 29.48 | 16.0 | 0.43 | 310 | 1318 |
| | | | 35 | 35.12 | 16.22 | 0.40 | 320 | 1330 |
| | | | 45 | 35.00 | 16.24 | 0.65 | 310 | 1340 |
| | | 30 | 10 | 28.45 | 15.81 | 0.8 | 85 | 1345 |
| | | | 15 | 29.36 | 15.76 | 0.4 | 105 | 1355 |
| | | | 25 | 32.42 | 15.89 | 0.65 | 270 | 1403 |
| | | | 35 | 35.14 | 16.26 | 0.4 | 306 | 1409 |
| | | | 45 | 35.17 | 16.22 | 0.4 | 340 | 1419 |
| | | 31 | 10 | 28.64 | 15.77 | 0.40 | 90 | 1429 |
| | | | 15 | 29.45 | 15.62 | 0.15 | 65 | 1442 |
| | | | 25 | 35.0 | 15.92 | 0.68 | 300 | 1452 |
| | | | 35 | 35.45 | 16.28 | 0.52 | 345 | 1500 |
| | | | 45 | 35.41 | 16.15 | 0.45 | 350 | 1510 |
| | | 32 | 5 | 29.04 | 15.86 | 0.65 | 95 | 1522 |
| | | | 10 | 29.45 | 15.66 | 0.10 | 85 | 1532 |
| | | | 15 | 31.45 | 15.76 | 0.18 | 45 | 1542 |
| | | | 25 | 35.85 | 16.14 | 0.55 | 345 | 1554 |

| Station | Date | Profile | Depth | Salinity | Temperature | Current Speed | Direction | Time |
|---|---|---|---|---|---|---|---|---|
| | | | 35 | 35.89 | 16.18 | 0.40 | 306 | 1610 |
| | | | 45 | 35.73 | 16.30 | 0 40 | 324 | 1617 |
| | | 33 | 5 | 29.15 | 15.92 | 0.70 | 90 | 1622 |
| | | | 10 | 29.28 | 15.77 | 0.30 | 90 | 1630 |
| | | | 15 | 31.45 | 15.92 | 0.55 | 270 | 1658 |
| | | | 25 | 35.55 | 16.26 | 0.38 | 345 | 1708 |
| | | | 35 | 35.44 | 16.24 | 0.35 | 345 | 1717 |
| | | | 45 | 35.66 | 16.21 | 0.42 | 345 | 1727 |
| | | 34 | 5 | 29.25 | 15.91 | 0.35 | 95 | 1818 |
| | | | 10 | 29.55 | 15.82 | 0.10 | 90 | 1822 |
| | | | 15 | 31.71 | 15.92 | 0.32 | 250 | 1829 |
| | | | 25 | 35.12 | 16.29 | 0.30 | 320 | 1837 |
| | | | 35 | 35.55 | 16.30 | 0.25 | 350 | 1852 |
| | | | 45 | 35.91 | 16.26 | 0.30 | 360 | 1902 |
| | | 35 | 5 | 29.24 | 16.05 | 0.30 | 225 | 1911 |
| | | | 10 | 31.76 | 15.92 | 0.30 | 288 | 1919 |
| | | | 15 | 33.00 | 16.24 | 0.10 | 306 | 1923 |
| | | | 25 | 35.88 | 16.32 | 0.10 | 342 | 1937 |
| | | | 35 | 35.82 | 16.40 | 0.25 | N | 1947 |
| | | | 45 | 36.10 | 16.25 | 0.30 | 350 | 1955 |
| | | 36 | 5 | 32.42 | 16.99 | 0.5 | 195 | 2005 |
| | | | 10 | 34.0 | 16.24 | 0.45 | 170 | 2018 |
| | | | 15 | 33.66 | 16.15 | 0.42 | 180 | 2027 |
| | | | 25 | 35.81 | 16.25 | 0.10 | 270 | 2036 |
| | | | 35 | 35.72 | 16.33 | 0.3 | 0 | 2045 |
| | | | 45 | 36.05 | 16.11 | 0.33 | 40 | 2055 |
| | | 37 | 5 | 33.03 | 16.14 | 0.32 | 170 | 2105 |
| | | | 10 | 33.08 | 16.26 | 0.62 | 170 | 2115 |
| | | | 15 | 33.58 | 16.25 | 0.48 | 185 | 2124 |
| | | | 25 | 34.12 | 16.18 | 0.36 | 100 | 2148 |
| | | | 35 | 36.08 | 16.24 | 0.34 | 75 | 2200 |
| | | | 45 | 36.28 | 16.17 | 0.28 | 360 | 2210 |

| Station | Date | Profile | Depth | Salinity | Temperature | Current Speed | Direction | Time |
|---|---|---|---|---|---|---|---|---|
| | | 38 | 5 | 33.66 | 16.18 | 0.38 | 175 | 2218 |
| | | | 10 | 33.45 | 16.25 | 0.45 | 165 | 2228 |
| | | | 15 | 35.05 | 16.18 | 0.58 | 165 | 2236 |
| | | | 25 | 35.65 | 16.28 | 0.38 | 175 | 2247 |
| | | | 35 | 36.05 | 16.32 | 0.32 | 105 | 2254 |
| | | | 45 | 36.62 | 16.16 | 0.25 | 75 | 2303 |
| | | 39 | 5 | 33.25 | 16.10 | 0.78 | 170 | 2311 |
| | | | 10 | 33.75 | 16.24 | 0.65 | 165 | 2322 |
| | | | 15 | 34.34 | 16.28 | 0.65 | 165 | 2329 |
| | | | 25 | 35.64 | 16.32 | 0.50 | 105 | 2340 |
| | | | 35 | 36.24 | 16.27 | 0.50 | 110 | 2350 |
| | | | 45 | 36.71 | 16.18 | 0.48 | 100 | 2359 |
| | 3/18 | 40 | 5 | 32.62 | 15.92 | 0.65 | 180 | 0013 |
| | | | 10 | 33.81 | 16.05 | 0.70 | 140 | 0022 |
| | | | 15 | 32.59 | 16.17 | 0.50 | 160 | 0029 |
| | | | 25 | 35.41 | 16.12 | 0.60 | 110 | 0038 |
| | | | 35 | 36.41 | 16.28 | 0.60 | 100 | 0047 |
| | | | 45 | 36.50 | 16.19 | 0.55 | 100 | 0055 |
| | | 41 | 5 | 33.47 | 16.09 | 0.85 | 170 | 0112 |
| | | | 10 | 32.70 | 16.07 | 0.80 | 150 | 0125 |
| | | | 15 | 33.89 | 16.05 | 0.70 | 180 | 0133 |
| | | | 25 | 35.37 | 16.29 | 0.55 | 180 | 0141 |
| | | | 35 | 36.37 | 16.27 | 0.50 | 120 | 0151 |
| | | | 45 | 36.29 | 16.16 | 0.60 | 110 | 0200 |
| | | 42 | 5 | 31.62 | 15.81 | 0.90 | 140 | 0218 |
| | | | 10 | 33.03 | 16.00 | 0.80 | 150 | 0250 |
| | | | 15 | 32.13 | 15.91 | 0.80 | 160 | 0258 |
| | | | 25 | 34.75 | 16.17 | 0.65 | 200 | 0307 |
| | | | 35 | 36.02 | 16.24 | 0.55 | 160 | 0317 |
| | | | 45 | 36.10 | 16.18 | 0.45 | 150 | 0326 |

| Station | Date | Profile | Depth | Salinity | Temperature | Current Speed | Direction | Time |
|---|---|---|---|---|---|---|---|---|
| | | 43 | 5 | 28.93 | 15.57 | 0.68 | 120 | 0345 |
| | | | 10 | 29.11 | 15.62 | 0.70 | 140 | 0352 |
| | | | 15 | 32.64 | 15.93 | 0.95 | 210 | 0400 |
| | | | 25 | 34.31 | 16.98 | 0.65 | 230 | 0407 |
| | | | 35 | 35.64 | 16.28 | 0.50 | 170 | 0414 |
| | | | 45 | 35.70 | 16.12 | 0.65 | 165 | 0423 |
| | | 44 | 5 | 28.53 | 15.46 | 0.85 | 120 | 0434 |
| | | | 10 | 29.20 | 15.61 | 0.75 | 150 | 0441 |
| | | | 15 | 30.30 | 15.92 | 0.80 | 220 | 0447 |
| | | | 25 | 34.29 | 16.07 | 0.70 | 230 | 0454 |
| | | | 35 | 35.10 | 16.23 | 0.50 | 180 | 0500 |
| | | | 45 | 35.29 | 16.06 | 0.65 | 170 | 0507 |
| | | 45 | 5 | 26.53 | 15.40 | 0.75 | 130 | 0536 |
| | | | 10 | 29.51 | 15.62 | 0.70 | 160 | 0543 |
| | | | 15 | 32.81 | 15.73 | 1.50 | 200 | 0550 |
| | | | 25 | 34.12 | 15.90 | 0.70 | 220 | 0600 |
| | | | 35 | 34.78 | 16.17 | 0.60 | 210 | 0608 |
| | | | 45 | 35.27 | 16.16 | 0.45 | 200 | 0615 |
| | | 46 | 5 | 28.96 | 15.55 | 0.75 | 150 | 0634 |
| | | | 10 | 31.98 | 15.74 | 0.85 | 170 | 0641 |
| | | | 15 | 33.76 | 15.75 | 0.80 | 210 | 0649 |
| | | | 25 | 34.15 | 16.00 | 0.70 | 234 | 0654 |
| | | | 35 | 35.16 | 16.04 | 0.65 | 207 | 0709 |
| | | | 45 | 35.33 | 16.20 | 0.65 | 180 | 0717 |
| | | 47 | 5 | 29.94 | 15.72 | 0.90 | 160 | 0726 |
| | | | 10 | 31.12 | 15.73 | 0.90 | 180 | 0733 |
| | | | 15 | 33.82 | 15.73 | 0.85 | 200 | 0740 |
| | | | 25 | 34.20 | 15.75 | 0.70 | 220 | 0748 |
| | | | 35 | 34.55 | 15.97 | 0.70 | 200 | 0800 |
| | | | 45 | | | 0.65 | 180 | 0808 |

| Station | Date | Profile | Depth | Salinity | Temperature | Current Speed | Direction | Time |
|---|---|---|---|---|---|---|---|---|
| | | 48 | 5 | 29.75 | 15.78 | 0.92 | 170 | 0821 |
| | | | 10 | 31.55 | 15.78 | 0.95 | 170 | 0835 |
| | | | 15 | 33.90 | 15.90 | 0.88 | 200 | 0840 |
| | | | 25 | 34.40 | 15.98 | 0.65 | 192 | 0847 |
| | | | 35 | 34.88 | 16.00 | 0.72 | 200 | 0855 |
| | | | 45 | 35.34 | 16.24 | 0.75 | 180 | 0914 |
| | | 49 | 5 | 30.56 | 15.68 | 0.85 | 180 | 0920 |
| | | | 10 | 31.65 | 15.78 | 1.50 | 180 | 0934 |
| | | | 15 | 33.92 | 15.82 | 1.40 | 200 | 0946 |
| | | | 25 | 34.58 | 15.84 | 0.55 | 220 | 0948 |
| | | | 35 | 35.23 | 15.92 | 0.65 | 200 | 0957 |
| | | | 45 | 35.45 | 16.00 | 0.75 | 180 | 1005 |
| | | 50 | 5 | 31.73 | 15.82 | 0.75 | 180 | 1025 |
| | | | 10 | 33.19 | 15.81 | 0.85 | 180 | 1032 |
| | | | 15 | 34.71 | 15.73 | 0.75 | 200 | 1040 |
| | | | 25 | 35.10 | 15.83 | 0.55 | 200 | 1053 |
| | | | 35 | 35.25 | 15.86 | 0.65 | 190 | 1102 |
| | | | 45 | 35.58 | 15.93 | 0.75 | 200 | 1113 |
| | | 51 | 5 | 31.85 | 15.82 | 0.75 | 180 | 1130 |
| | | | 10 | 32.09 | 15.66 | 0.85 | 190 | 1150 |
| | | | 15 | 34.56 | 15.79 | 0.60 | 200 | 1154 |
| | | | 25 | 34.55 | 16.00 | 0.45 | 234 | 1200 |
| | | | 35 | 34.64 | 15.72 | 0.55 | 216 | 1210 |
| | | | 45 | 35.12 | 15.81 | 0.65 | 198 | 1214 |
| | | 52 | 5 | 31.81 | 15.89 | 0.75 | 180 | 1222 |
| | | | 10 | 34.19 | 15.79 | 0.65 | 180 | 1233 |
| | | | 15 | 34.94 | 15.72 | 0.50 | 200 | 1251 |
| | | | 25 | 35.99 | 15.75 | 0.40 | 220 | 1255 |
| | | | 35 | 35.01 | 15.68 | 0.60 | 230 | 1304 |
| | | | 45 | 35.0 | 15.70 | 0.70 | 200 | 1312 |

| Station | Date | Profile | Depth | Salinity | Temperature | Current Speed | Direction | Time |
|---|---|---|---|---|---|---|---|---|
| | | 53 | 5 | 32.12 | 15.61 | 0.75 | 190 | 1318 |
| | | | 10 | 34.15 | 15.65 | 0.55 | 200 | 1327 |
| | | | 15 | 34.64 | 16.06 | 0.50 | 200 | 1332 |
| | | | 25 | 34.44 | 15.96 | 0.40 | 224 | 1342 |
| | | | 35 | 34.70 | 15.75 | 0.55 | 220 | 1355 |
| | | | 45 | 34.78 | 15.78 | 0.70 | 198 | 1405 |
| | | 54 | 5 | 34.15 | 15.80 | 0.60 | 200 | 1425 |
| | | | 10 | 34.55 | 15.80 | 0.55 | 200 | 1438 |
| | | | 15 | 34.42 | 15.78 | 0.40 | 216 | 1500 |
| | | | 25 | 34.23 | 15.76 | 0.40 | 234 | 1514 |
| | | | 35 | 34.37 | 15.61 | 0.40 | 180 | 1532 |
| | | | 45 | 34.55 | 15.62 | 0.60 | 198 | 1542 |
| | | 55 | 5 | 34.26 | 15.87 | 0.45 | 216 | 1548 |
| | | | 10 | 34.38 | 15.79 | 0.40 | 210 | 1605 |
| | | | 15 | 33.96 | 15.80 | 0.35 | 200 | 1608 |
| | | | 25 | 34.20 | 15.82 | 0.30 | 216 | 1620 |
| | | | 35 | 34.52 | 15.74 | 0.55 | 216 | 1630 |
| | | | 45 | 34.75 | 15.61 | 0.65 | 207 | 1628 |
| | | 56 | 5 | 33.47 | 16.07 | 0.50 | 198 | 1643 |
| | | | 10 | 34.12 | 15.84 | 0.45 | 216 | 1703 |
| | | | 15 | 33.94 | 15.77 | 0.30 | 225 | 1707 |
| | | | 25 | 34.25 | 15.70 | 0.30 | 210 | 1719 |
| | | | 35 | 34.35 | 15.58 | 0.50 | 195 | 1721 |
| | | | 45 | 34.4 | 15.53 | 0.55 | 195 | 1735 |
| | | 57 | 5 | 33.34 | 16.1 | 0.30 | 155 | 1744 |
| | | | 10 | 34.01 | 15.70 | 0.50 | 265 | 1753 |
| | | | 15 | 34.14 | 15.83 | 0.35 | 190 | 1807 |
| | | | 25 | 34.22 | 15.75 | 0.45 | 190 | 1817 |
| | | | 35 | 34.41 | 15.54 | 0.50 | 200 | 1825 |
| | | | 45 | 34.46 | 15.5 | 0.55 | 200 | 1833 |

| Station | Date | Profile | Depth | Salinity | Temperature | Current Speed | Direction | Time |
|---|---|---|---|---|---|---|---|---|
| | | 58 | 5 | 33.62 | 16.12 | 0.50 | 270 | 1842 |
| | | | 10 | 33.84 | 16.15 | 0.45 | 234 | 1845 |
| | | | 15 | 35.50 | 15.82 | 0.30 | 216 | 1852 |
| | | | 25 | 34.51 | 15.72 | 0.35 | 198 | 1858 |
| | | | 35 | 34.42 | 15.48 | 0.40 | 225 | 1905 |
| | | | 45 | 34.50 | 15.54 | 0.60 | 198 | 1917 |
| | | 59 | 5 | 33.95 | 16.24 | 0.45 | 252 | 1924 |
| | | | 10 | 34.14 | 16.02 | 0.40 | 225 | 1936 |
| | | | 15 | 34.05 | 15.86 | 0.35 | 216 | 1945 |
| | | | 25 | 34.16 | 15.72 | 0.40 | 198 | 1954 |
| | | | 35 | 34.62 | 15.56 | 0.50 | 198 | 2001 |
| | | | 45 | 34.42 | 15.58 | 0.55 | 198 | 2007 |
| | | 60 | 5 | 33.93 | 16.05 | 0.20 | 270 | 2014 |
| | | | 10 | 33.96 | 16.06 | 0.30 | 234 | 2024 |
| | | | 15 | 36.69 | 15.97 | 0.25 | 216 | 2031 |
| | | | 25 | 34.40 | 15.78 | 0.45 | 189 | 2039 |
| | | | 35 | 34.48 | 15.58 | 0.50 | 198 | 2047 |
| | | | 45 | 34.94 | 15.50 | 0.55 | 198 | 2055 |
| | | 61 | 5 | 34.49 | 16.09 | 0.10 | 288 | 2106 |
| | | | 10 | 34.66 | 15.97 | 0.15 | 220 | 2114 |
| | | | 15 | 36.77 | 16.98 | 0.30 | 216 | 2120 |
| | | | 25 | 33.53 | 15.70 | 0.55 | 180 | 2140 |
| | | | 35 | 33.57 | 15.75 | 0.50 | 180 | 2148 |
| | | | 45 | 33.70 | 15.65 | 0.55 | 198 | 2154 |
| | | 62 | 5 | 33.42 | 15.99 | 0.10 | 342 | 2200 |
| | | | 10 | 33.50 | 16.03 | 0.20 | 188 | 2218 |
| | | | 15 | 33.46 | 15.97 | 0.30 | 198 | 2228 |
| | | | 25 | 33.49 | 15.94 | 0.45 | 180 | 2236 |
| | | | 35 | 33.87 | 15.57 | 0.65 | 180 | 2246 |
| | | | 45 | 33.92 | 15.48 | 0.70 | 190 | 2254 |

| Station | Date | Profile | Depth | Salinity | Temperature | Current Speed | Direction | Time |
|---|---|---|---|---|---|---|---|---|
| | | 63 | 5 | 33.94 | 15.99 | 0.05 | 324 | 2304 |
| | | | 10 | 33.72 | 16.03 | 0.25 | 144 | 2313 |
| | | | 15 | 33.76 | 16.06 | 0.35 | 162 | 2324 |
| | | | 25 | 33.74 | 16.05 | 0.50 | 180 | 2334 |
| | | | 35 | 33.98 | 15.64 | 0.75 | 180 | 2344 |
| | | | 45 | 34.06 | 15.44 | 0.70 | 171 | 2357 |
| | 3/19 | 64 | 5 | 33.60 | 16.02 | 0.05 | 108 | 0010 |
| | | | 10 | 33.78 | 16.08 | 0.30 | 115 | 0022 |
| | | | 15 | 33.67 | 15.97 | 0.35 | 135 | 0030 |
| | | | 25 | 33.70 | 16.17 | 0.55 | 170 | 0042 |
| | | | 35 | 34.02 | 15.40 | 0.85 | 175 | 0054 |
| | | | 45 | 34.0 | 15.41 | 0.75 | 180 | 0105 |
| | | 65 | 5 | 33.46 | 15.92 | 0.05 | 100 | 0112 |
| | | | 10 | 33.38 | 15.98 | 0.35 | 105 | 0122 |
| | | | 15 | 33.42 | 15.95 | 0.50 | 100 | 0131 |
| | | | 25 | 33.46 | 15.95 | 0.55 | 165 | 0141 |
| | | | 35 | 34.0 | 15.32 | 0.85 | 185 | 0150 |
| | | | 45 | 34.05 | 15.38 | 0.70 | 180 | 0200 |
| | | 66 | 5 | 32.64 | 16.04 | 0.55 | 130 | 0212 |
| | | | 10 | 32.58 | 16.08 | 0.80 | 110 | 0221 |
| | | | 15 | 32.7 | 15.84 | 0.80 | 135 | 0231 |
| | | | 25 | 33.93 | 15.49 | 0.85 | 170 | 0241 |
| | | | 35 | 34.03 | 15.34 | 0.75 | 175 | 0250 |
| | | | 45 | 34.13 | 14.43 | 0.60 | 175 | 0300 |
| | | 67 | 5 | 32.2 | 16.18 | 0.10 | 100 | 0312 |
| | | | 10 | 32.3 | 16.0 | 0.70 | 105 | 1323 |
| | | | 15 | 32.7 | 16.1 | 0.75 | 135 | 0331 |
| | | | 25 | 33.83 | 15.68 | 0.85 | 170 | 0340 |
| | | | 35 | 34.08 | 15.39 | 0.75 | 180 | 0347 |
| | | | 45 | 34.04 | 15.36 | 0.65 | 180 | 0357 |

| Station | Date | Profile | Depth | Salinity | Temperature | Current Speed | Direction | Time |
|---|---|---|---|---|---|---|---|---|
| | | 68 | 5 | 32.3 | 16.31 | 0.10 | 80 | 0407 |
| | | | 10 | 32.9 | 16.11 | 1.50 | 115 | 0426 |
| | | | 15 | 31.73 | 16.24 | 1.10 | 140 | 0434 |
| | | | 25 | 33.2 | 16.01 | 1.40 | 185 | 0443 |
| | | | 35 | 34.08 | 15.64 | 1.50 | 205 | 0452 |
| | | | 45 | 34.26 | 15.40 | 0.84 | 210 | 0502 |
| | | 69 | 5 | 28.65 | 16.72 | 0.90 | 100 | 0514 |
| | | | 10 | 29.78 | 16.56 | 0.75 | 135 | 0524 |
| | | | 15 | 31.58 | 16.50 | 0.65 | 170 | 0534 |
| | | | 25 | 32.84 | 16.23 | 0.90 | 185 | 0544 |
| | | | 35 | 34.11 | 15.92 | 0.85 | 220 | 0554 |
| | | | 45 | 34.28 | 15.56 | 0.70 | 280 | 0604 |
| | | 70 | 5 | 28.76 | 16.67 | 1.90 | 100 | 0616 |
| | | | 10 | 31.92 | 16.30 | 1.10 | 135 | 0625 |
| | | | 15 | 32.44 | 16.27 | 0.75 | 175 | 0633 |
| | | | 25 | 34.21 | 15.94 | 0.70 | 205 | 0641 |
| | | | 35 | 34.30 | 16.00 | 0.65 | 230 | 0650 |
| | | | 45 | 34.32 | 15.86 | 0.45 | 235 | 0659 |
| | | 71 | 5 | 30.88 | 16.62 | 0.75 | 110 | 0708 |
| | | | 10 | 32.04 | 16.30 | 0.70 | 155 | 0717 |
| | | | 15 | 32.47 | 16.24 | 0.65 | 160 | 0725 |
| | | | 25 | 34.14 | 16.05 | 0.55 | 210 | 0732 |
| | | | 35 | 34.36 | 16.0 | 0.55 | 220 | 0739 |
| | | | 45 | 34.45 | 15.8 | 0.35 | 220 | 0747 |
| | | 72 | 5 | 30.43 | 16.61 | 0.75 | 135 | 0811 |
| | | | 10 | 32.70 | 16.02 | 0.65 | 170 | 0819 |
| | | | 15 | 33.68 | 15.94 | 0.45 | 188 | 0826 |
| | | | 25 | 34.65 | 16.19 | 0.35 | 235 | 0830 |
| | | | 35 | 34.71 | 15.82 | 0.35 | 235 | 0838 |
| | | | 45 | 34.68 | 15.89 | 0.35 | 235 | 0845 |

| Station | Date | Profile | Depth | Salinity | Temperature | Current Speed | Direction | Time |
|---|---|---|---|---|---|---|---|---|
| | | 73 | 5 | 32.12 | 16.24 | 0.80 | 135 | 0850 |
| | | | 10 | 33.41 | 5.92 | 0.60 | 162 | 0905 |
| | | | 15 | 34.45 | .15 | 0.30 | 180 | 0915 |
| | | | 25 | 34.74 | .06 | 0.30 | 216 | 092C |
| | | | 35 | 35.02 | 15.78 | 0.30 | 234 | 0930 |
| | | | 45 | 35.12 | 15.84 | 0.35 | 235 | 0940 |
| | | 74 | 5 | 31.80 | 16.51 | 0.65 | 120 | 0955 |
| | | | 10 | 33.05 | 15.99 | 0.40 | 160 | 1005 |
| | | | 15 | 35.49 | 16.37 | 0.35 | 180 | 1015 |
| | | | 25 | 36.12 | 15.81 | 0.45 | 210 | 1025 |
| | | | 35 | 35.53 | 15.84 | 0.35 | 250 | 1035 |
| | | | 45 | 35.65 | 15.85 | 0.25 | 250 | 1047 |
| | | 75 | 5 | 33.37 | 16.45 | 0.65 | 150 | 1100 |
| | | | 10 | 35.05 | 16.18 | 0.30 | 162 | 1109 |
| | | | 15 | 35.84 | 16.39 | 0.25 | 198 | 1118 |
| | | | 25 | 36.44 | 16.17 | 0.40 | 225 | 1125 |
| | | | 35 | 36.67 | 15.90 | 0.45 | 216 | 1133 |
| | | | 45 | 36.06 | 15.76 | 0.35 | 180 | 1141 |
| | | 76 | 5 | 33.45 | 16.98 | 0.10 | 234 | 1147 |
| | | | 10 | 34.86 | 16.44 | 0.30 | 234 | 1200 |
| | | | 15 | 36.10 | 16.39 | 0.40 | 270 | 1207 |
| | | | 25 | 36.02 | 16.30 | 0.45 | 250 | 1215 |
| | | | 35 | 35.68 | 15.90 | 0.30 | 198 | 1225 |
| | | | 45 | 35.65 | 15.80 | 0.35 | 200 | 1233 |
| | | 77 | 5 | 28.84 | 18.00 | 0.25 | 234 | 1245 |
| | | | 10 | 34.62 | 16.56 | 0.25 | 250 | 1307 |
| | | | 15 | 35.15 | 16.52 | 0.30 | 270 | 1315 |
| | | | 25 | 36.42 | 16.10 | 0.35 | 270 | 1320 |
| | | | 35 | 35.65 | 15.90 | 0.35 | 270 | 1332 |
| | | | 45 | 35.58 | 15.92 | 0.35 | 252 | 1340 |

| Station | Date | Profile | Depth | Salinity | Temperature | Current Speed | Direction | Time |
|---|---|---|---|---|---|---|---|---|
| | | 78 | 5 | 31.42 | 17.72 | 0.10 | 279 | 1350 |
| | | | 10 | 34.25 | 16.79 | 0.25 | 228 | 1403 |
| | | | 15 | 35.40 | 16.48 | 0.20 | 288 | 1413 |
| | | | 25 | 35.79 | 16.09 | 0.45 | 198 | 1455 |
| | | | 35 | 35.56 | 15.92 | 0.45 | 262 | 1505 |
| | | | 45 | 35.55 | 15.90 | 0.30 | 270 | 1512 |
| | | 79 | 5 | 28.00 | 17.98 | 0.15 | 36 | 1557 |
| | | | 10 | 34.18 | 16.50 | 0.20 | 216 | 1610 |
| | | | 15 | 34.96 | 16.56 | 0.25 | 270 | 1615 |
| | | | 25 | 35.54 | 15.94 | 0.35 | 270 | 1624 |
| | | | 35 | 35.43 | 15.86 | 0.40 | 252 | 1637 |
| | | | 45 | 35.29 | 15.87 | 0.45 | 270 | 1645 |
| | | 80 | 5 | 29.14 | 17.76 | 0.10 | 315 | 1700 |
| | | | 10 | 34.22 | 16.59 | 0.20 | 322 | 1708 |
| | | | 15 | 33.55 | 16.26 | 0.35 | 315 | 1717 |
| | | | 25 | 35.36 | 15.96 | 0.30 | 298 | 1725 |
| | | | 35 | 35.34 | 15.92 | 0.25 | 262 | 1733 |
| | | | 45 | 35.36 | 15.88 | 0.30 | 270 | 1740 |
| | | 81 | 5 | 23.30 | 17.67 | 0.05 | 330 | 1837 |
| | | | 10 | 34.17 | 16.30 | 0.10 | 320 | 1845 |
| | | | 15 | 34.90 | 16.24 | 0.25 | 280 | 1856 |
| | | | 25 | 35.23 | 15.97 | 0.30 | 290 | 1904 |
| | | | 35 | 35.25 | 15.92 | 0.35 | 270 | 1912 |
| | | | 45 | 35.15 | 15.91 | 0.30 | 275 | 1920 |
| | | 82 | 5 | 23.63 | 17.44 | 0.05 | 330 | 1935 |
| | | | 10 | 33.76 | 16.35 | 0.15 | 300 | 1944 |
| | | | 15 | 34.33 | 16.35 | 0.25 | 290 | 1952 |
| | | | 25 | 35.24 | 15.90 | 0.30 | 270 | 2000 |
| | | | 35 | 35.18 | 15.96 | 0.30 | 270 | 2010 |
| | | | 45 | 35.16 | 16.08 | 0.30 | 280 | 2019 |

| Station | Date | Profile | Depth | Salinity | Temperature | Current Speed | Direction | Time |
|---|---|---|---|---|---|---|---|---|
| | | 83 | 5 | 24.30 | 17.28 | 0.05 | 340 | 2030 |
| | | | 10 | 34.93 | 16.37 | 0.15 | 270 | 2038 |
| | | | 15 | 34.90 | 16.45 | 0.15 | 270 | 2043 |
| | | | 25 | 35.30 | 15.90 | 0.25 | 255 | 2053 |
| | | | 35 | 35.20 | 15.90 | 0.25 | 270 | 2103 |
| | | | 45 | 35.23 | 15.95 | 0.20 | 260 | 2111 |
| | | 84 | 5 | 24.08 | 17.40 | 0.10 | 360 | 2127 |
| | | | 10 | 34.28 | 16.38 | 0.05 | 70 | 2135 |
| | | | 15 | 34.66 | 16.32 | 0.15 | 270 | 2144 |
| | | | 25 | 34.80 | 16.08 | 0.30 | 210 | 2153 |
| | | | 35 | 35.20 | 15.88 | 0.3[illegible] | 270 | 2201 |
| | | | 45 | 35.30 | 15.96 | 0.25 | 270 | 2210 |
| | | 85 | 5 | 23.51 | 17.42 | 0.10 | 270 | 2223 |
| | | | 10 | 34.77 | 16.43 | 0.15 | 260 | 2232 |
| | | | 15 | 34.74 | 16.52 | 0.10 | 250 | 2239 |
| | | | 25 | 35.31 | 15.84 | 0.20 | 225 | 2246 |
| | | | 35 | 35.42 | 15.94 | 0.25 | 260 | 2253 |
| | | | 45 | 35.34 | 15.98 | 0.20 | 255 | 2300 |
| | | 86 | 5 | 24.46 | 17.30 | 0.10 | 110 | 2315 |
| | | | 10 | 33.85 | 16.65 | 0.05 | 110 | 2323 |
| | | | 15 | 34.75 | 16.57 | 0.15 | 170 | 2330 |
| | | | 25 | 35.23 | 16.03 | 0.15 | 205 | 2338 |
| | | | 35 | 35.40 | 15.88 | 0.20 | 250 | 2350 |
| | | | 45 | 35.28 | 15.94 | 0.15 | 243 | 2357 |
| | 3/20 | 87 | 5 | 26.70 | 17.04 | 0.15 | 126 | 0000 |
| | | | 10 | 33.14 | 16.65 | 0.15 | 180 | 0010 |
| | | | 15 | 34.90 | 16.36 | 0.25 | 162 | 0020 |
| | | | 25 | 35.27 | 15.92 | 0.15 | 198 | 0030 |
| | | | 35 | 35.28 | 15.92 | 0.10 | 216 | 0040 |
| | | | 45 | 35.42 | 15.93 | 0.10 | 234 | 0050 |

| Station | Date | Profile | Depth | Salinity | Temperature | Current Speed | Direction | Time |
|---|---|---|---|---|---|---|---|---|
| | | 88 | 5 | 32.47 | 16.93 | 0.25 | 118 | 0100 |
| | | | 10 | 32.41 | 16.81 | 0.20 | 154 | 0110 |
| | | | 15 | 34.73 | 16.52 | 0.20 | 154 | 0120 |
| | | | 25 | 35.18 | 15.88 | 0.25 | 180 | 0130 |
| | | | 35 | 35.24 | 15.90 | 0.15 | 198 | 0140 |
| | | | 45 | 35.39 | 15.97 | 0.25 | 198 | 0150 |
| | | 89 | 5 | 31.82 | 16.94 | 0.30 | 180 | 0200 |
| | | | 10 | 33.34 | 17.03 | 0.20 | 144 | 0210 |
| | | | 15 | 34.78 | 16.45 | 0.25 | 144 | 0220 |
| | | | 25 | 35.09 | 15.90 | 0.20 | 180 | 0230 |
| | | | 35 | 35.30 | 15.93 | 0.15 | 216 | 0240 |
| | | | 45 | 35.32 | 15.93 | 0.10 | 208 | 0250 |
| | | 90 | 5 | 32.08 | 16.80 | 0.40 | 130 | 0300 |
| | | | 10 | 33.50 | 16.85 | 0.25 | 134 | 0310 |
| | | | 15 | 34.62 | 16.64 | 0.25 | 134 | 0320 |
| | | | 25 | 35.14 | 15.98 | 0.30 | 162 | 0330 |
| | | | 35 | 35.22 | 15.86 | 0.15 | 198 | 0344 |
| | | | 45 | 35.24 | 15.90 | 0.05 | 206 | 0350 |
| | | 91 | 5 | 30.56 | 16.76 | 0.25 | 116 | 0400 |
| | | | 10 | 32.05 | 16.96 | 0.20 | 180 | 0410 |
| | | | 15 | 34.60 | 16.79 | 0.15 | 180 | 0420 |
| | | | 25 | 35.40 | 16.00 | 0.15 | 180 | 0430 |
| | | | 35 | 35.40 | 16.00 | 0.15 | 235 | 0440 |
| | | | 45 | 35.64 | 15.99 | 0.05 | 355 | 0450 |
| | | 92 | 5 | 27.92 | 16.62 | 0.95 | 108 | 0500 |
| | | | 10 | 29.24 | 16.52 | 0.55 | 144 | 0510 |
| | | | 15 | 33.26 | 16.98 | 0.20 | 198 | 0520 |
| | | | 25 | 35.36 | 15.92 | 0.10 | 198 | 0530 |
| | | | 35 | 35.52 | 15.92 | 0.05 | 180 | 0540 |
| | | | 45 | 35.55 | 15.96 | 0.05 | 244 | 0543 |

| Station | Date | Profile | Depth | Salinity | Temperature | Current Speed | Direction | Time |
|---|---|---|---|---|---|---|---|---|
| | | 93 | 5 | 29.05 | 16.67 | 0.65 | 151 | 0615 |
| | | | 10 | 33.23 | 16.86 | 0.20 | 180 | 0623 |
| | | | 15 | 34.80 | 16.87 | 0.05 | 188 | 0630 |
| | | | 25 | 35.29 | 15.98 | 0.10 | 206 | 0640 |
| | | | 35 | 35.54 | 15.91 | 0.05 | 144 | 0650 |
| | | | 45 | 35.82 | 15.98 | 0.05 | 90 | 0655 |
| | | 94 | 5 | 31.12 | 16.88 | 0.30 | 144 | 0700 |
| | | | 10 | 31.48 | 16.93 | 0.15 | 185 | 0720 |
| | | | 15 | 34.50 | 16.96 | 0.10 | 180 | 0730 |
| | | | 25 | 35.58 | 15.89 | 0.10 | 180 | 0740 |
| | | | 35 | 35.64 | 15.91 | 0.05 | 200 | 0750 |
| | | | 45 | 35.67 | 15.97 | 0.10 | 310 | 0800 |
| | | 95 | 5 | 31.88 | 16.97 | 0.35 | 165 | 0810 |
| | | | 10 | 34.16 | 16.93 | 0.05 | 170 | 0820 |
| | | | 15 | 34.37 | 16.81 | 0.15 | 215 | 0835 |
| | | | 25 | 35.55 | 15.83 | 0.10 | 235 | 0845 |
| | | | 35 | 35.60 | 15.86 | 0.05 | 260 | 0855 |
| | | | 45 | 35.66 | 15.88 | 0.25 | 250 | 0905 |

## REFERENCES


Abramowitz, M., and I. A. Stegun, 1965, Handbook of mathematical functions. New York (Dover Publications, Inc.).

Bowden, K. F., 1962, Measurements of turbulence near the sea bed in a tidal current. J. Geophys. Res., 67(8):3181.

Haltiner, G. J., and F. L. Martin, 1959, Dynamical and physical meteorology. New York (McGraw-Hill Book Co., Inc.), 470 pp.

Johnson, J. W., and H. C. Hwang, 1961, Mixing and dispersion by wind waves. Inst. Engineering Research Tech. Rept., Series 138, Issue 5, Univ. California, Berkeley.

Kalinske, A. A., and C. F. Pien, 1944, Eddy diffusion. Industrial and Engineering Chemistry, 36:220-223.

Marmer, H. A., 1932, Tides and tidal currents. In Physics of the earth, V. Oceanography, Bull. National Research Council, No. 85, pp. 229-309.

Masch, F. D., 1961, Mixing and dispersing action of wind waves. Inst. Engineering Research Tech. Rept., Series 138, Issue 6, Univ. California, Berkeley, 106 pp.

McNown, J., and P. N. Lin, 1952, Sediment concentration and fall velocity. Proc. Second Midwestern Conf. on Fluid Mechanics. Ohio State Univ.

Murray, S. P., 1969, Current meters in use at the Coastal Studies Institute. Coastal Studies Bulletin, Louisiana State Univ., No. 3, pp. 1-15.

Orlob, G. T., 1959, Eddy diffusion in homogeneous turbulence. J. Hydraulics Div. Am. Soc. Civil Engrs., 85(HY9):75-101.

Orton, R. B., 1964, The climate of Texas and the adjacent Gulf waters. U.S. Dept. Commerce, Weather Bureau, p. 112.

Pritchard, D. W., 1966, Comment on the paper "Small-scale horizontal diffusion near the coast," by N. Ito, M. Fukuda, and Y. Tanigawa. International Atomic Agency Symposium on the Disposal of Radioactive Wastes into Seas, Oceans, and Surface Waters, Vienna, p. 482.

Reid, R. O., 1957, Modification of the quadratic bottom-stress law for turbulent channel flow in the presence of surface wind stress. Corps of Engineers, Beach Erosion Board Tech. Memo. No. 93, 33 pp.

Roberts, O. F. T., 1923, Scattering of smoke in a turbulent atmosphere. Proc. Royal Society of London, Series A, 104:640-654.

Scruton, P. C., 1956, Oceanography of Mississippi Delta sedimentary environments. Bull., Am. Assoc. Petrol. Geologists, 40:2864-2952.

Sutton, O. G., 1953, Micrometeorology. New York (McGraw-Hill Book Co., Inc.), 333 pp.

Sverdrup, H. U., M. W. Johnson, and R. H. Fleming, 1942, The oceans, their physics, chemistry, and general biology. New York (Prentice Hall), 1087 pp.

Taylor, G. I., 1921, Diffusion by continuous movements. Proc. London Math. Society, 20:196-212.

_____, 1935, Statistical theory of turbulence, Parts I-IV. Proc. Royal Society of London, Series A, 151:421-478.

U.S. Coast and Geodetic Survey, ESSA, 1970, Tide tables, high and low water predictions, east coast, North and South America, including Greenland. U.S. Government Printing Office, p. 239.

Weather Bureau, U.S. Dept. of Commerce, 1959, Climatological and oceanographic atlas for mariners. Vol. 1, North Atlantic Ocean.

Wiegel, R. L., 1962, Wind waves and swell. Proc. 7th Conf. on Coastal Engineering.

Yudine, M. I., 1959, Physical considerations on heavy particle diffusion. Advances in geophysics, atmospheric diffusion and air pollution, 6: 185-192.

Security Classification

## DOCUMENT CONTROL DATA - R & D

*(Security classification of title, body of abstract and indexing annotation must be entered when the overall report is classified)*

1. ORIGINATING ACTIVITY (Corporate author)
Coastal Studies Institute
Louisiana State University
Baton Rouge, Louisiana 70803

2a. REPORT SECURITY CLASSIFICATION
UNCLASSIFIED

2b. GROUP

3. REPORT TITLE
Oceanographic Observations and Theoretical Analysis of Oil Slicks During The Chevron Spill, March 1970

4. DESCRIPTIVE NOTES (Type of report and inclusive dates)
Final Report (March 1970 - July 1970)

5. AUTHOR(S) (First name, middle initial, last name)
Stephen P. Murray, W. G. Smith, Choule J. Sonu

| 6. REPORT DATE | 7a. TOTAL NO. OF PAGES | 7b. NO. OF REFS |
|---|---|---|
| July 1970 | 110 | 23 |

| 8a. CONTRACT OR GRANT NO. | 9a. ORIGINATOR'S REPORT NUMBER(S) |
|---|---|
| DOT-CG-03,592-A | NONE |
| b. PROJECT NO. 714104/A/006 | |
| c. | 9b. OTHER REPORT NO(S) (Any other numbers that may be assigned this report) |
| d. | 714104/A/006-2 |

10. DISTRIBUTION STATEMENT
Availability Unlimited. Document may be released to the Clearinghouse for Federal Scientific and Technical Information, Springfield, Virginia 22151, for sale to the public.

11. SUPPLEMENTARY NOTES
Key words: oil slick, oil spill, oil slick growth and movement

12. SPONSORING MILITARY ACTIVITY
U. S. Coast Guard
Department of Transportation
Washington, D. C. 20591

13. ABSTRACT

Oceanographic observations near the Chevron spilling well off the Mississippi Delta in March 1970 revealed relative roles of various physical factors of the regional estuarine system in the behavior of oil slicks. Surface stress from the wind was most important, at speeds above 15 mph the slick orientation was generally determined by the wind direction. The wind also indirectly affected oil which was sunk by dispersant in the wind waves promoted mixing, which in turn affected the vertical stability, hence eventually the velocity profile. Wind setups and setdowns were correlated with downward and upward isopycnal movements, respectively. Both calculations and observations showed that tidal currents produced an L-shaped slick geometry when winds were below about 15 mph. The diurnal rotation of the tidal currents served to limit the excursion length of oil from the source, keeping it short of the nearest shore. The presence of fresh water from the Mississippi River in the surface layer and the consequent development of convergence lines often formed a natural barrier, preventing oil from encroaching upon the shore. Theoretical analysis using turbulent diffusion theory disclosed that the area and length of a steady-state oil slick increased with oil discharge but decreased with current speed and the lateral diffusion coefficient. Slick width increased with the rate of discharge and decreased with current speed but was independent of the diffusion coefficient. The width/length ratio of an oil slick, which was notably independent of current speed, was controlled only by the diffusion coefficient and the oil discharge. In order to be able to predict oil slick behavior, understanding of the interaction between these multiple factors is essential and, for that end, the use of a multiple-sensor array with automatic data transfer and processing capability is recommended. (U)

DD FORM 1 NOV 1473

Security Classification

44444